



Hydrocarbon Potential of Impact Craters: Unconventional Exploration Play

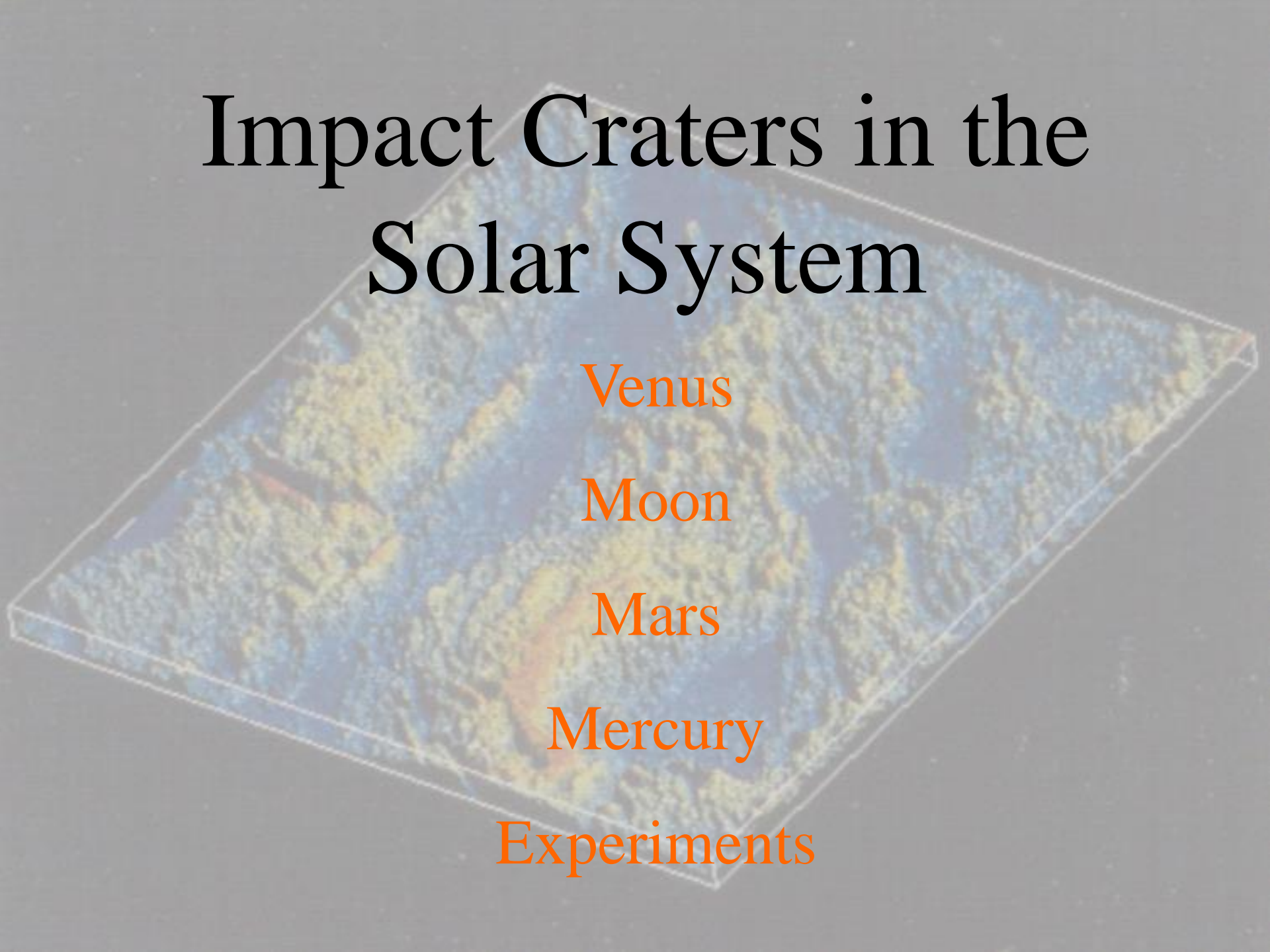
Analogue impact craters in outer space

Experimental impact craters

Proven impact craters on Earth

Probable and Possible impact craters on Earth

Impact Craters in the Solar System



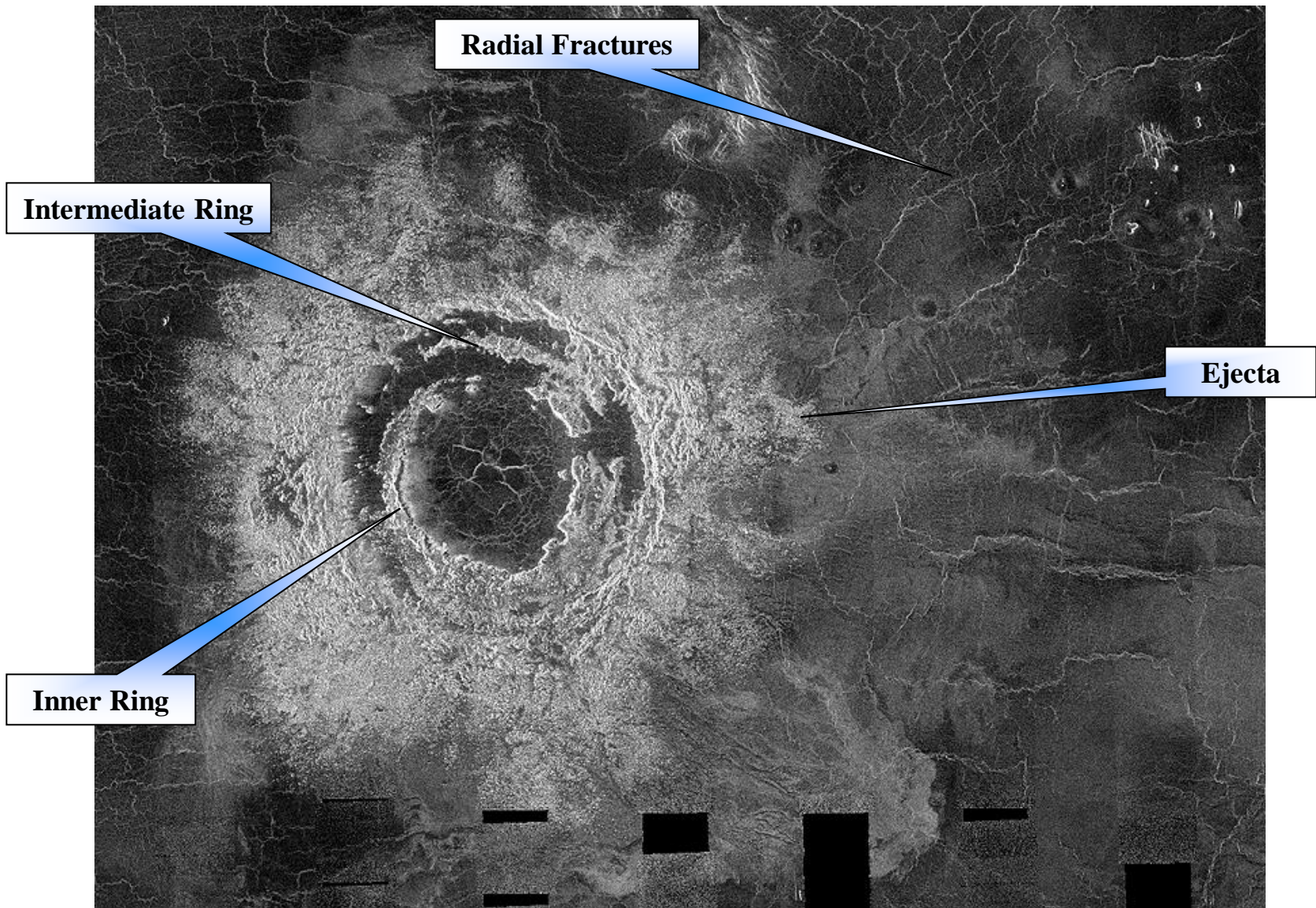
Venus

Moon

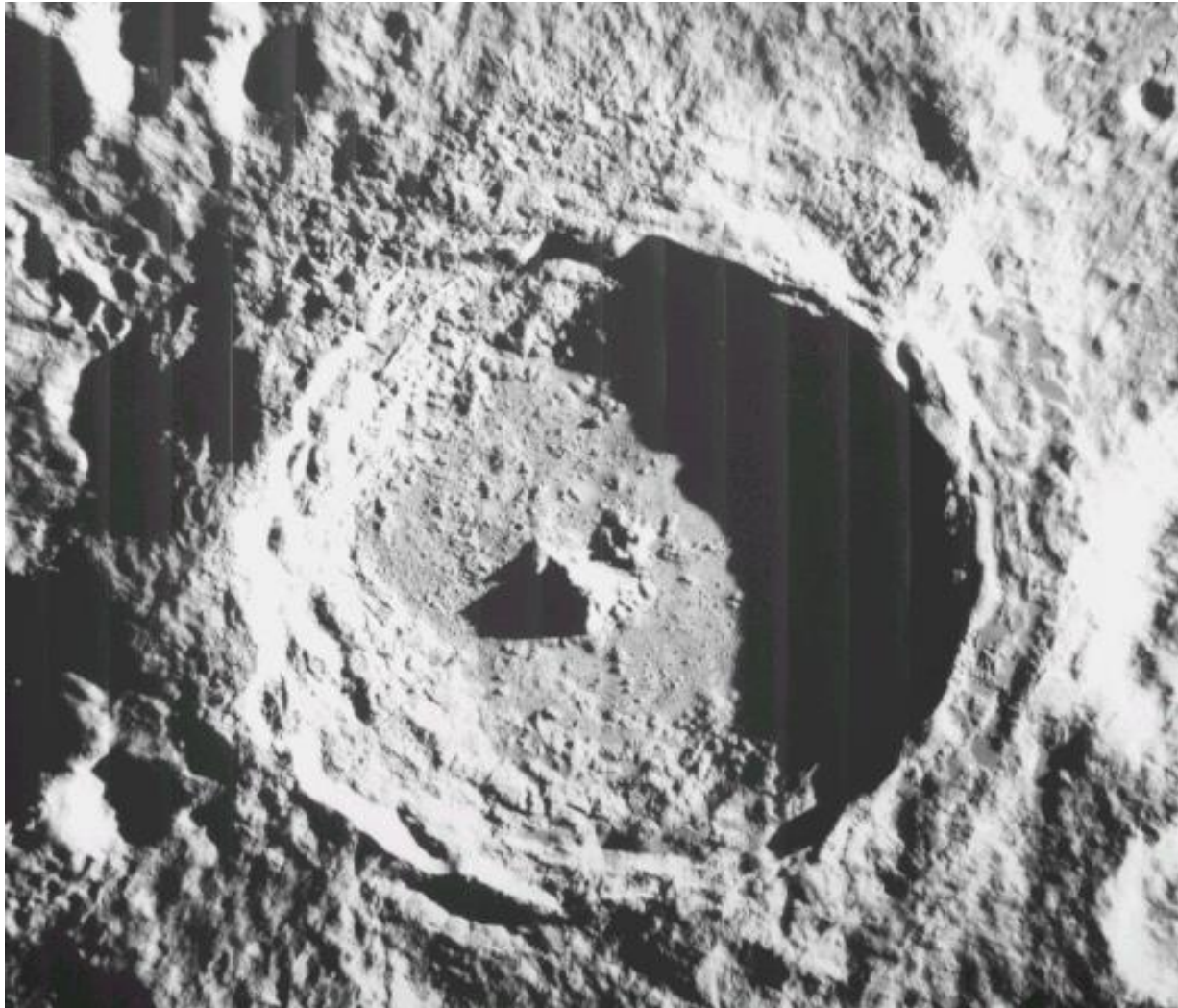
Mars

Mercury

Experiments



Mona Lisa multiringed basin, Venus, synthetic aperture radar left-look incident 39.1-44.5. NASA ID C1-30N027;1. North is up. Crater is 86 kilometers in diameter. The average age of the surface of Venus is estimated to be 250 to 450 Ma, and approximately 900 impact craters have been identified thus far on this lightly explored planet..

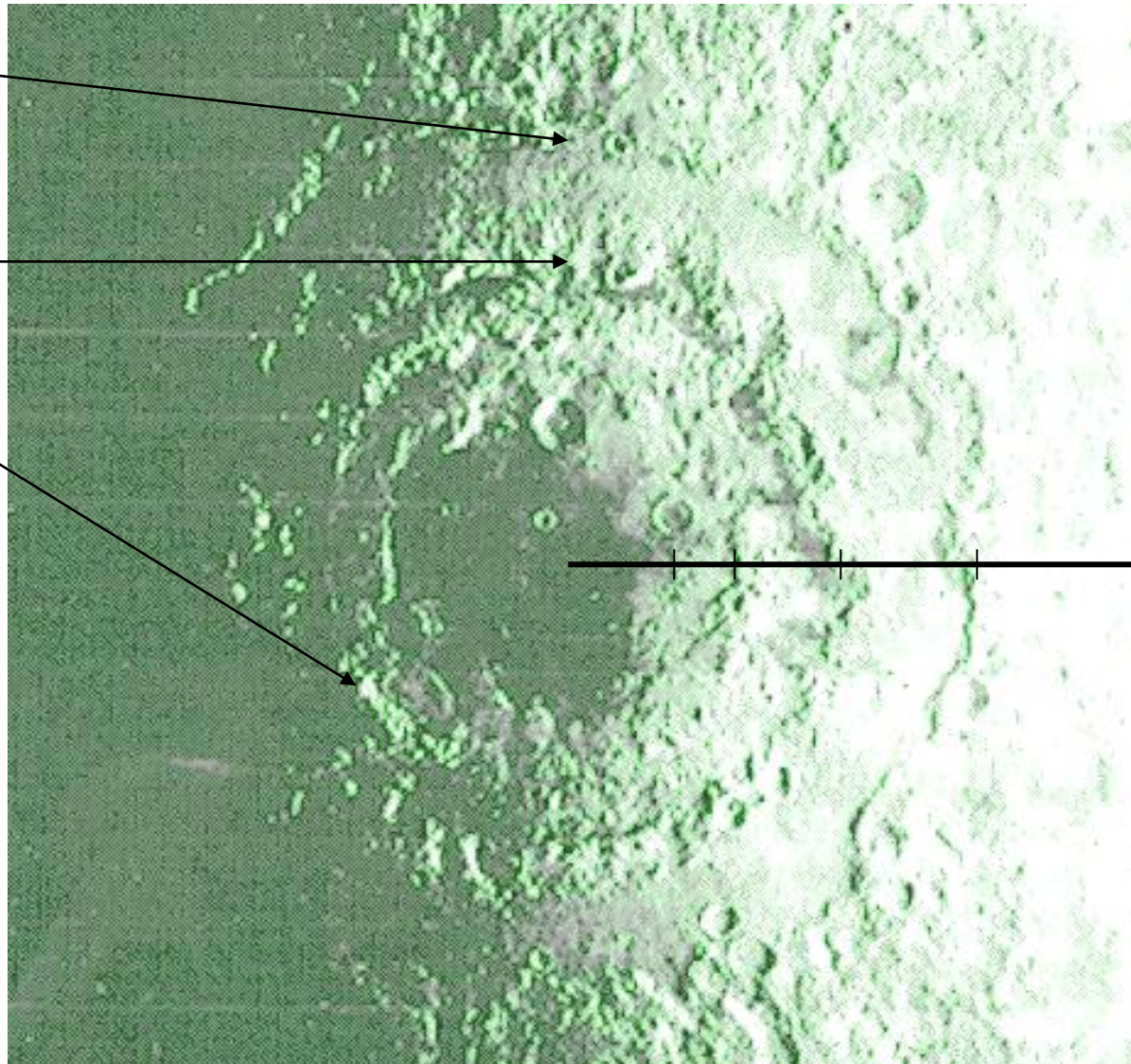


Tycho Crater, Moon, Lunar Orbiter 05 (NASA/JPL). The Moon hosts over 50 giant impact craters with diameters ranging from 300 to over 3,200 kilometers in diameter. Examples of these Copernican-scale craters include Procellarum (3200 kilometers diameter), South Pole-Aitken (2500 kilometers diameter), and Orientale (930 kilometers diameter).

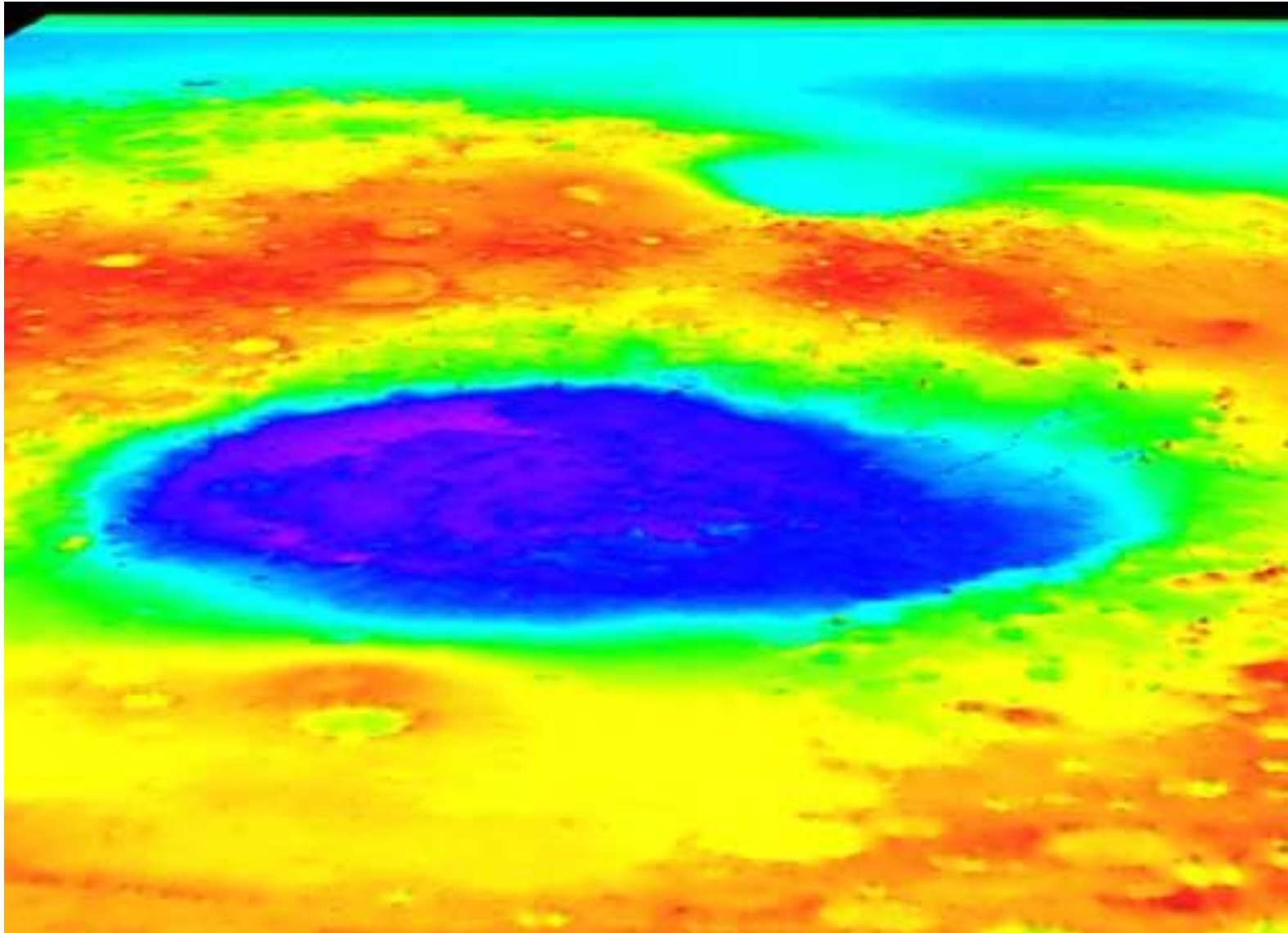
Cordillera

Outer Montes
Rook

Inner Montes
Rook

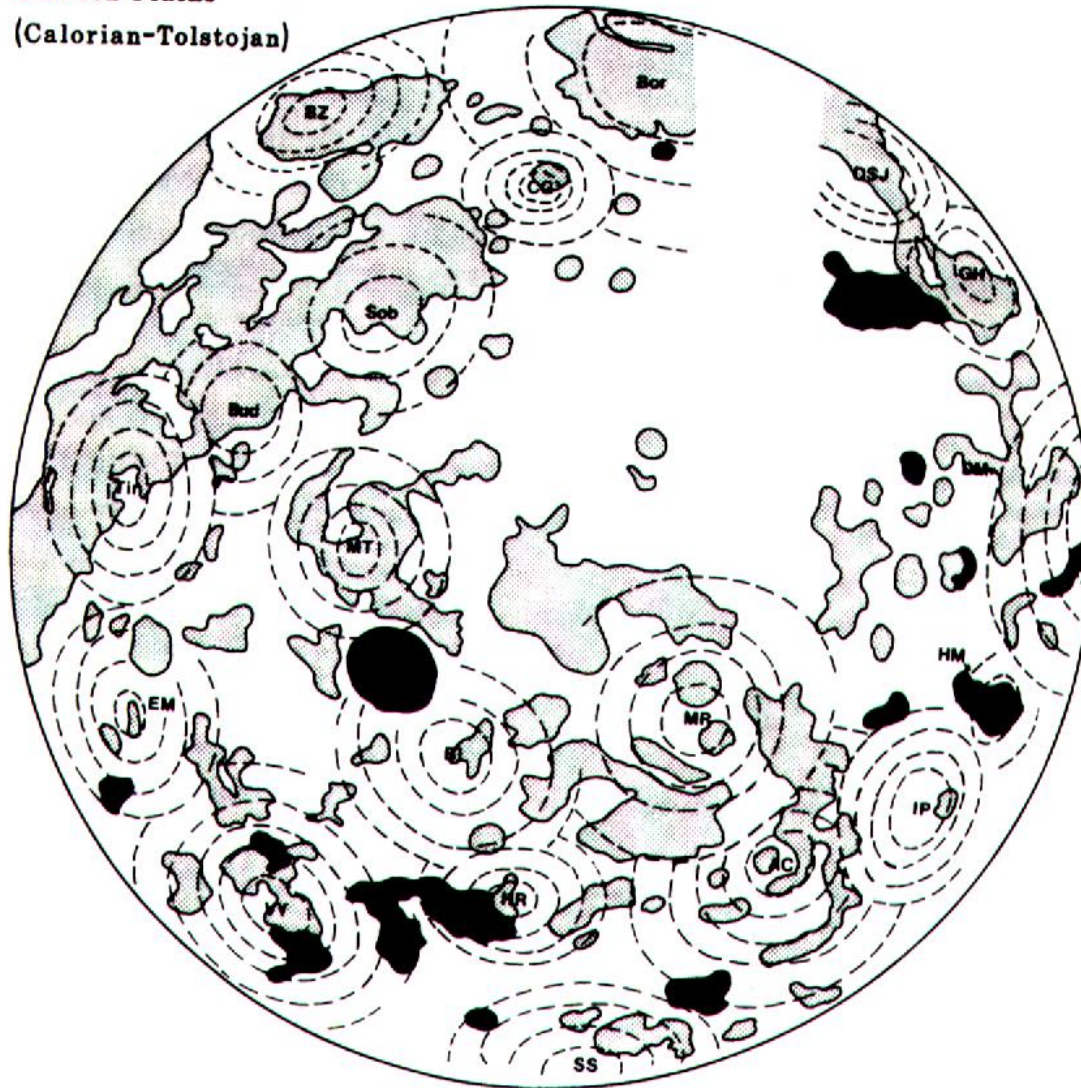


Mare Orientale Multiringed Basin, 980 km diameter, Moon (NASA), is the prototype multiring basin. The Inner Montes Rook, Outer Montes Rook, and main Cordillera rings are indicated. Note 4 rings.

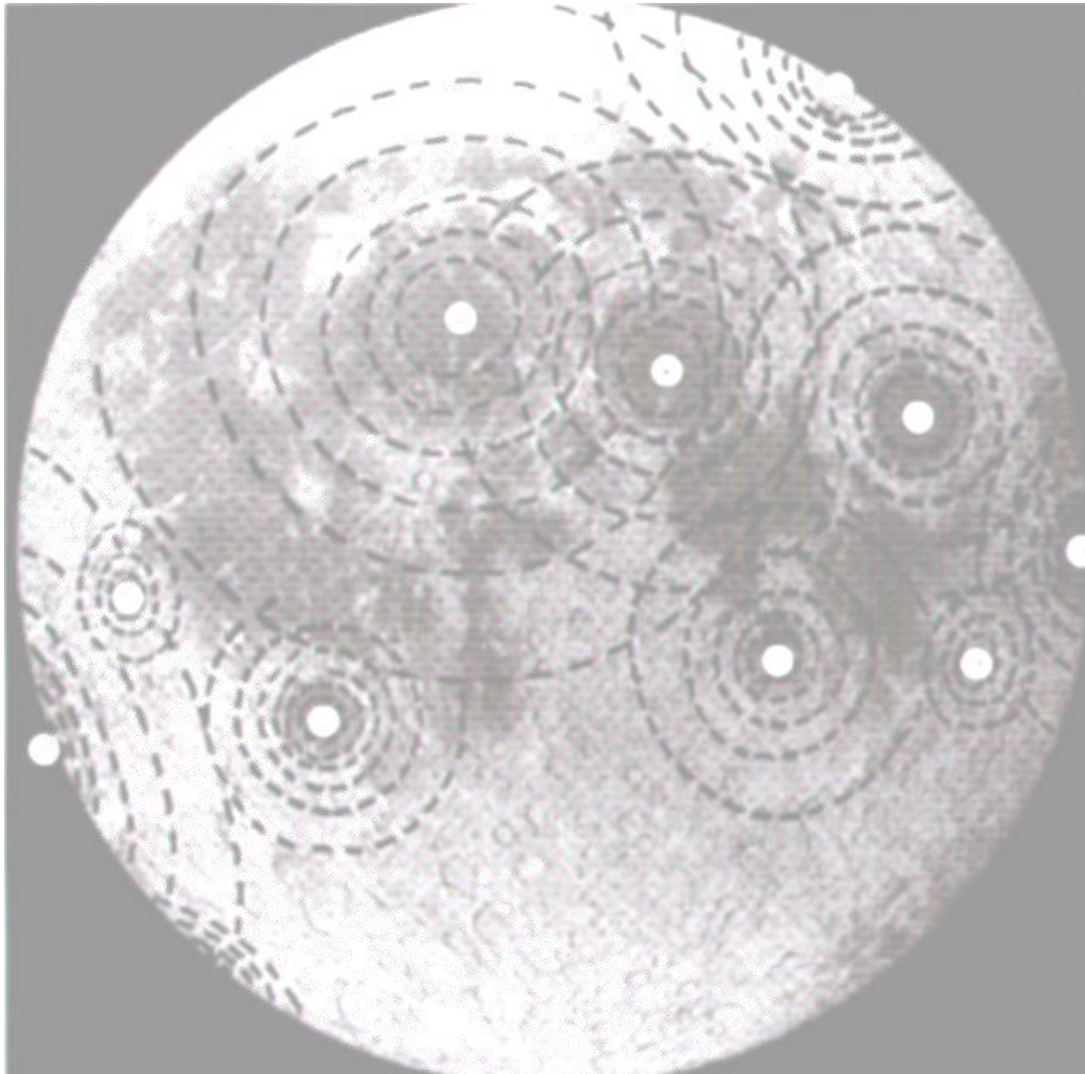


Hellas Basin, Mars. Global Surveyor laser altimetry (NASA, 1999). Location 41 S / 295 W. Rings are at 840, 1200, 1700, 2200, 3100, 4400, and 5500 kilometer diameters, with the main topographic rim (above) at 2200 kilometers diameter.

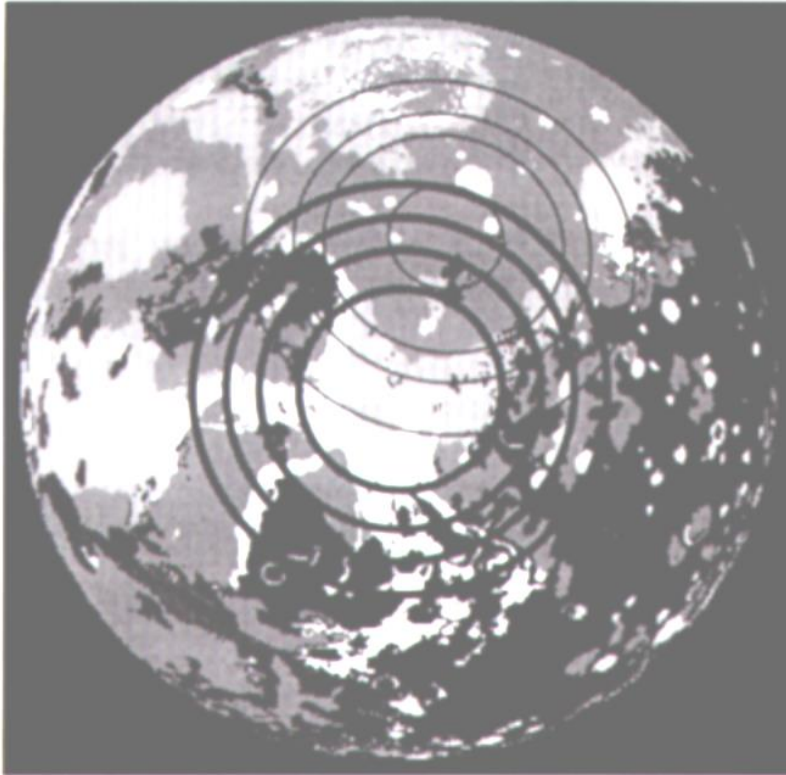
Smooth Plains
(Calorian-Tolstojan)



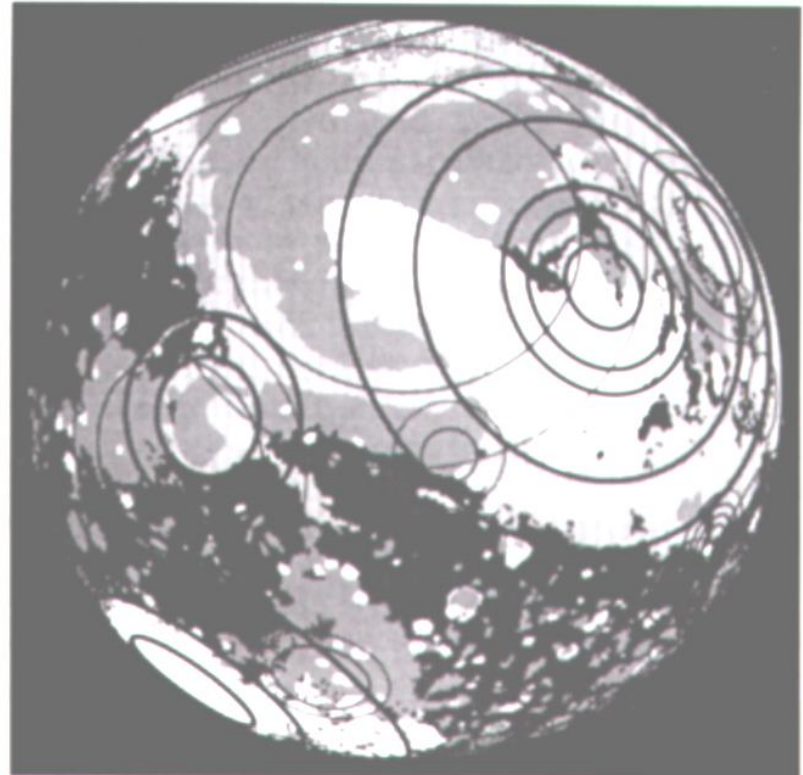
Lambert equal-area projection showing the distribution of smooth plains and multiringed basins on Mercury (Spudi, 1993, p. 227). On both Mercury and the Moon, basins control the distribution of volcanic units.



Lambert equal-area projection of the near (left) and far (right) sides of the Moon showing the locations and rings of lunar rings (Spudis, 1993, p. 39). Multiring geologic analyses of this type have been done on the terrestrial planets and moons for over 30 years.

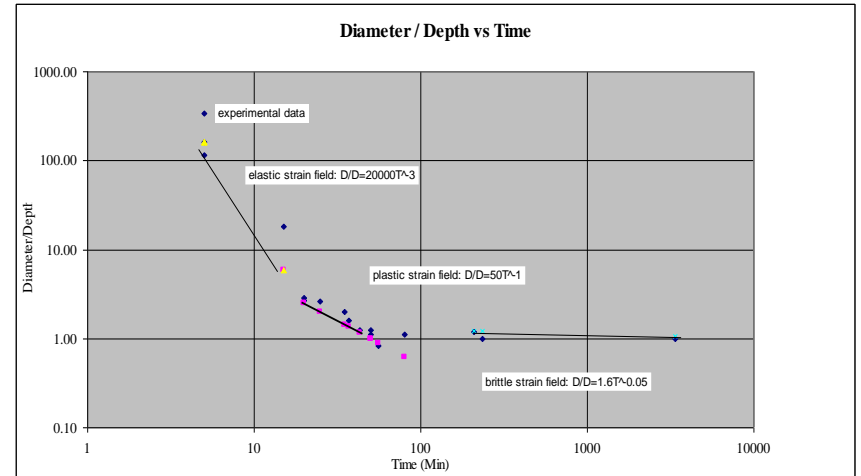
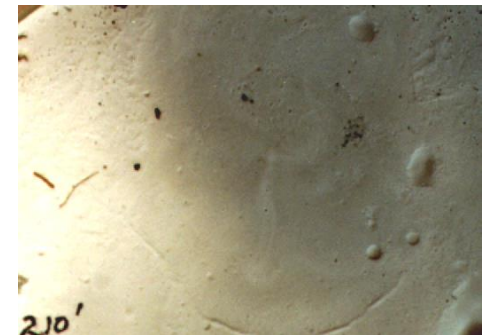
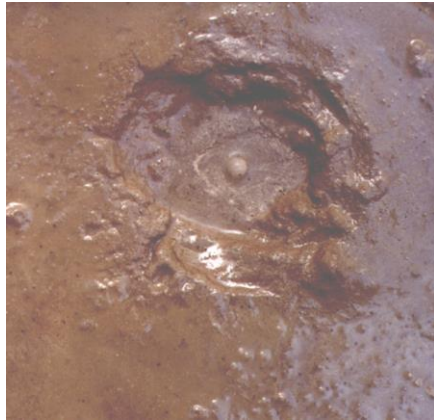
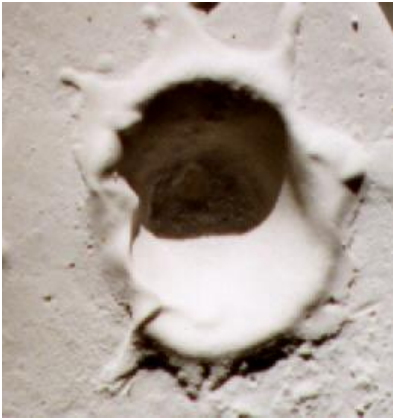


Chryse: 24N / 45W. Rings at diameters of 840, 1320 (main rim), 1920, 2840, and 3940 kilometers.



Utopia: 48N / 324. Ring diameters at 170, 250, 355 (main rim), 520, 680, and 1100 kilometers.

Multi-ring analyses by researchers from Goddard Space Flight Center, for Mars (Frey et al, LPSC XXV p 388, p390).



Range of impact morphologies with increasing pore pressure / decreasing shear strength from upper left to lower right. Note that the most easily recognized impact-generated structures (upper left) represent only a small set of the range of impact-generated structures possible (lower right). UR graph x=time, y=diameter/depth.

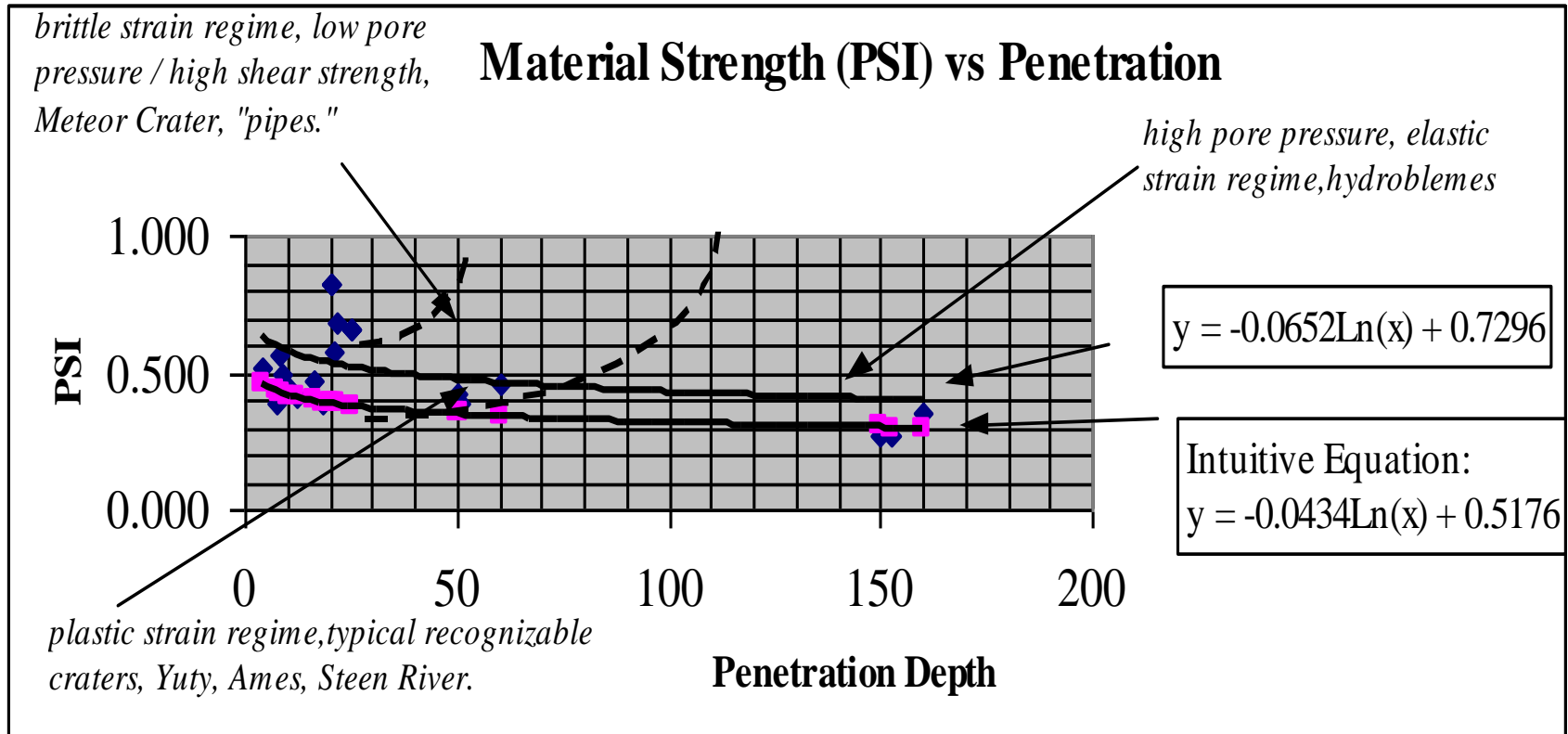


Figure ____. Experimental penetration depth determination. Relationship between penetration depth (DOP) and rheology constant PSI (Ψ). Hydroblemes typically have very large DOPs, with correlative Ψ 's of $<0.3 \pm$. Most typical impact craters, those with raised rims, hemispherical excavations, splotch ejects, have Ψ 's ranging from 0.35 to 0.45.

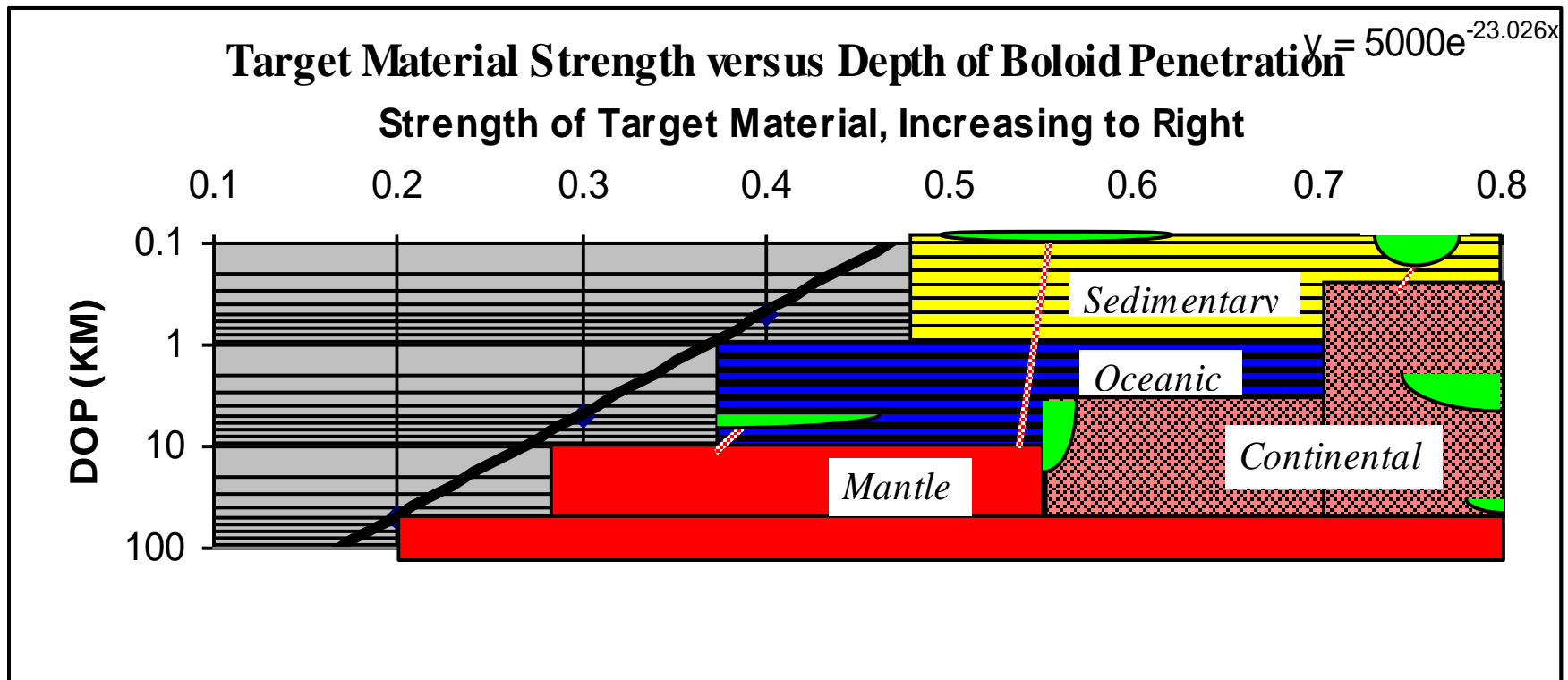


Figure ____. Schematic showing depth of penetration of meteorite (DOP) versus strength of the target material. Where very deep depths of penetration, for example 10 kilometers, targets continental crust, large depth to diameter craters that do not penetrate the lower crust result; deep penetrations which intersect relatively thin oceanic crust should be expected to disturb the mantle and initiate thermal conduction. High pore pressure sediments sitting on oceanic crust can disturb the mantle and initiate thermal conduction.

‘Proven’ Impact Craters on Earth

Meteor Crater

Ames

Calvin 28

Sierra Madera

Araguainha

Vredefort

Decaturville

Marquez Dome

Chicxulub

Bukit Paloh

Haughton

Redwing Creek

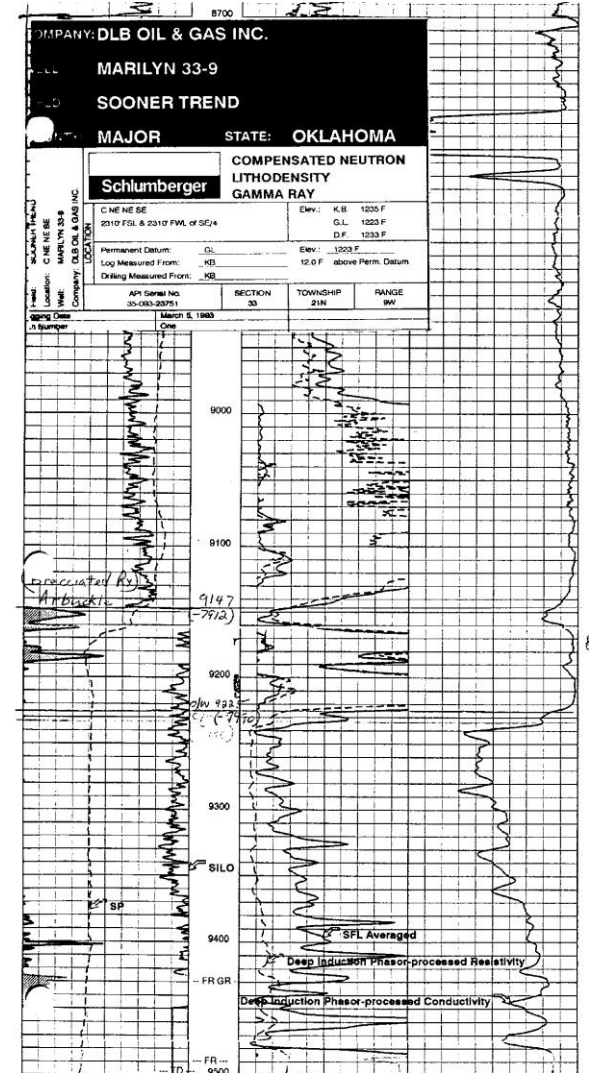
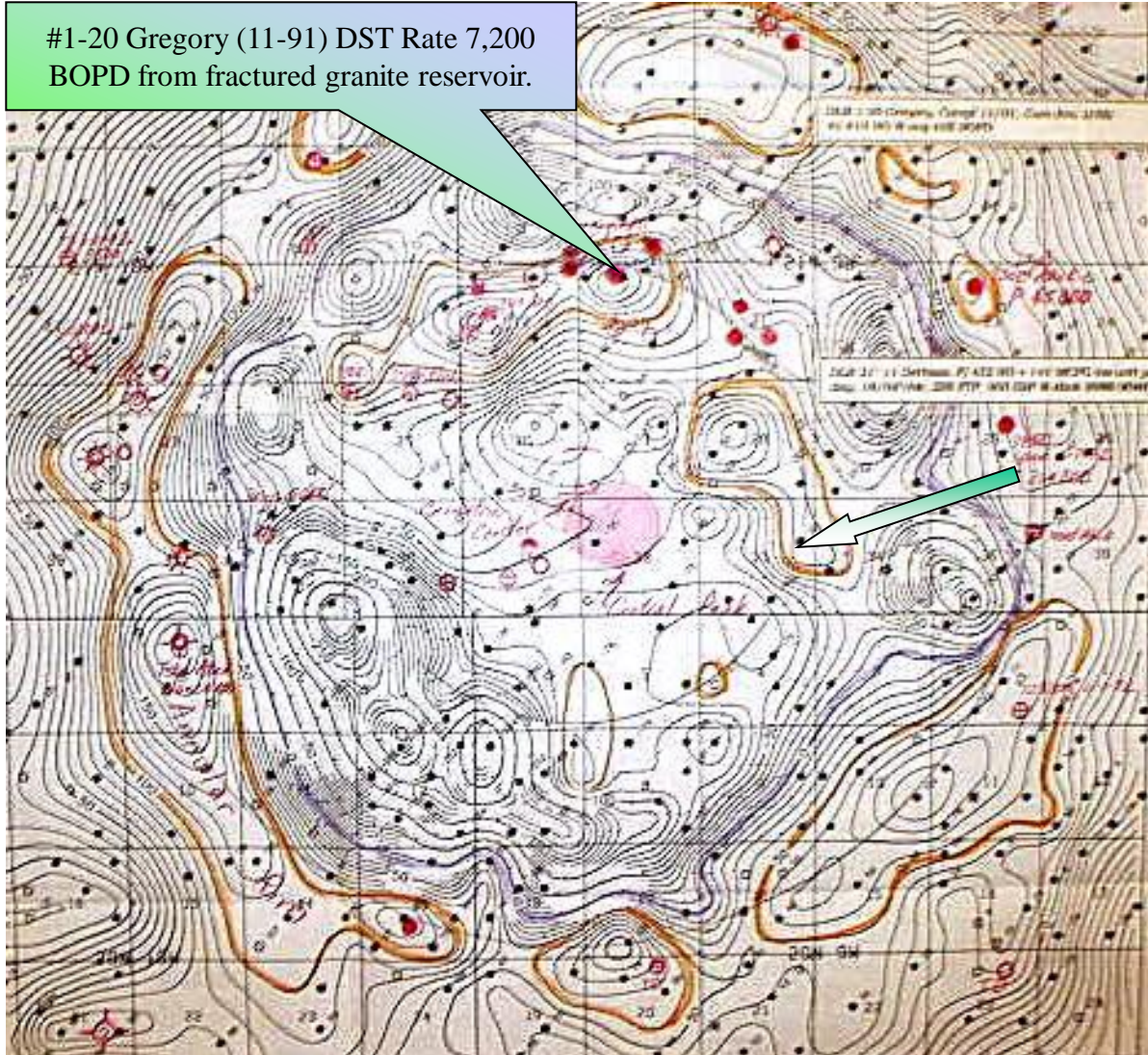
Avak



USGS Chief Geologist G.K. Gilbert visited this feature in 1891 and concluded that it was of volcanic origin. In 1902 D. Barringer, a mining engineer, concluded it was an impact crater, and he spent the next 26 years (and all his money) trying to find the giant iron meteorite lode.

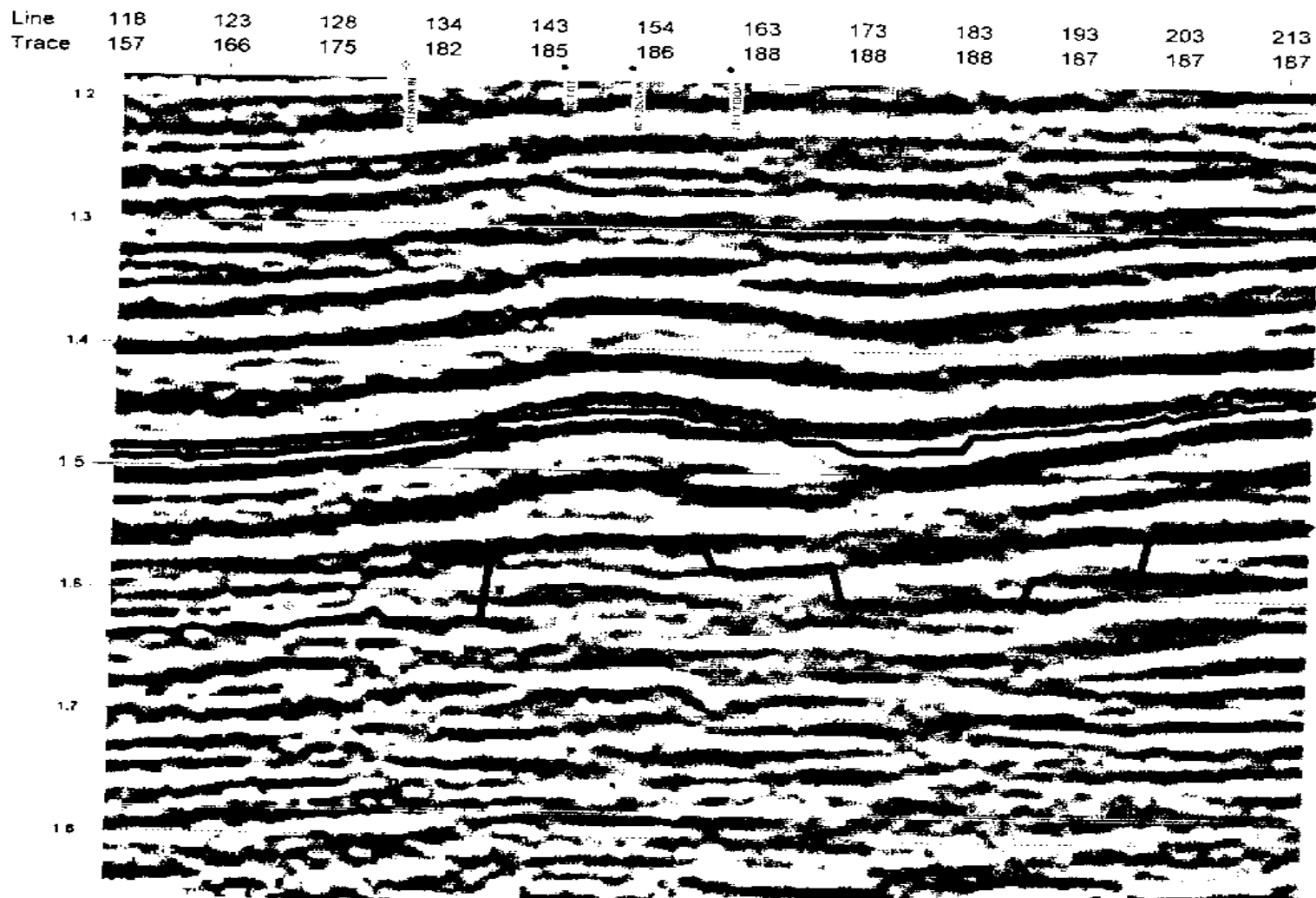


#1-20 Gregory (11-91) DST Rate 7,200 BOPD from fractured granite reservoir.

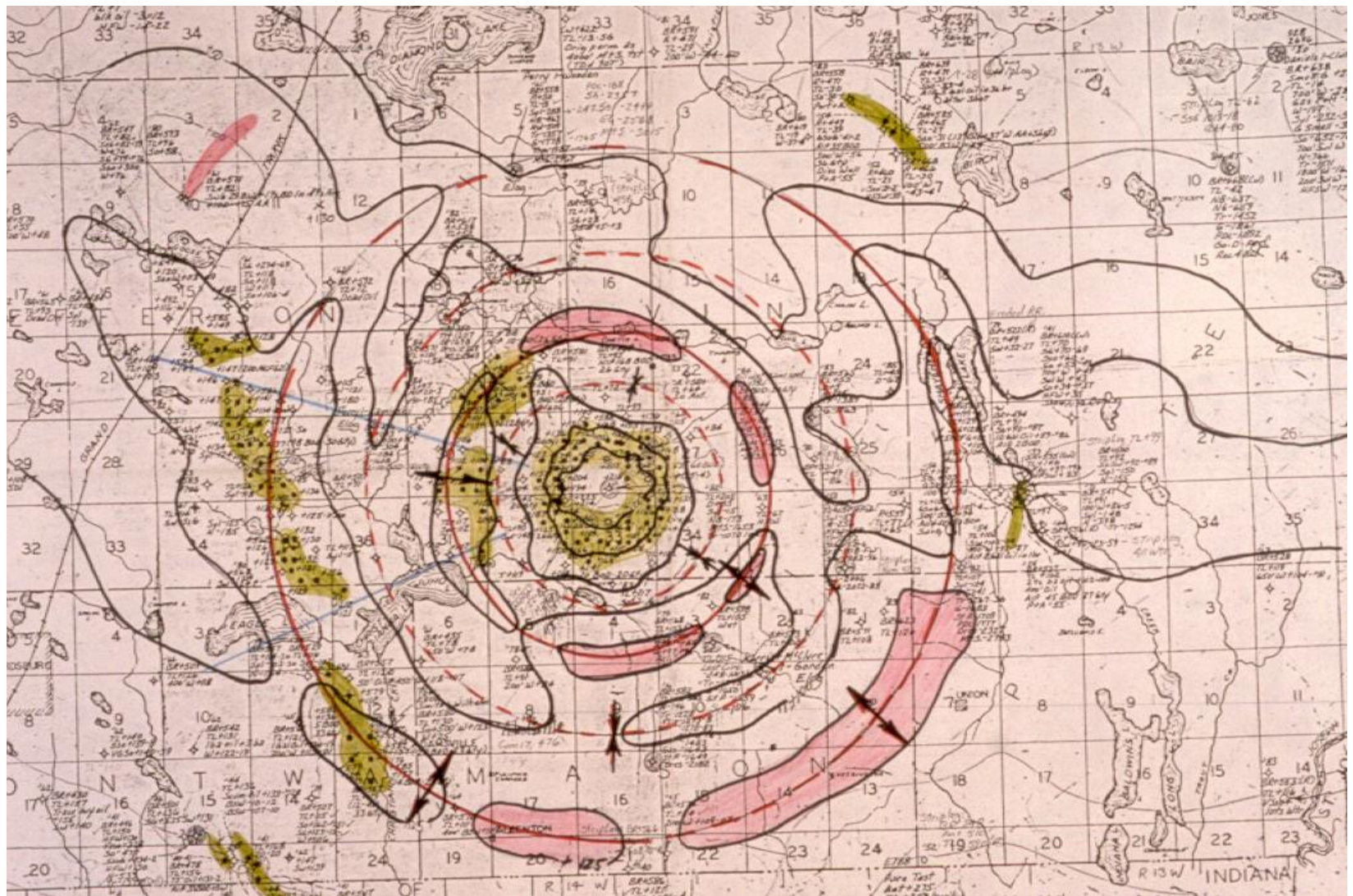


Ames Astrobleme, Sylvan Residual, 4/10/92, DB.

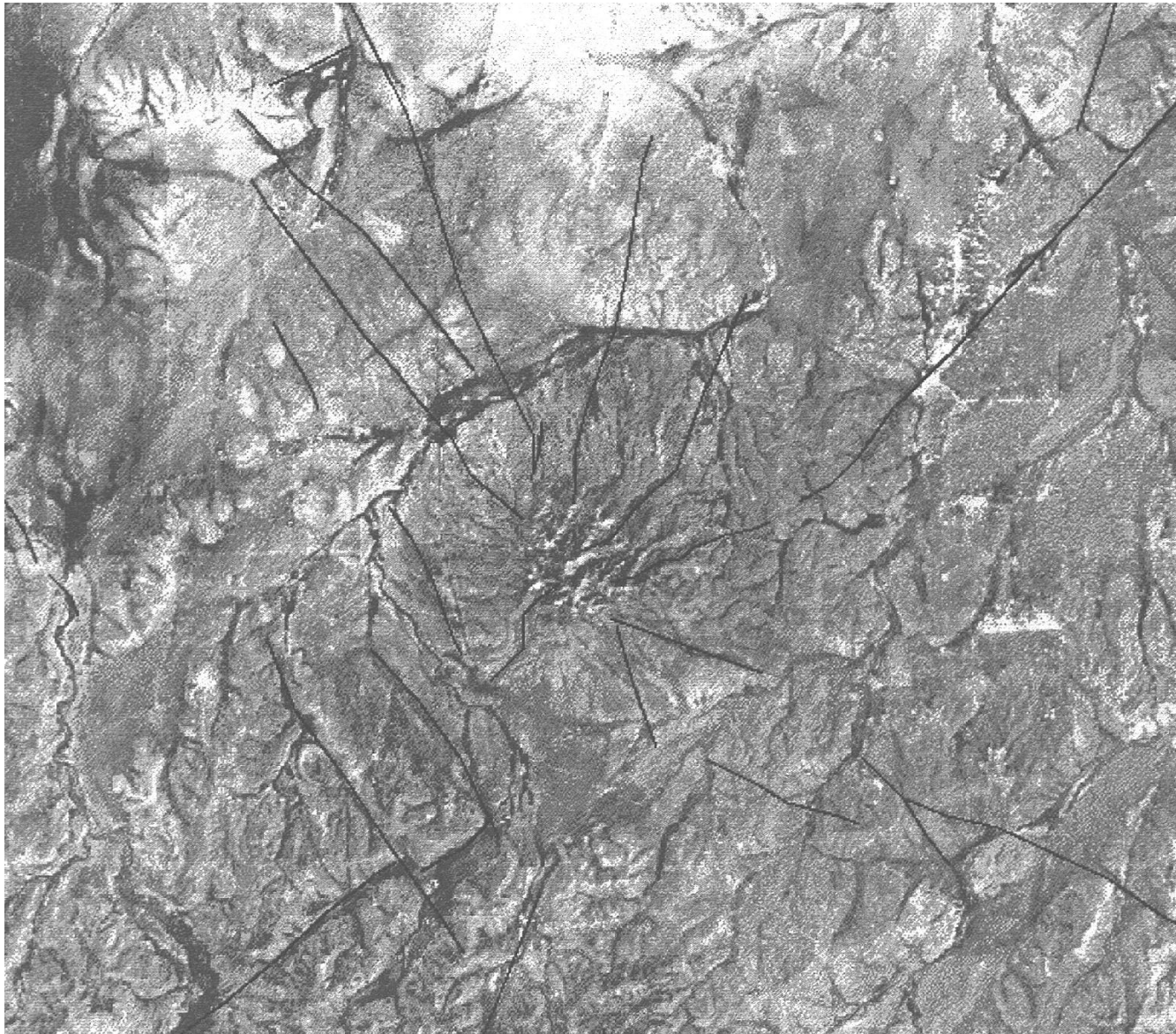
DLB Marilyn 33-9. DST GTS 6", OTS 14", Rate 4,234 BOPD + 202 MCFGPD. Brecciated Arbuckle avg. 9% porosity, 557 md, 78 net feet.



South-north arbitrary seismic line across central rebound peak, across crater floor, then onto the north rim (from Sandridge & Ainsworth, 1997). Estimated ultimate recovery 50 MMBO oil discovered 1992.



Calvin-28, Cass County Michigan, Traverse Limestone. 13.6 km diameter, 395 ma, 600 MBO from 800-900'.

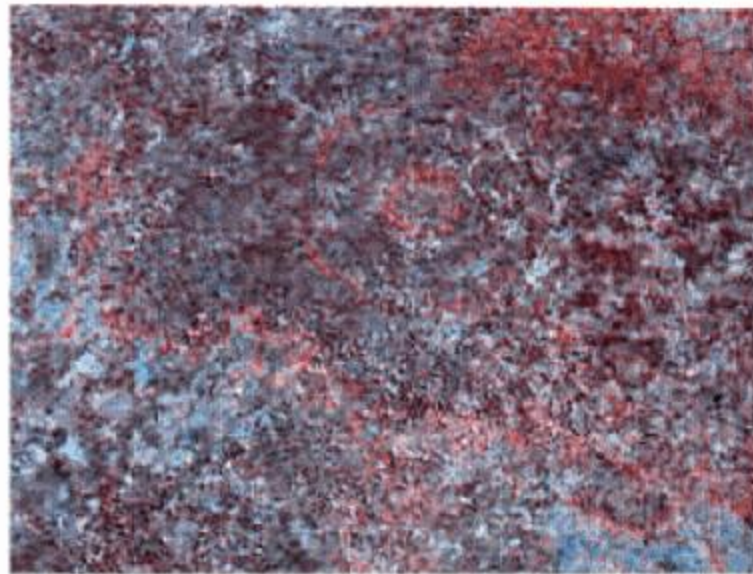
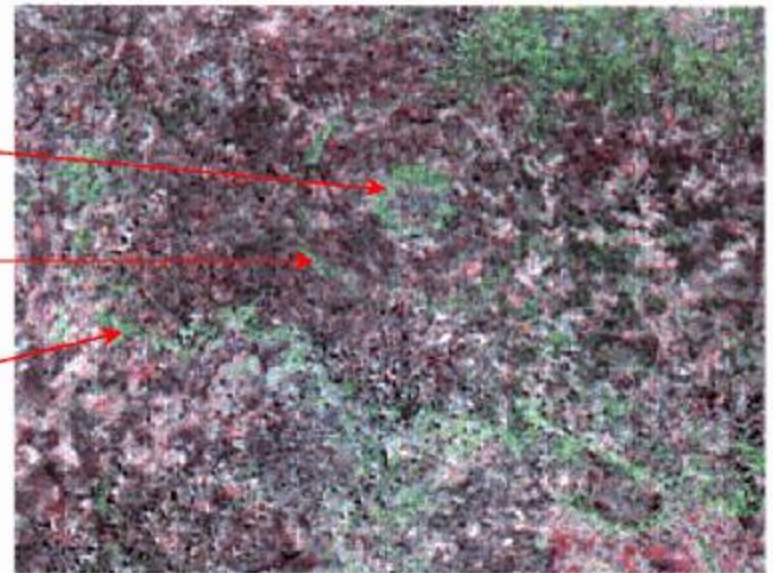


Sierra Madera central uplift peak, Landsat TM image. Gas well on south rim area, Texas Pacific #6 Montgomery-Fulk (75), with CAOF 4.3 BCFGPD. Case of fracture enhancement in sub-crater reservoir, similar to Marquez Astrobleme.

Inner ring Ponta Grossa Formation

Outer ring Passa Dois Formation

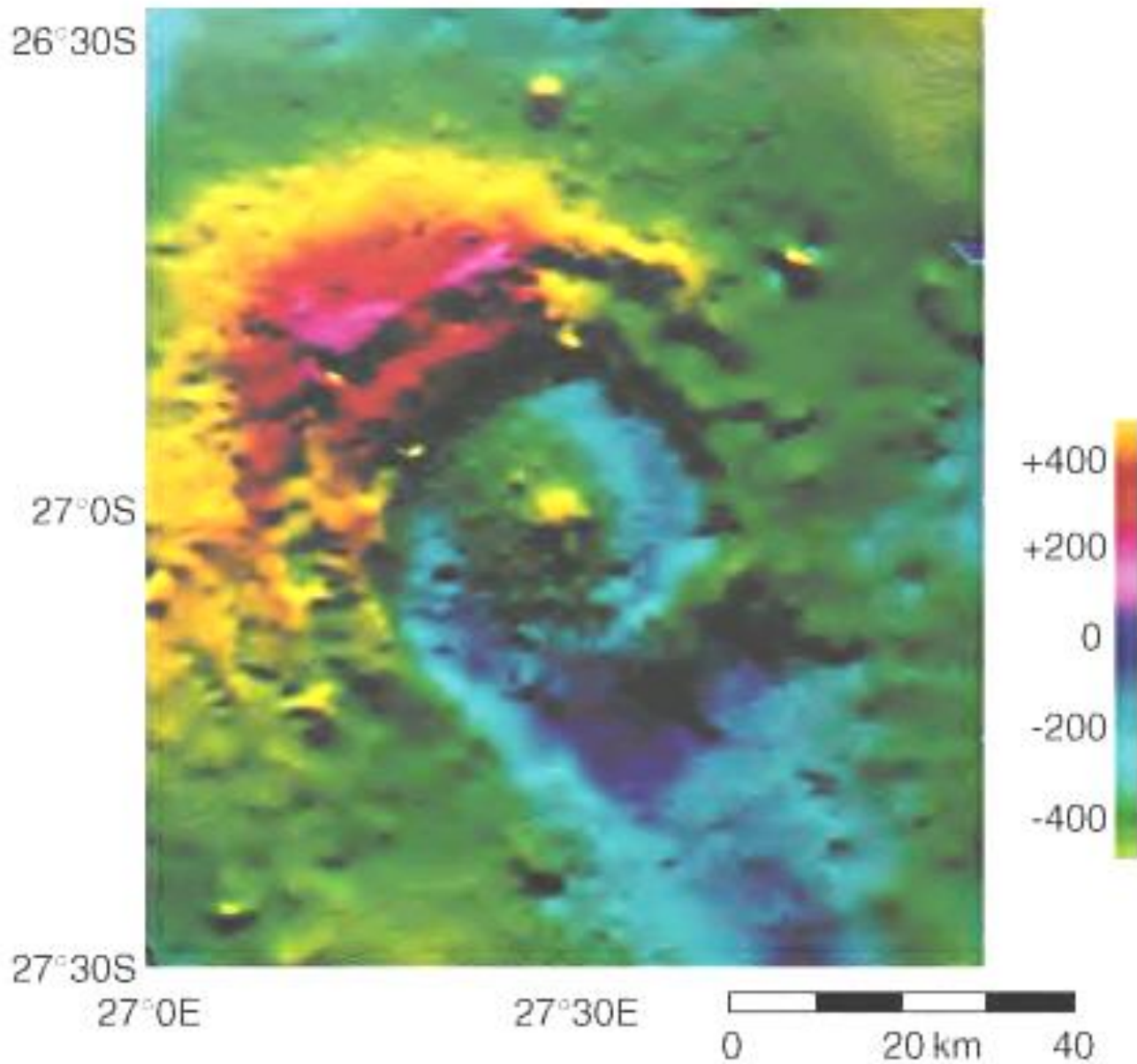
Limits of Ejecta Blanket



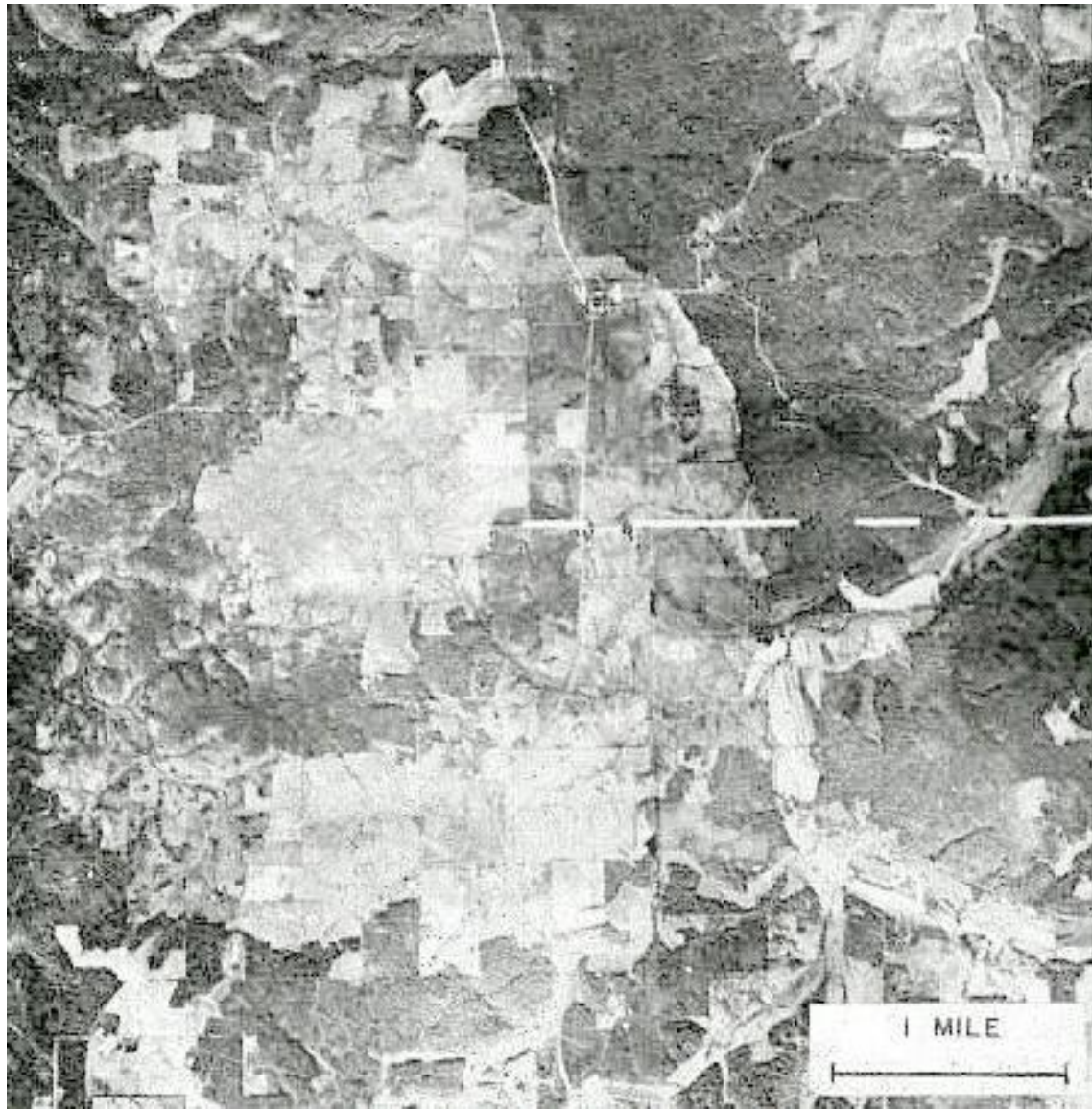
Araguainha Dome Impact Crater, Brazil. Complex, 40 km diameter crater, dated at 250 Ma. Landsat TM acquired 4/3/86. Bands 3, 4, 5.

Landsat TM data acquired 4/3/86.

Araguainha Crater, Brazil. Landsat TM.

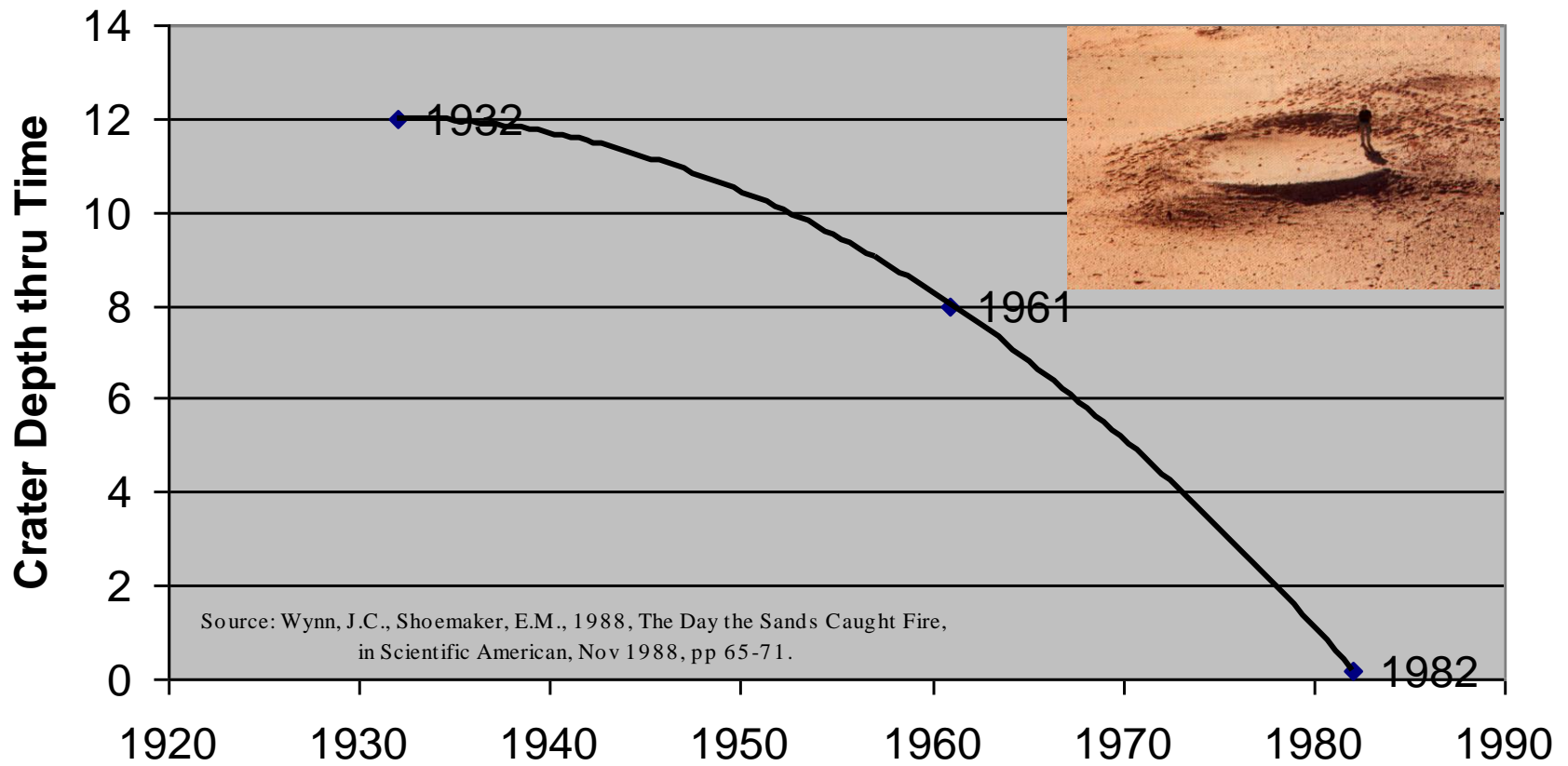


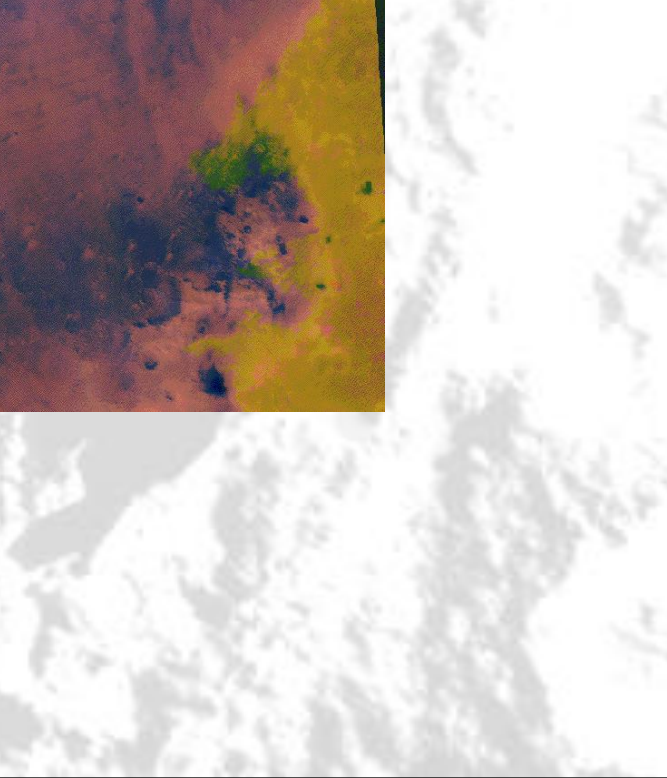
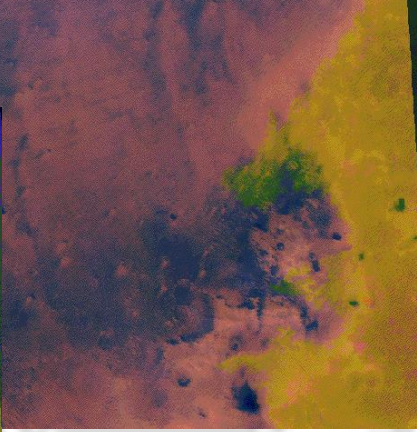
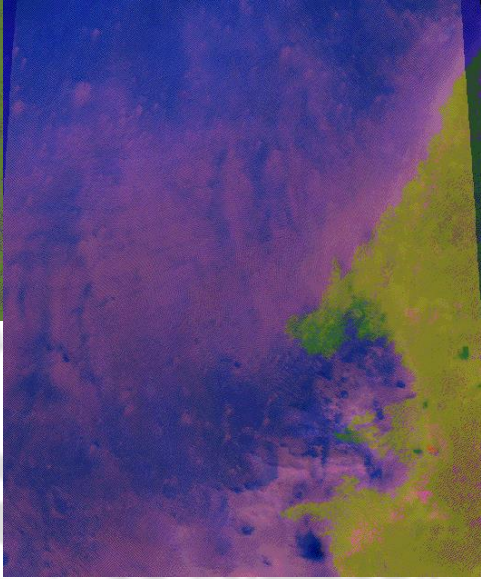
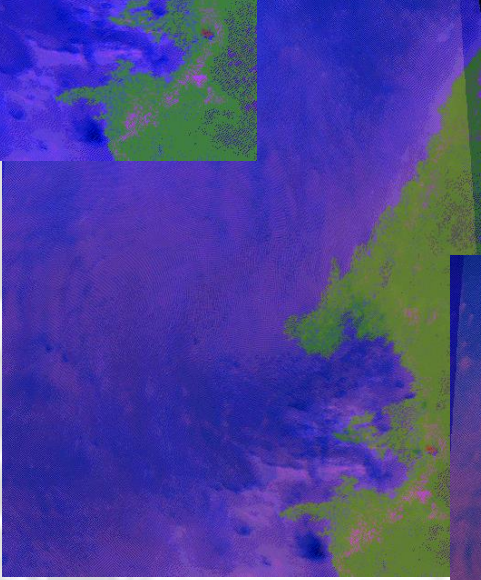
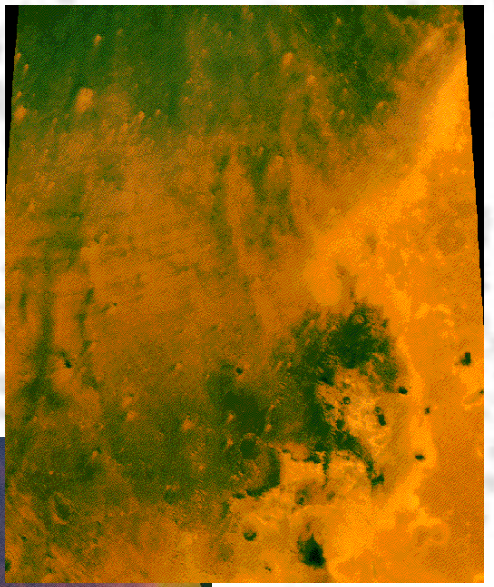
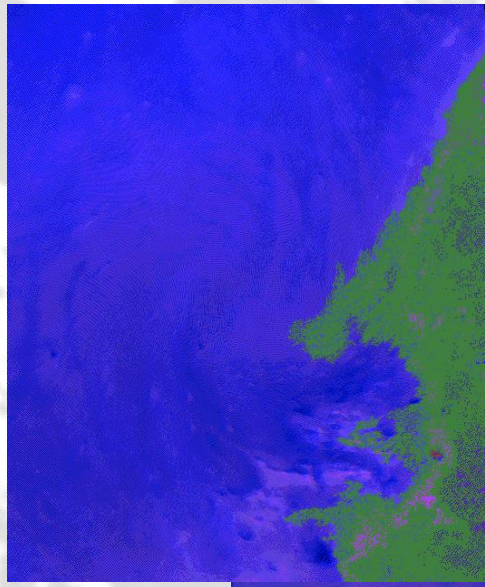
Vredefort Ring, South Africa, 1VD Gravity.



Decaturville Crater, Missouri, aerial photograph.

Wabar Crater Burial, Saudi Arabia





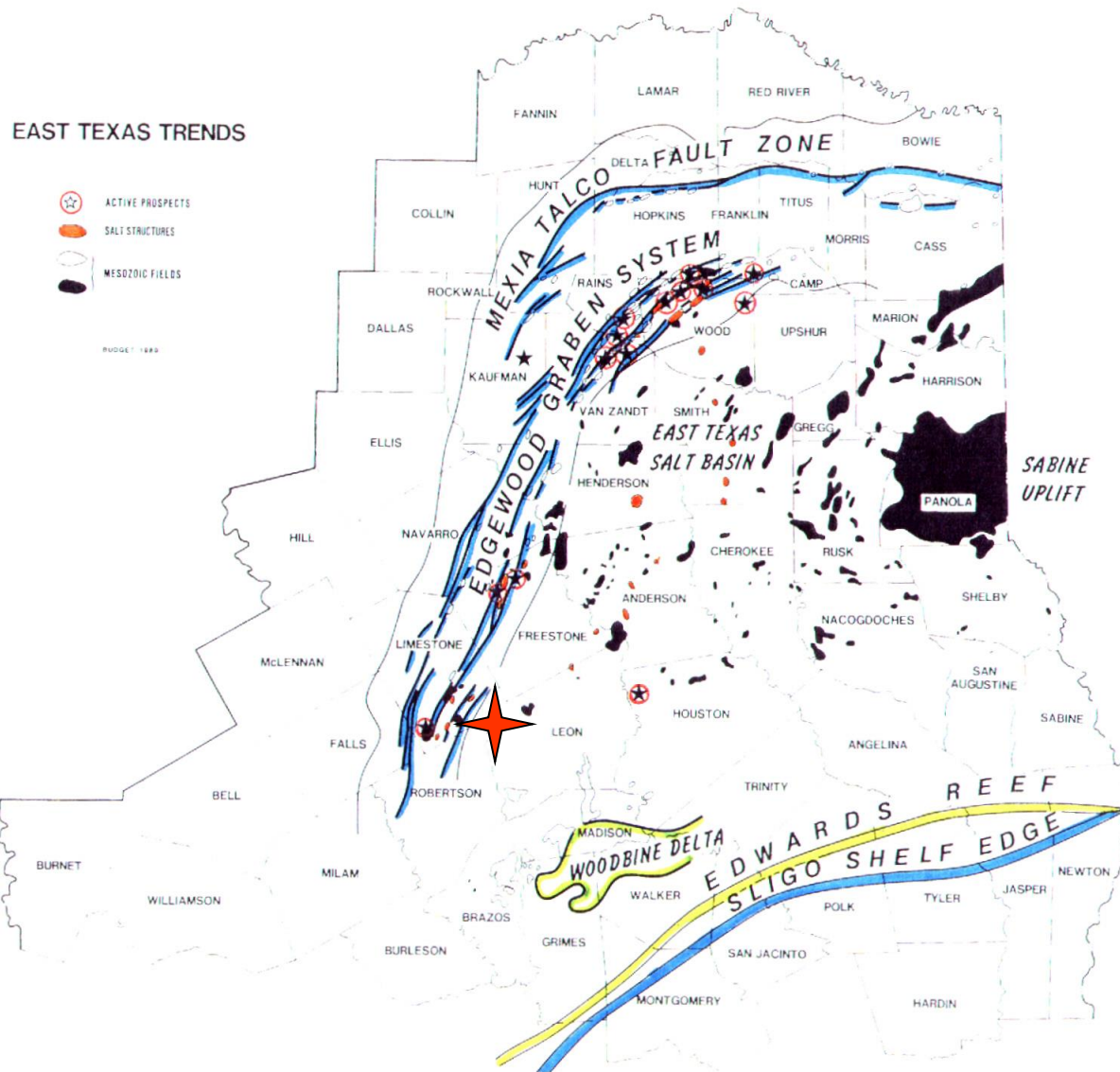
Marquez Dome Impact Structure, Leon County, Texas

3D Seismic Investigation of Marquez Dome, East Texas

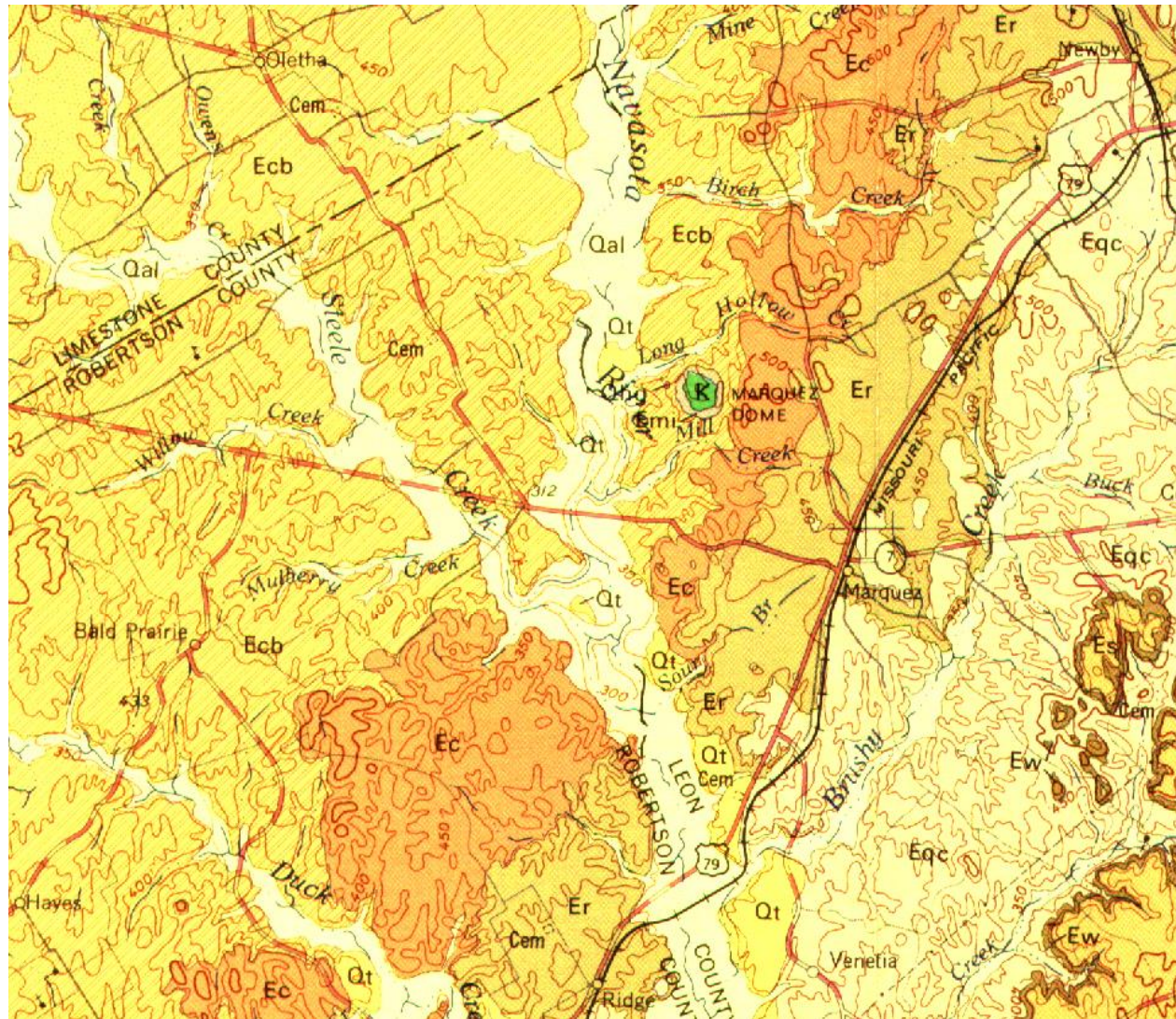
D. B. Buthman

Unocal, 14141 Southwest Freeway, Sugar Land, Texas, 77478

Industry recently acquired 285 square kilometers of 3D reflection seismic data over the 13 kilometer diameter Marquez Dome impact crater, Leon County, Texas. The area is located within the gas prospective Cotton Valley trend in the East Texas Salt Basin between the Edgewood Graben System and the Woodbine Delta. Arbitrary reflection seismic profiles across the dome shows an approximately one square kilometer area where seismic reflectors are disrupted, incoherent, and flanked by coherent away-dipping reflectors. The base of the seismic incoherence occurs at approximately 1.3 seconds two-way time, this strong positive reflection indicating a soft to hard rock boundary characteristic of crater fill and relatively undisturbed dome-flanking country rock. Reflectors below the base of the disruption also exhibit doming. The “dome” maps seismically as a closed low, with west-northwest, northeast, and south-southeast synclinal spokes emanating from its perimeter. The presence of Pecan Gap Limestone material at the surface, exhumed from 1067 meters depth, together with the lack of coherent seismic reflectors within the dome, suggests that the dome formed by catastrophic pulverization and exhumation rather than plastic folding.

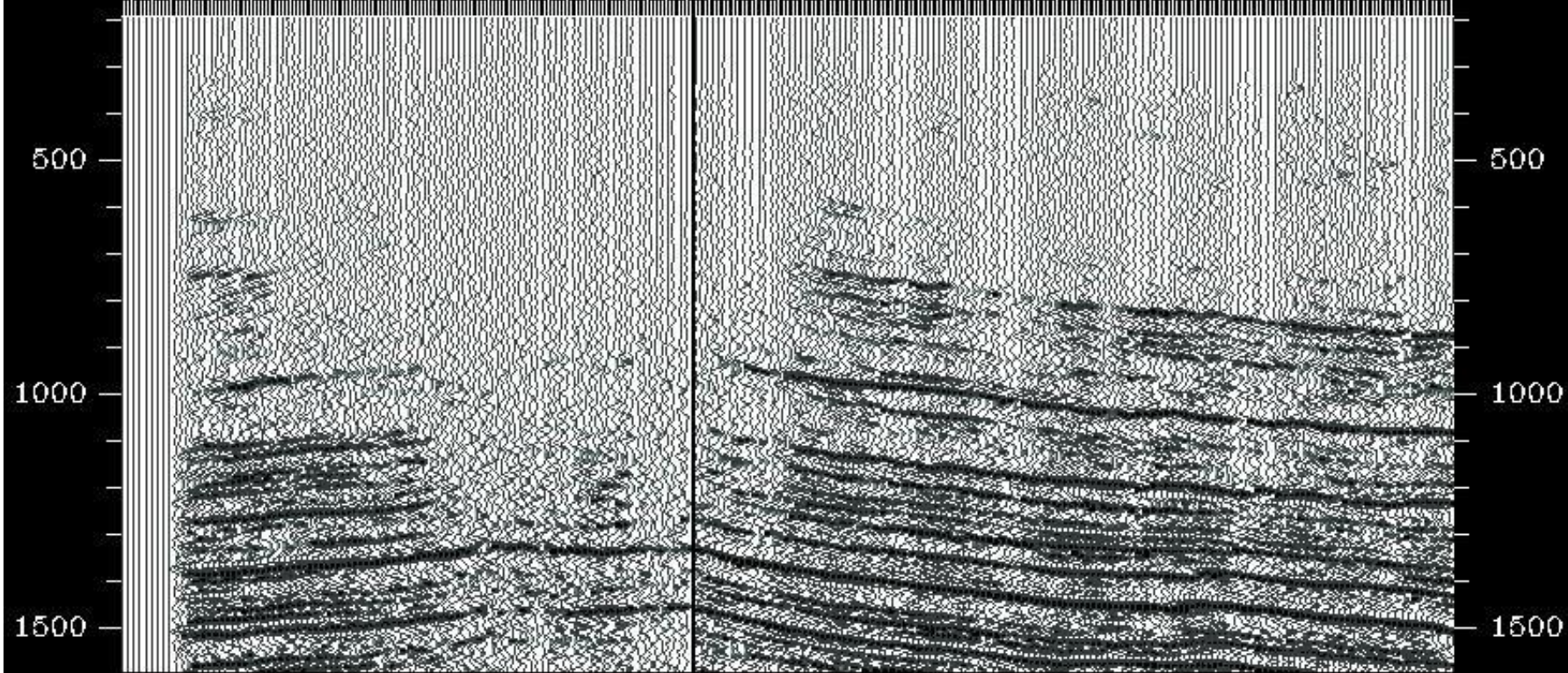


East Texas Oil and Gas Trends Map showing location of Marquez Dome Impact Structure.



Geologic map, Marquiz Dome, Leon County, Texas. The Pecan Gap Limestone has been exhumed 3500' from the subsurface by rebound from the impact. Geologic field excursion conducted at the dome October 2-3, 1999. Collected breccias, peculiar "burnt" rocks, Pecan Gap Limestone, and experienced overwhelming maneure/vomit gas stench 10/2/99 (PM) that did not persist and may represent either H₂S gas seep or nearby well or pipeline release or Emu maneure (?).

L1000 L1300 L1600 L1900 L2200 L2430 L2615 L2800 L2980 L3165 L3350 L3535
T6775 T6880 T6990 T7095 T7205 T7250 T7000 T6750 T6500 T6250 T6000 T5750



filt01.3dv

ArbitraryLine

←9034'→

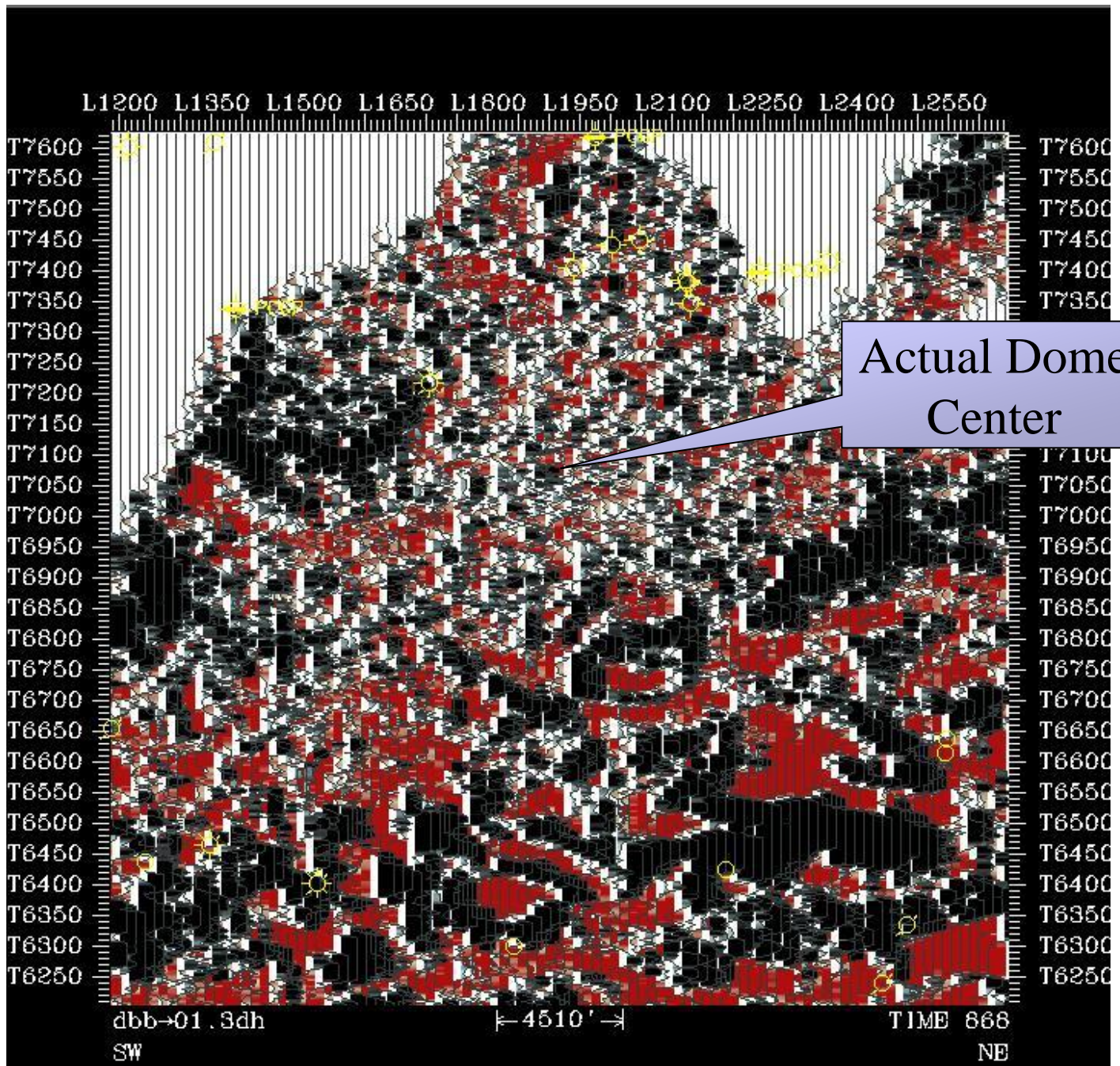
ArbitraryLine

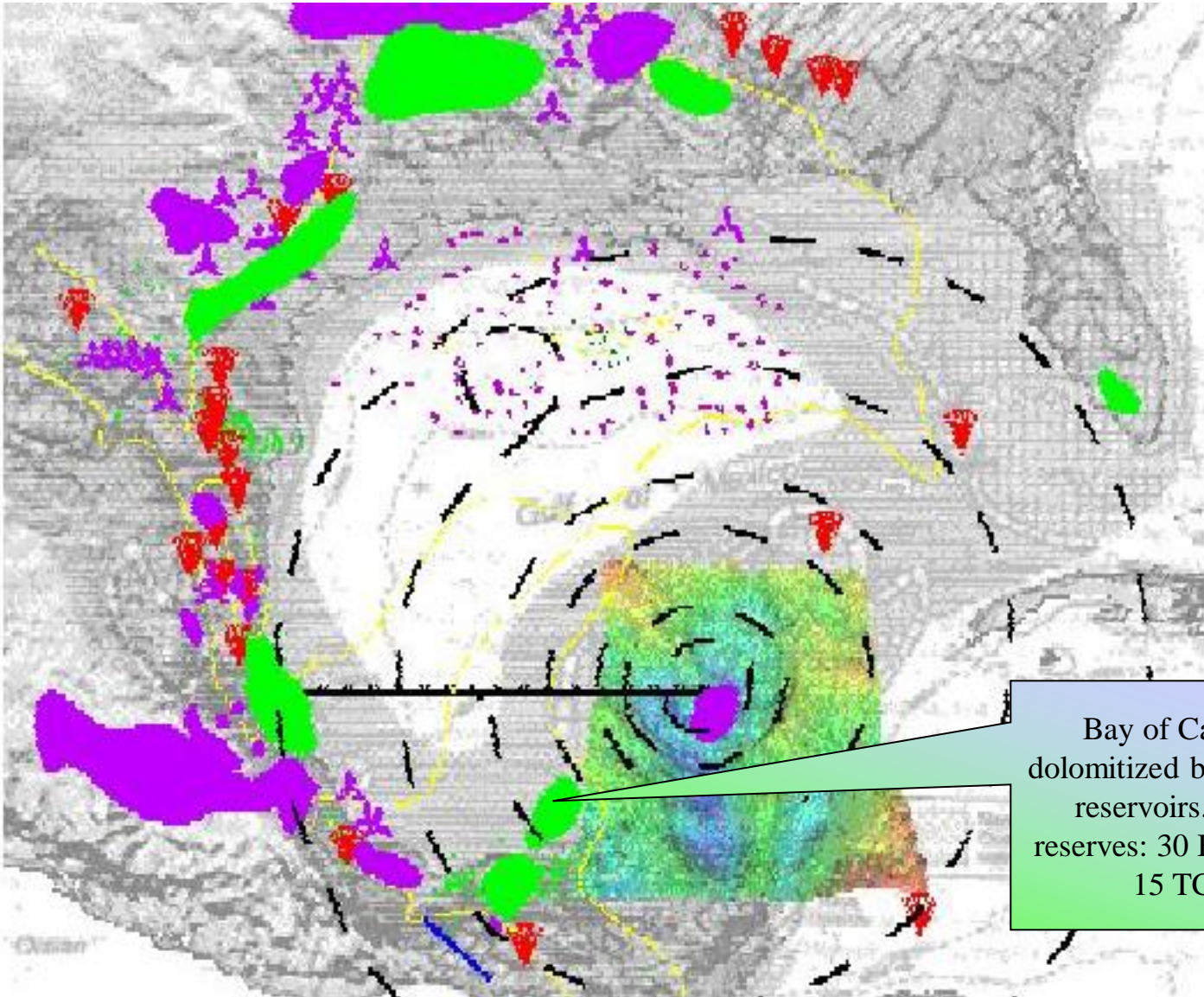
S 82 TPI 3.0 IPS

NW

82 TPI 3.0 IPS

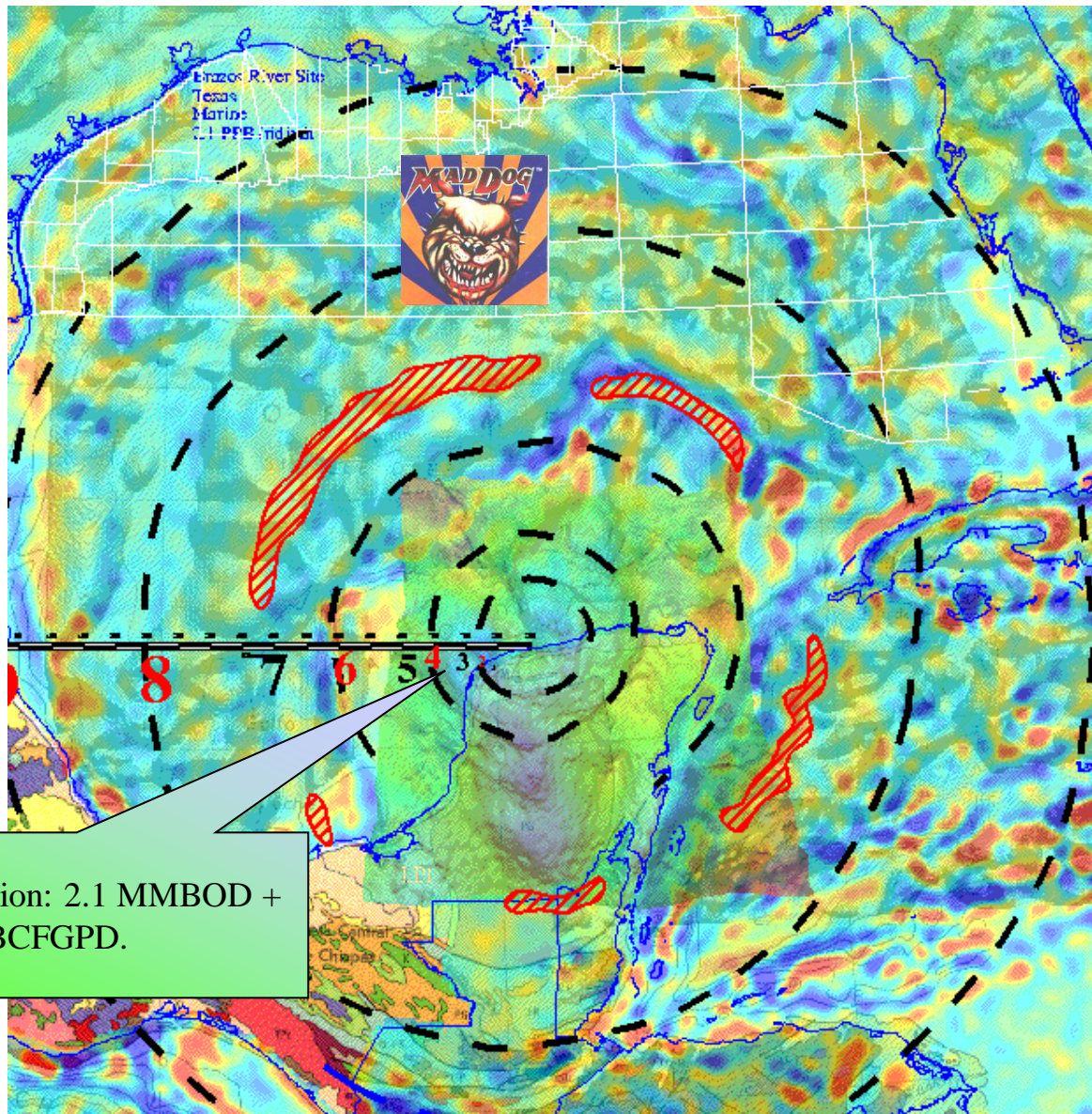
E





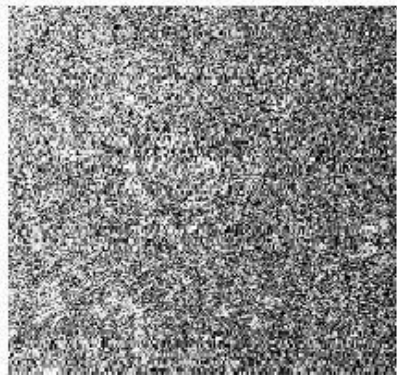
Bay of Campeche
dolomitized breccia ejecta
reservoirs. Primary
reserves: 30 BBbls Oil &
15 TCFG.

Chicxulub multiringed impact basin, Gulf of Mexico Lower Cretaceous paleogeography, volcanics, tsunami ejecta deposits, Chicxulub gravity.

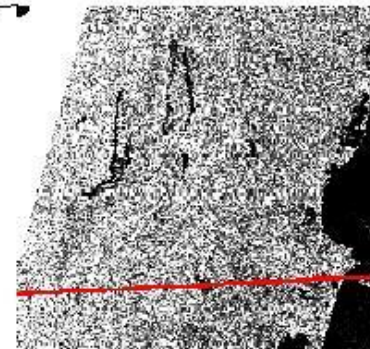
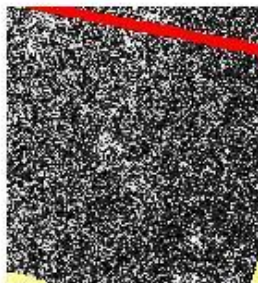
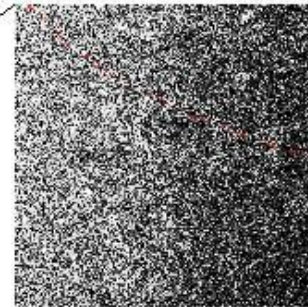


Current production: 2.1 MMBOD +
1.4 BCFGPD.

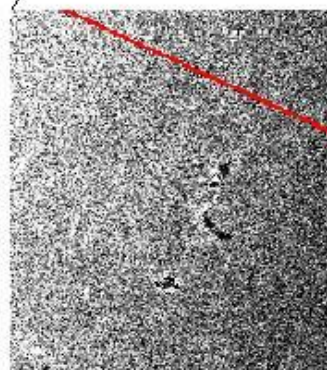
Chicxulub multiringed impact basin, Gulf of Mexico fused SR RTP magnetics, vertical derivative of gravity, onshore geologic map. With interpretation, including geometric.



Cenote rings are northwest-southeast, with foci to the ne.



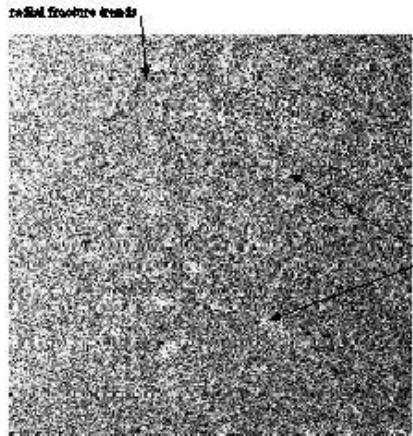
Onshore Belize, radial fracture sets.



Cenote rings, radial fractures and splashes with ring.



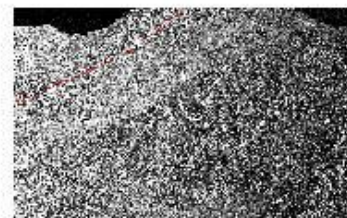
Onshore Honduras, concentric rings.



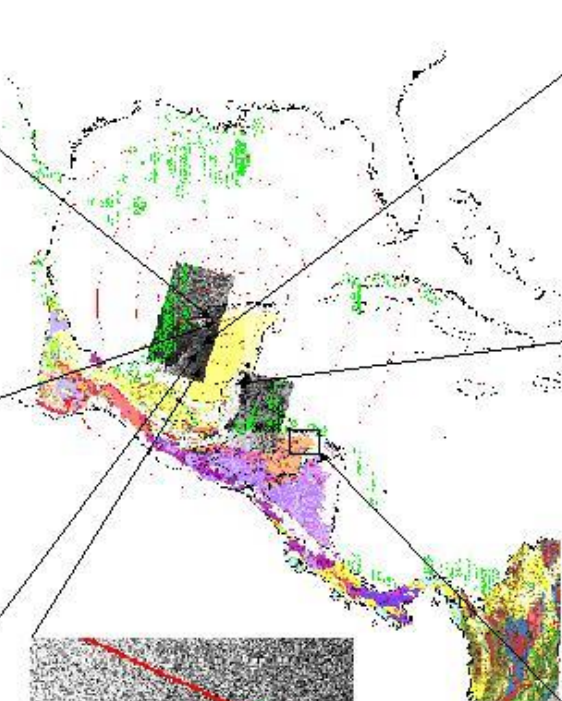
radial fracture tracks

cenote rings

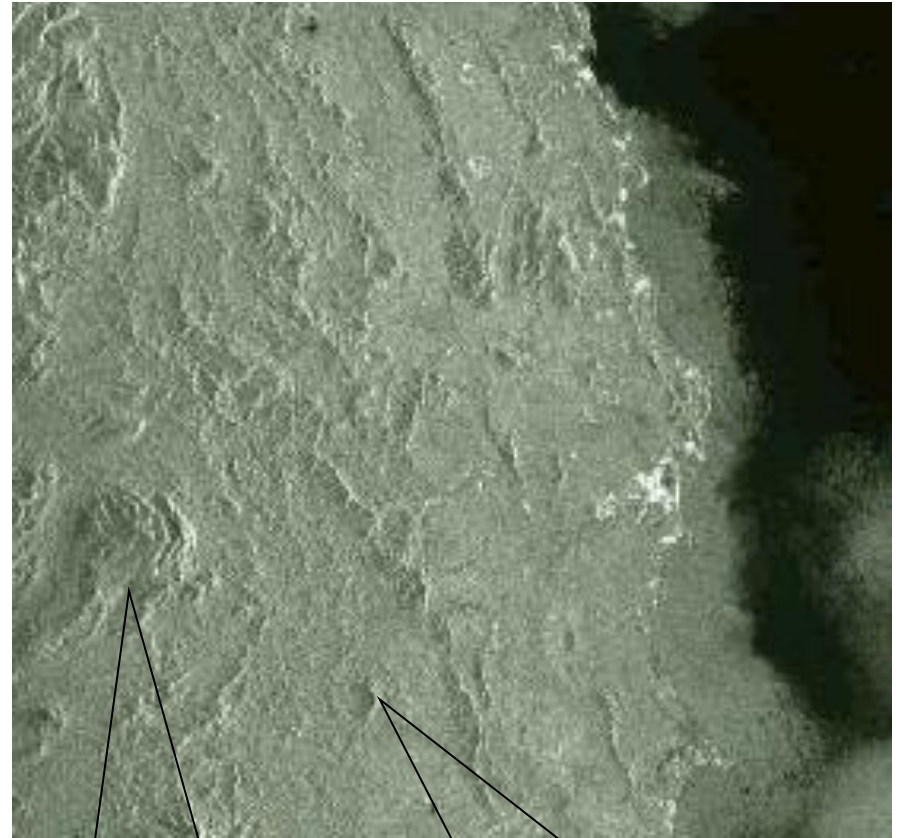
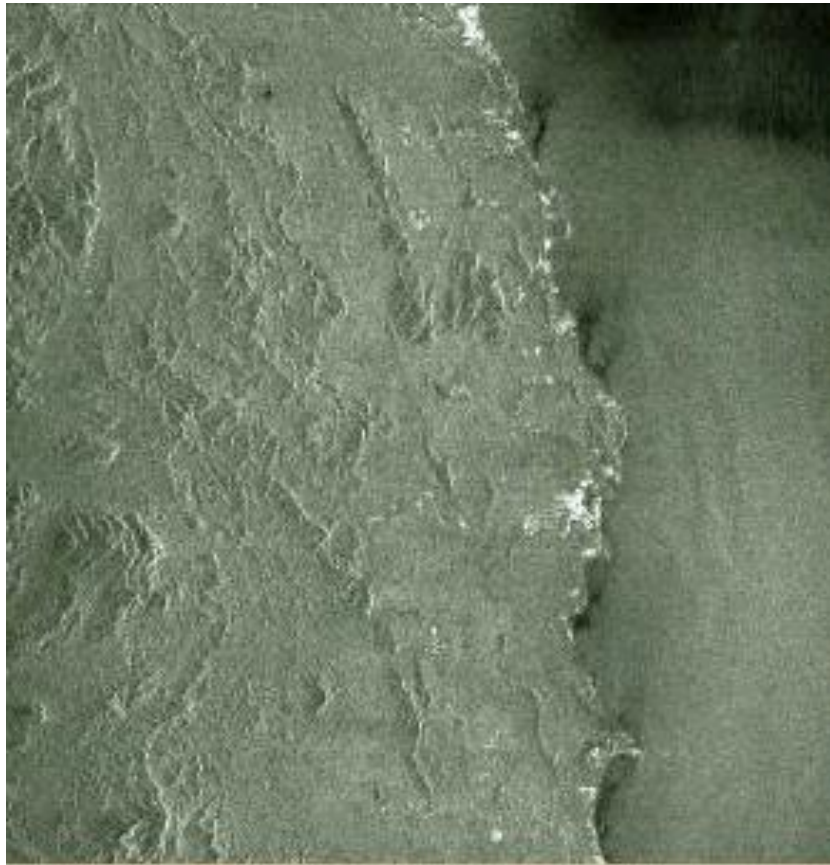
Cenote rings are northwest-southeast, with foci to the ne.



Onshore Honduras, concentric rings.



Unocal
SAR Central America
SAR GIS Crater Tectonics



Identified possible primary impact site for Bukit Paloh secondary.

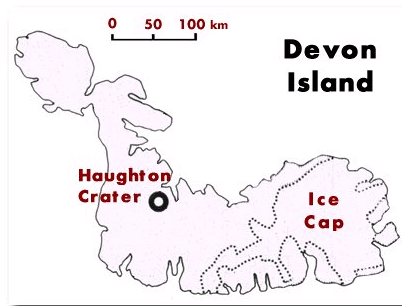
Circular depression at Bukit Paloh. Diameter 3.5 km.

Synthetic aperture radar, craters at Bukit Paloh, Terengganu-Pahang border. Multi-ringed feature in peninsular Malaysia (Tjia, H.D., *Warta Geologi*, v. 22, n. 4, Jul-Aug 1996, pp. 289-91, 1996). The eastern arcuate ridge is crowned by Bukit Paloh, which is 620 meters above sea level. This Bukit Paloh crater may represent a secondary impact resulting from a nearby primary impact which caused the early Quaternary volcanism in the Jabor area nearby (Tjia, 1996).



The Houghton meteorite impact crater, on Devon Island, Nunavut, in the Canadian high arctic, is 20 km in diameter and formed 23 million years ago. It is one of the highest-latitude terrestrial impact craters known on land ($75^{\circ}22'N$, $89^{\circ}41'W$). It lies in the "frost rubble zone" of the Earth, i.e., in a polar desert environment and is the only crater known to lie in such an environment.

A complex diversity of lithologies are exposed at Houghton, reflecting the fact that the impact event punched through the entire stack of Paleozoic sediments present at the time and excavated material from a depth of over 1.7 km, biting into the gneissic basement. Some shocked formations at Houghton have retained their integrity and are now exposed as tilted or downfaulted magablocks within the structure and at its periphery. However, particularly distinctive at Houghton is the crater's allochthonous impact breccia formation, a rubble deposit resulting from the launching, airborne mixing, fallback and weak rewelding of impact-shattered fragments derived from the entire stack of excavated rocks. Thus at Houghton, (shocked) basement crystalline rocks can be now found in abundance at the surface.

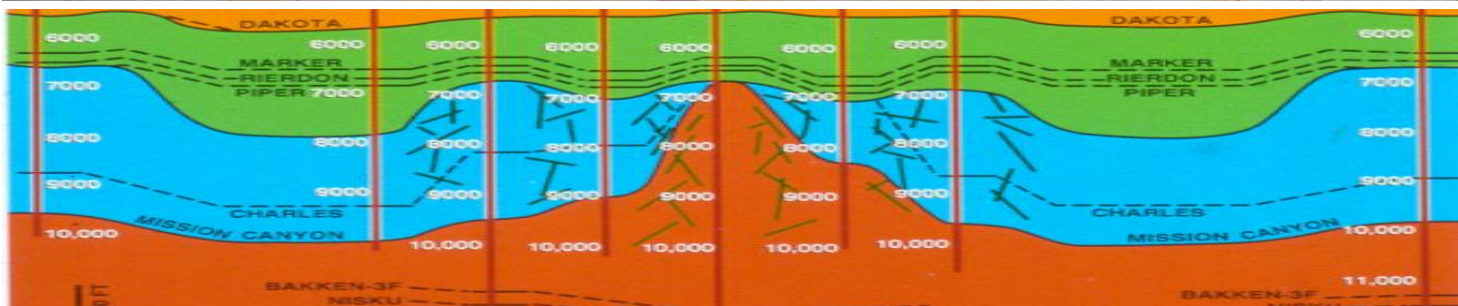
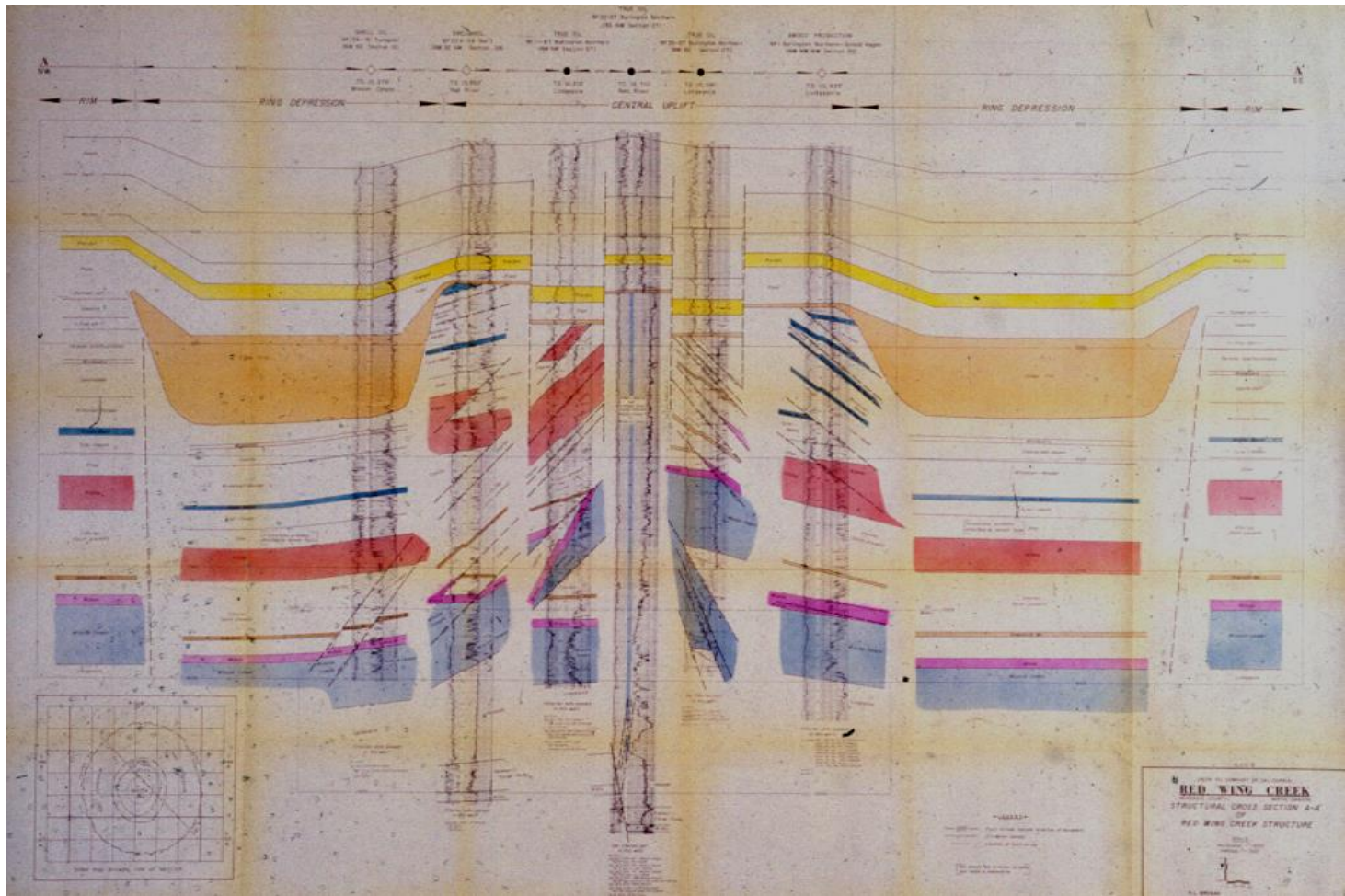


A map of Devon Island showing the location of the Houghton crater and the ice cap.

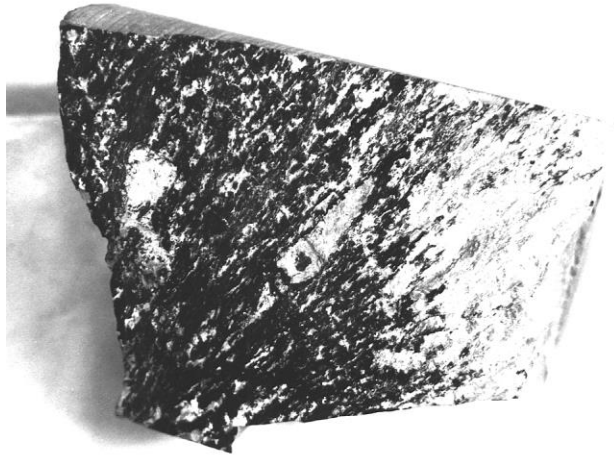
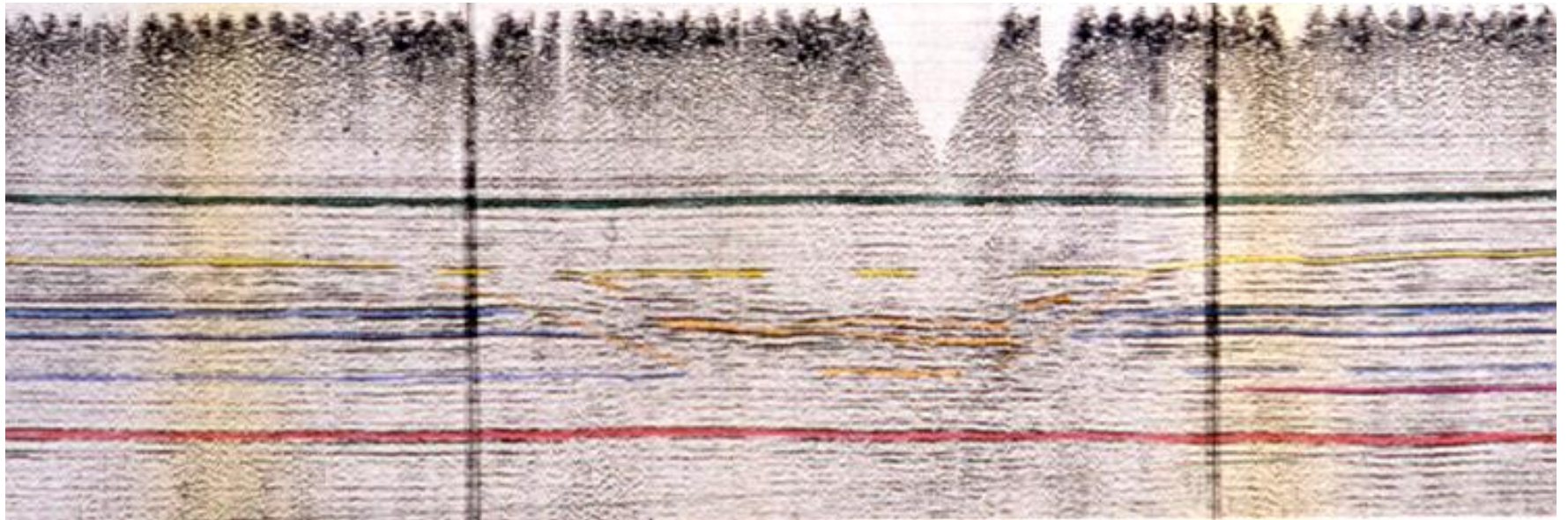


Radar image of the Haughton crater.

Airborne synthetic aperture radar image of Haughton Crater acquired in 1998 by the Intera STAR X-band radar system. The width of the scene is 36 km. Image courtesy Geological Survey of Canada. North is to the top and the crater is about 20 km wide. Note that the Haughton River breaches the crater rim to the northeast and flows into Thomas Lee Inlet.



Red Wing Creek Field log correlations (difficult!) and diagrammatic cross sections.

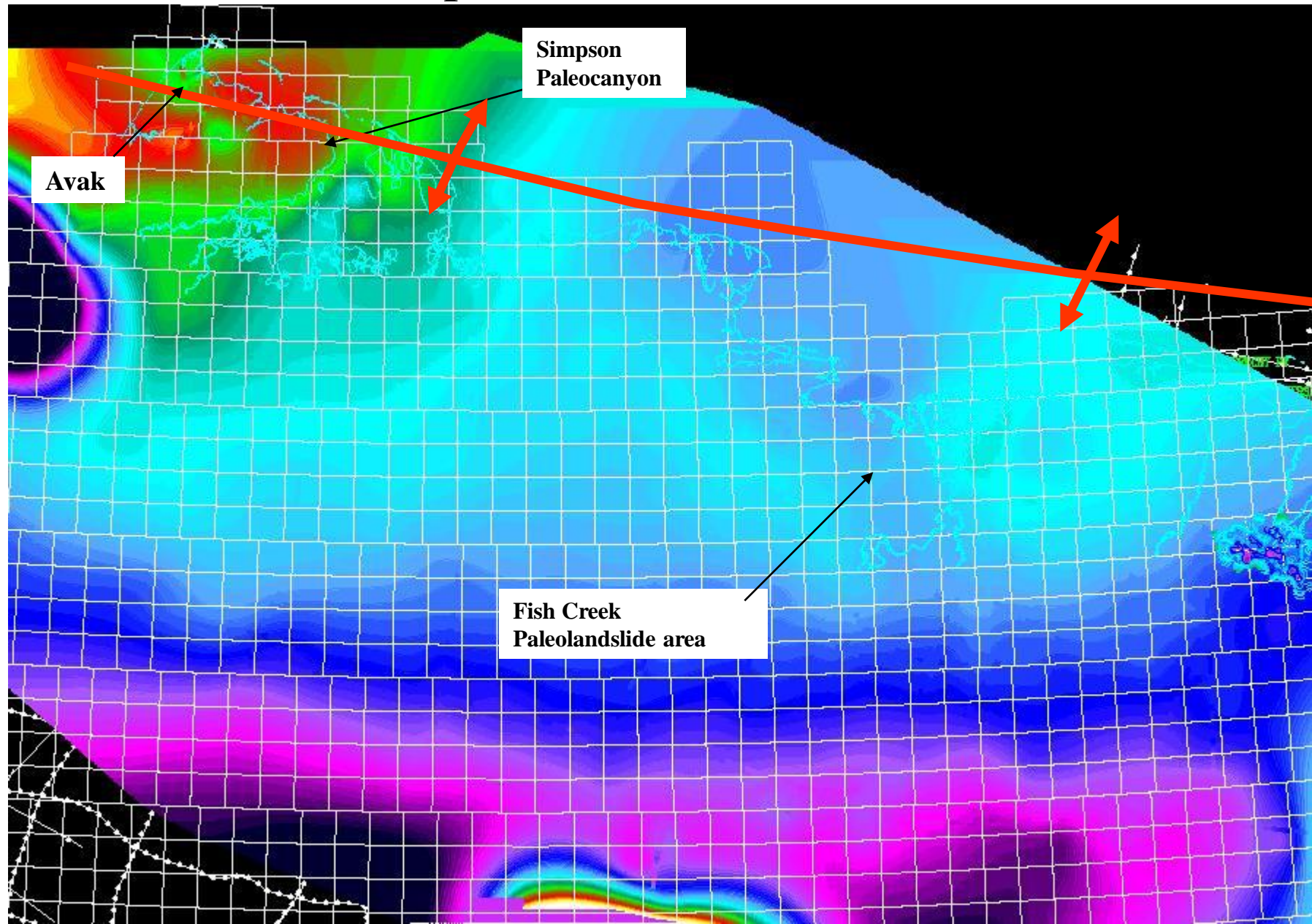


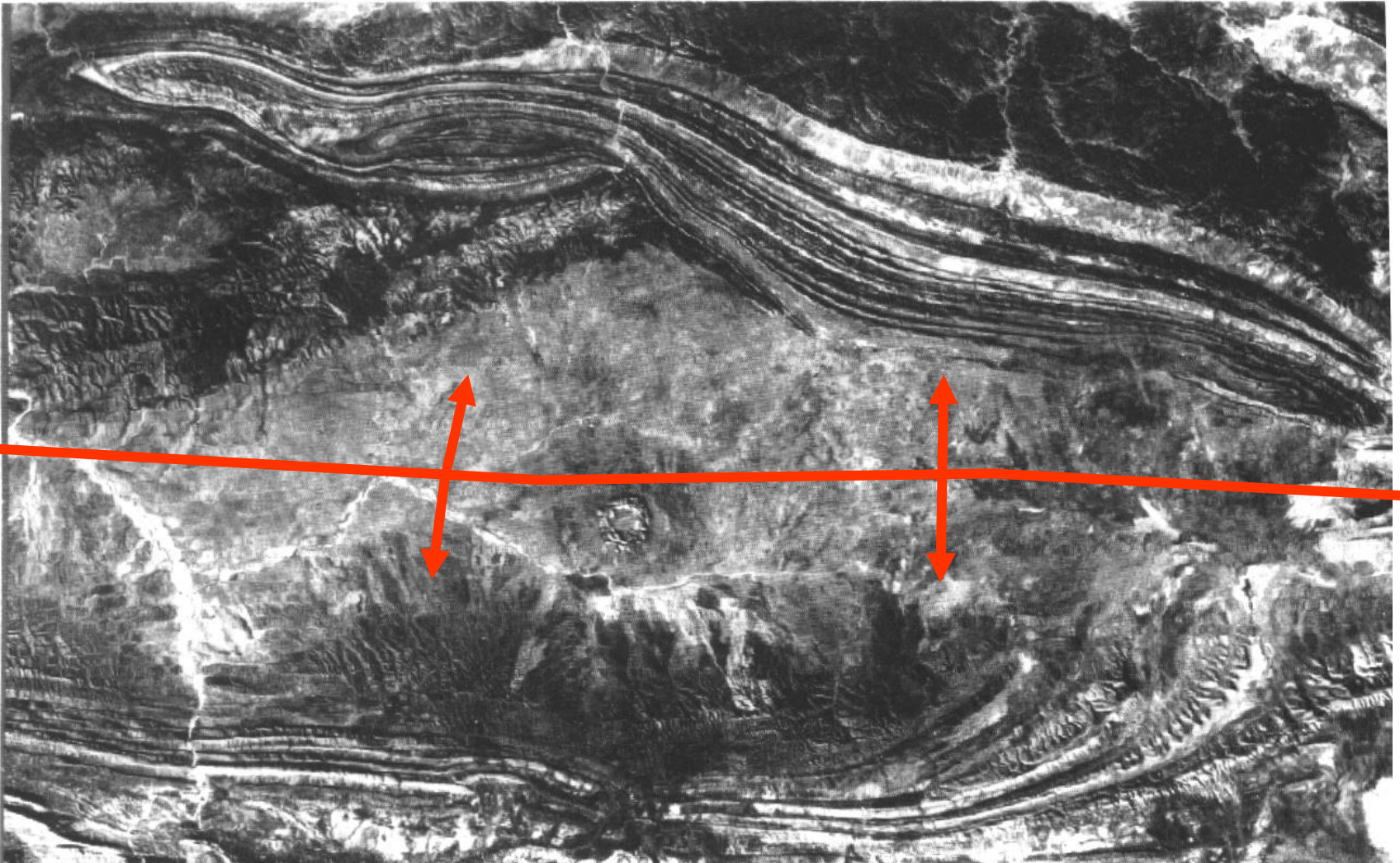
Red Wing Creek Field, McKenzie County, North Dakota. North-South seismic line showing disturbance. Bottom left: Fragment of large shatter cone stained with residual oil, 7375', True #13-27, and small shattercones from 7374.5, right.

Avak Structure, Arctic Alaska

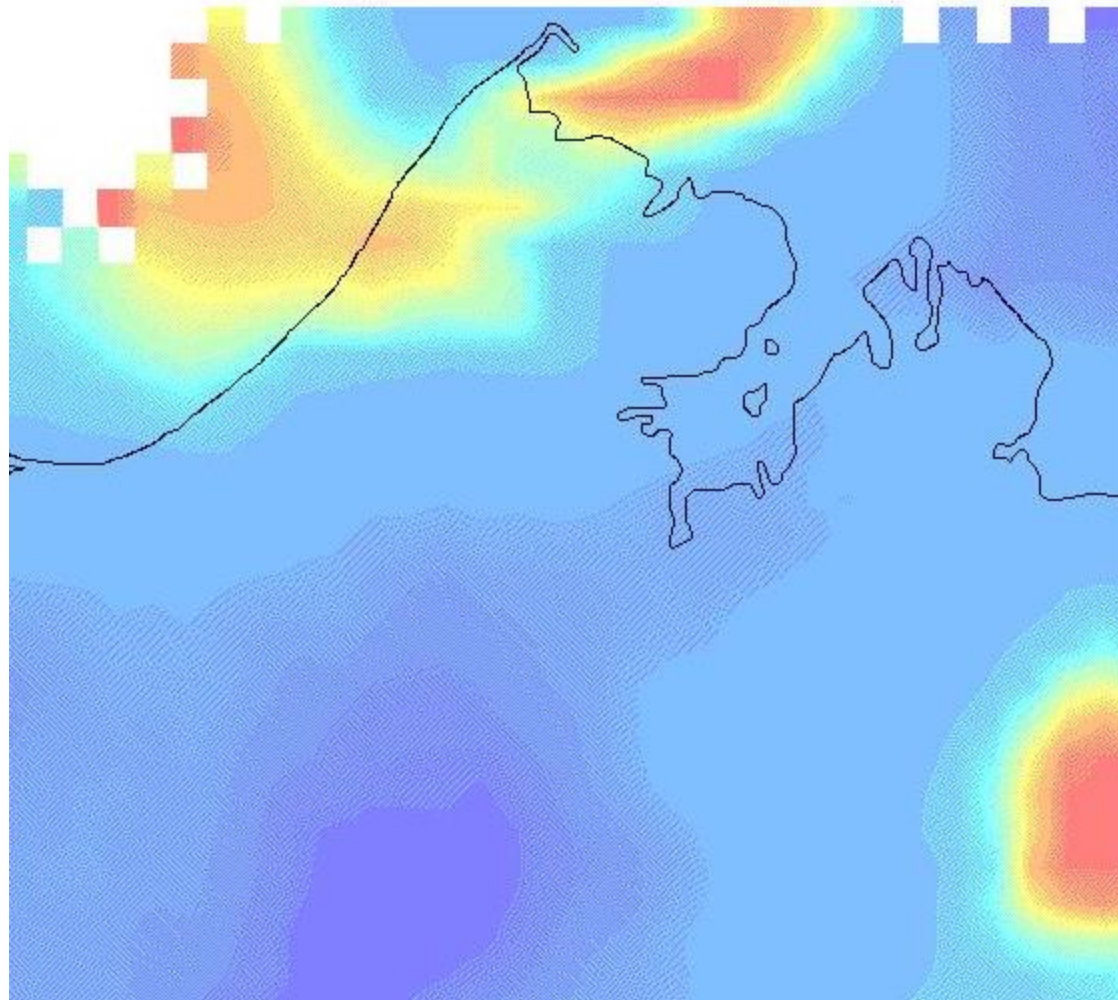
- Age: Late Cretaceous to Tertiary marine shelf or coastal plain between 95 and 3 Ma.
- Dimensions: 8 km diameter x 1 km deep; central uplift 4 km diameter with L. Cret. Rocks uplifted 500 m.
- Reserves: 37 BCFG from **updip pinchout traps in Jurassic sandstones against the outer walls of the crater.**
- Regional Setting: Avak sits atop the 150-180 km x 100 km wide Barrow high.

Avak Top ICS (PBU) Seismic TWT

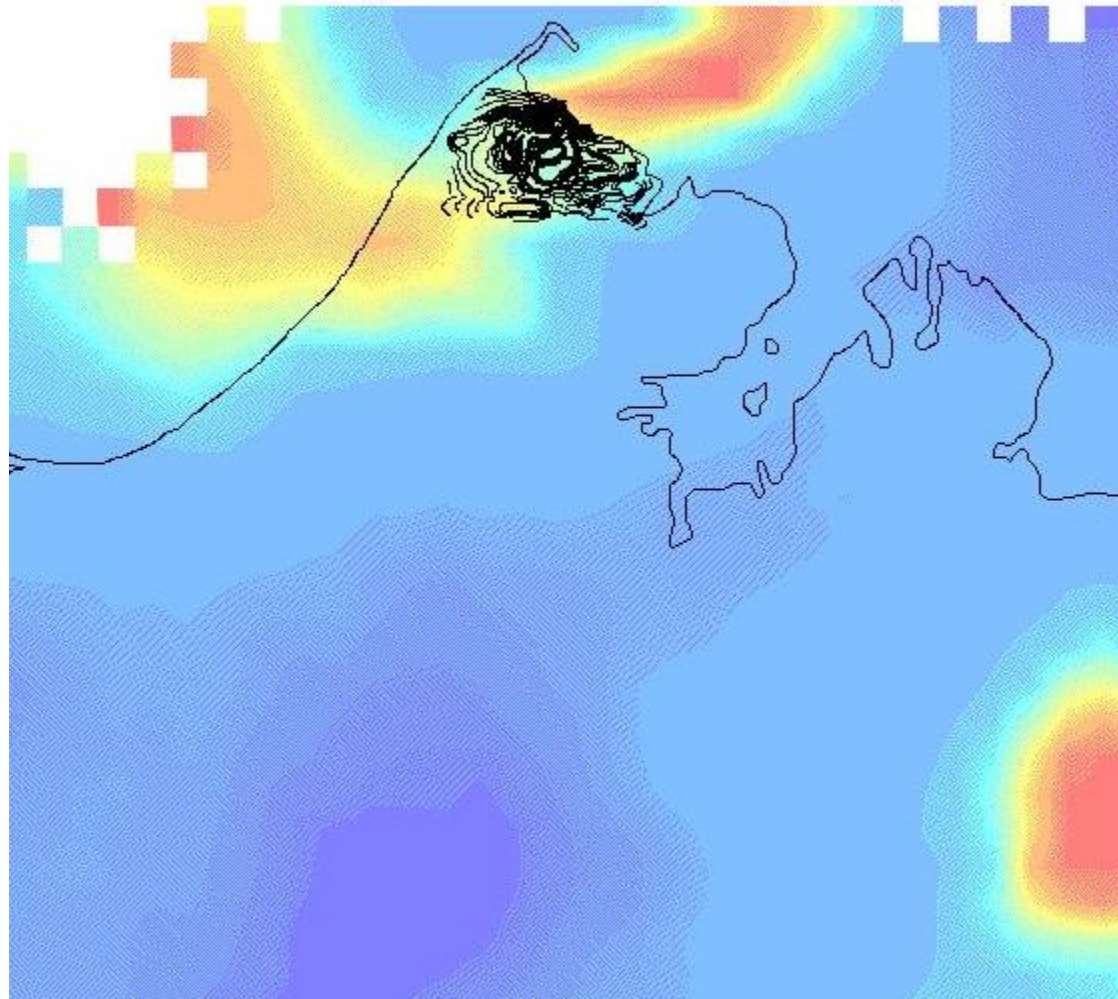




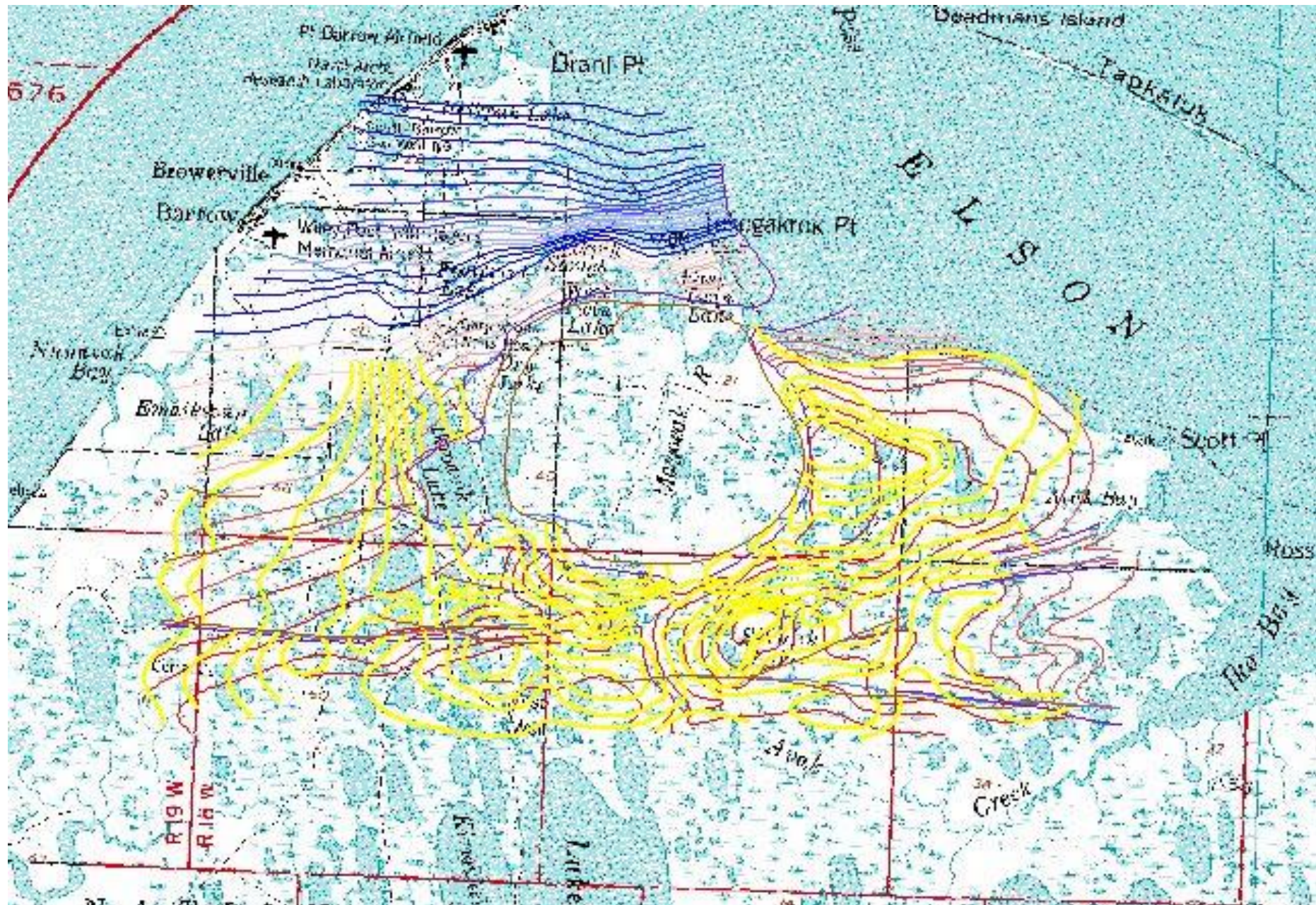
Analogue for Avak is the Grosses Bluff complex annular structure in central Australia, crater formed during the Late Jurassic. From Tingate, P.R., et al, 1996, in AGSO Journal of Australian Geology & Geophysics, 16 (4), 529-552. At Grosses Bluff, Tingate theorized that the dome beneath the impact structure was caused by impact rebound.



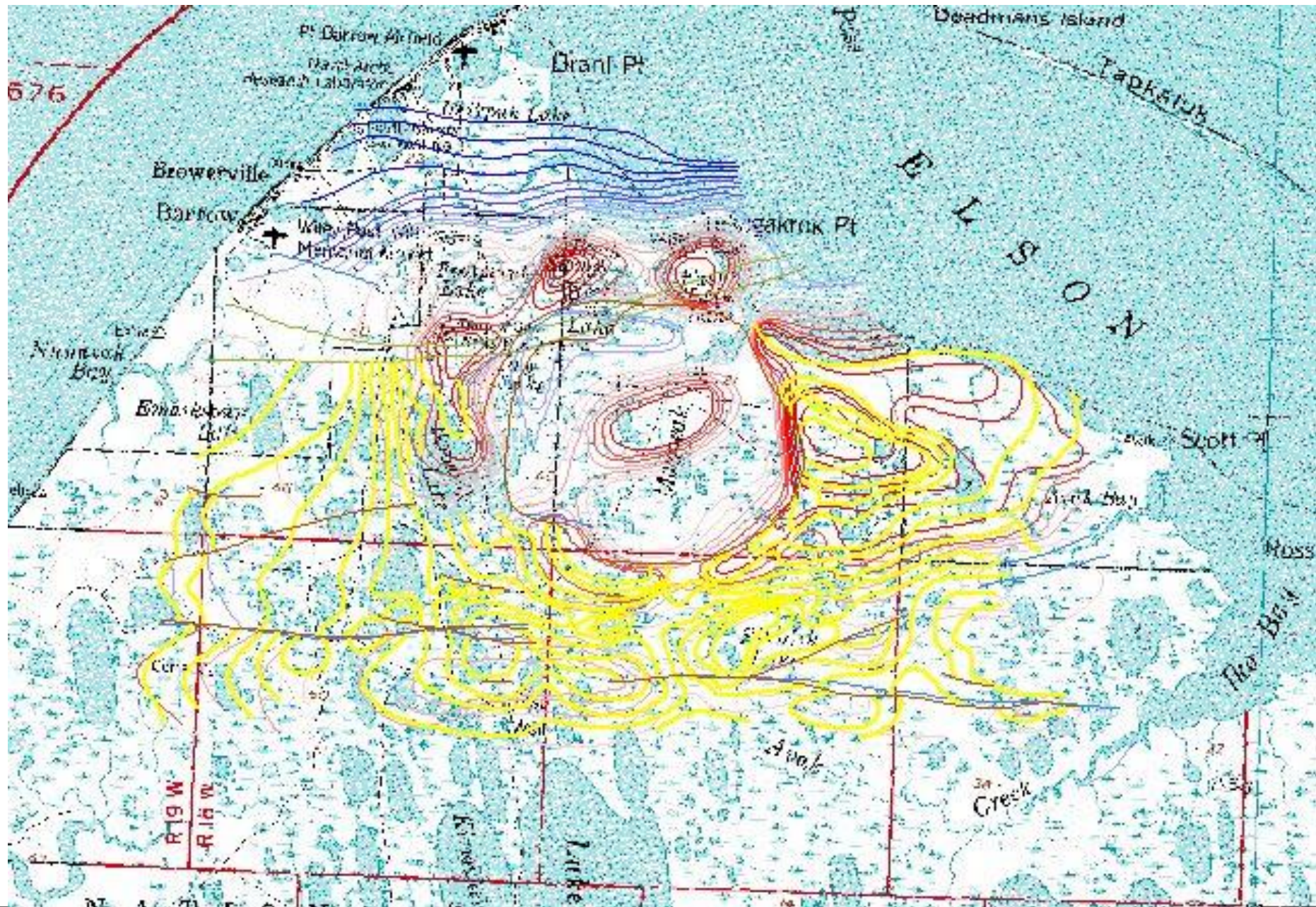
Avak. USGS 5K Isostatic Gravity.



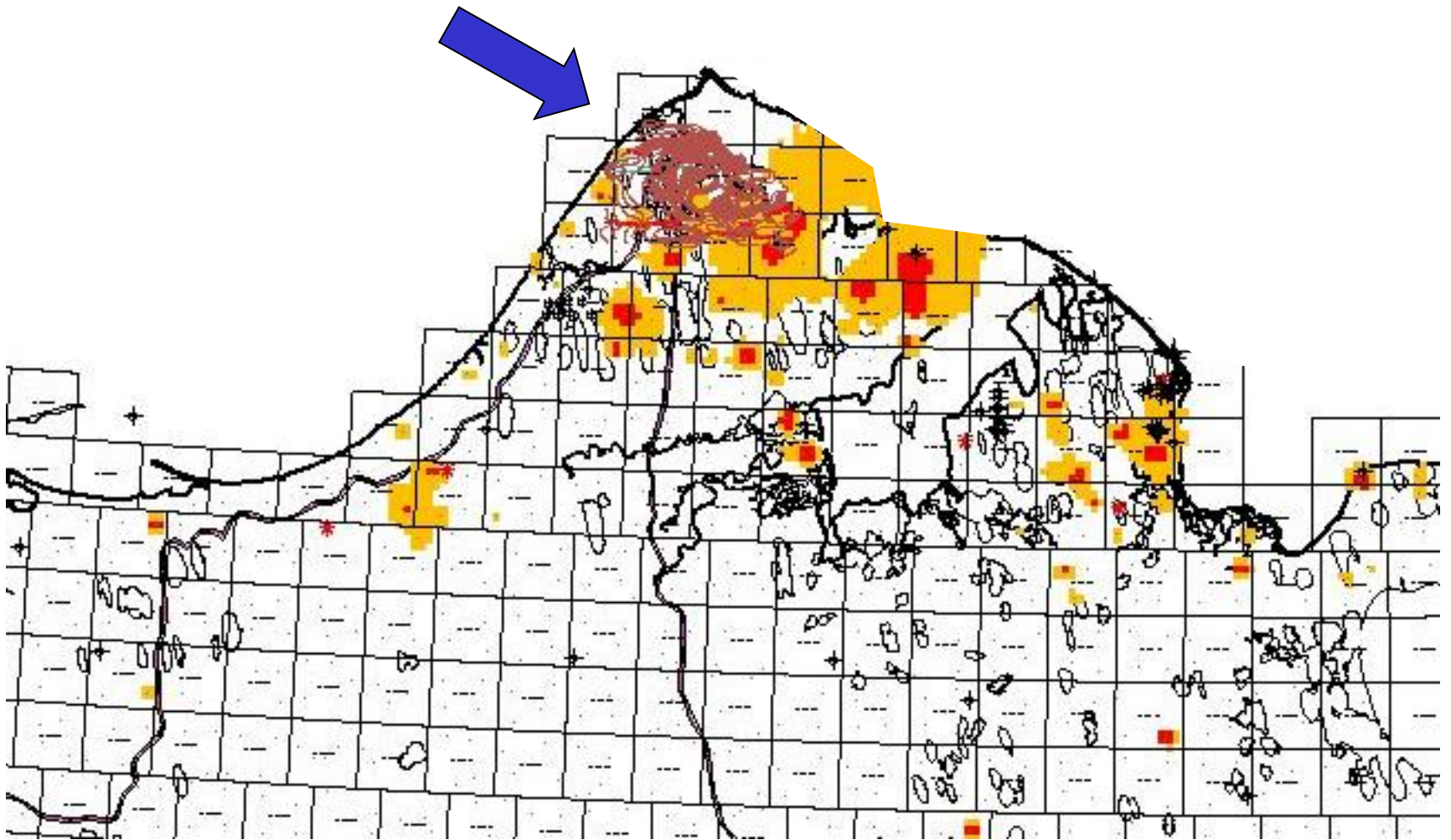
Avak. USGS 5K Isostatic Gravity and Top Argillite Structure.



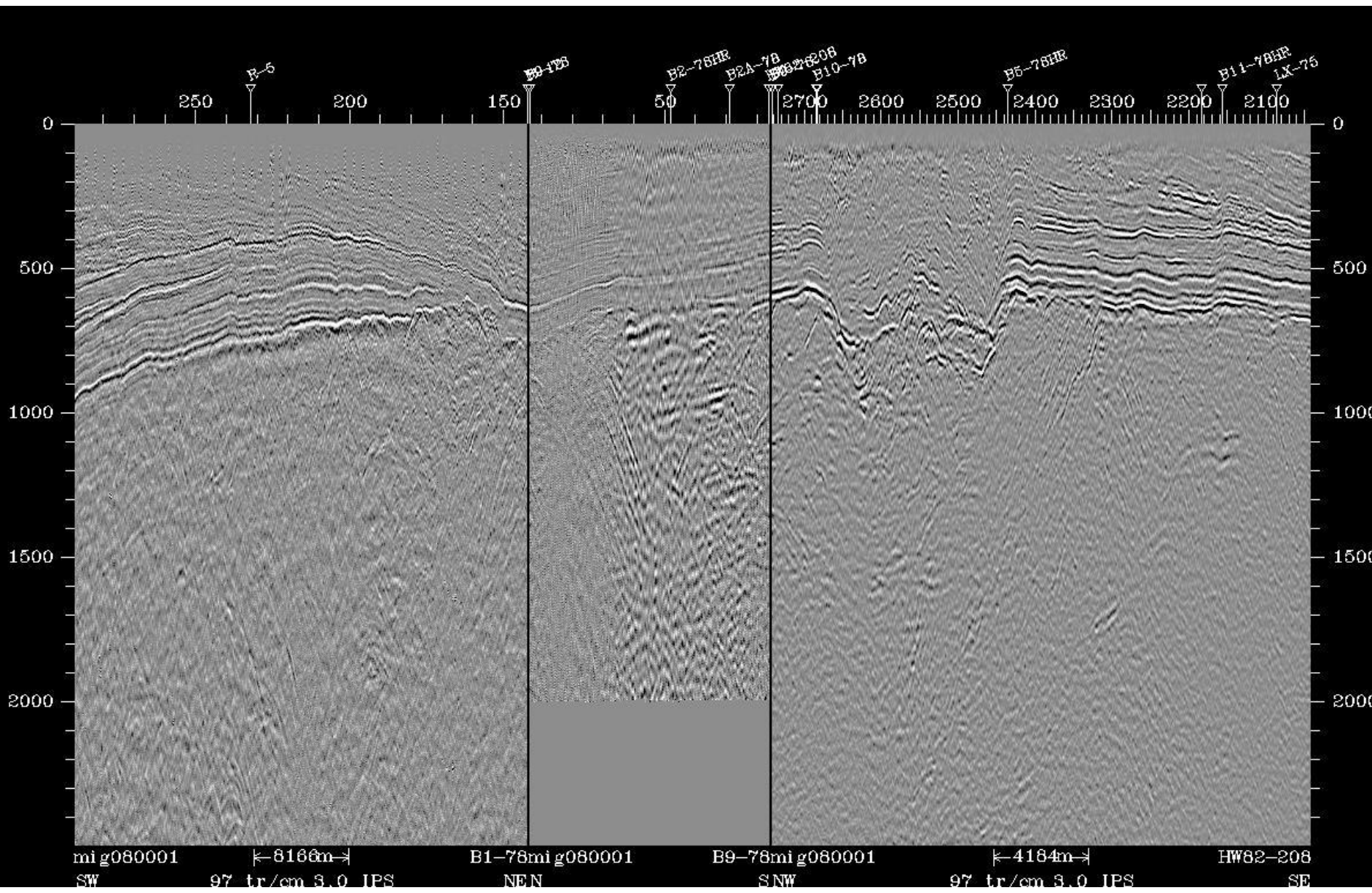
Avak Impact structure, Barrow, North Slope, Alaska. Top of Gamma Ray Shale Marker structure and top Barrow Sandstone (yellow), on 1:250,000 topographic map.



Avak Impact structure, Barrow, North Slope, Alaska. Top of Argillite and top Barrow Sandstone (yellow), on 1:250,000 topographic map.



Avak Structure. Nure Nickel concentrations greater than 30,000 ppm in surface sediments, with Top Argillite Seismic Structure and wells. If the nickel is reflective of nickel-iron meteoritic material responsible for the impact, then the trajectory was from the northwest.



mi g080001
SW 97 tr/cm 3.0 IPS

B1-78mi g080001
NEN

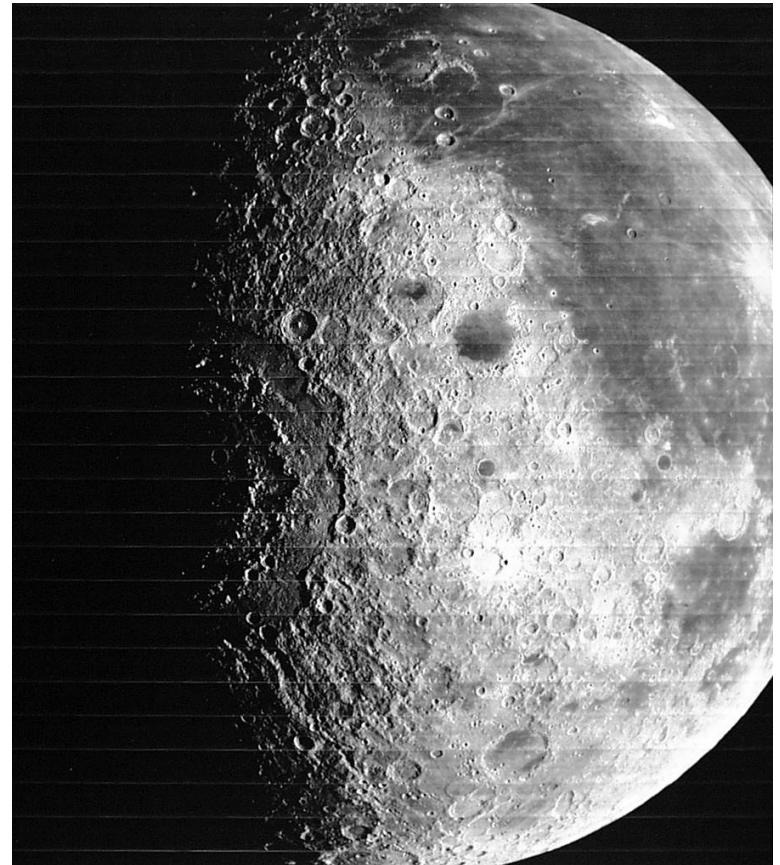
B9-78mi g080001
SNW

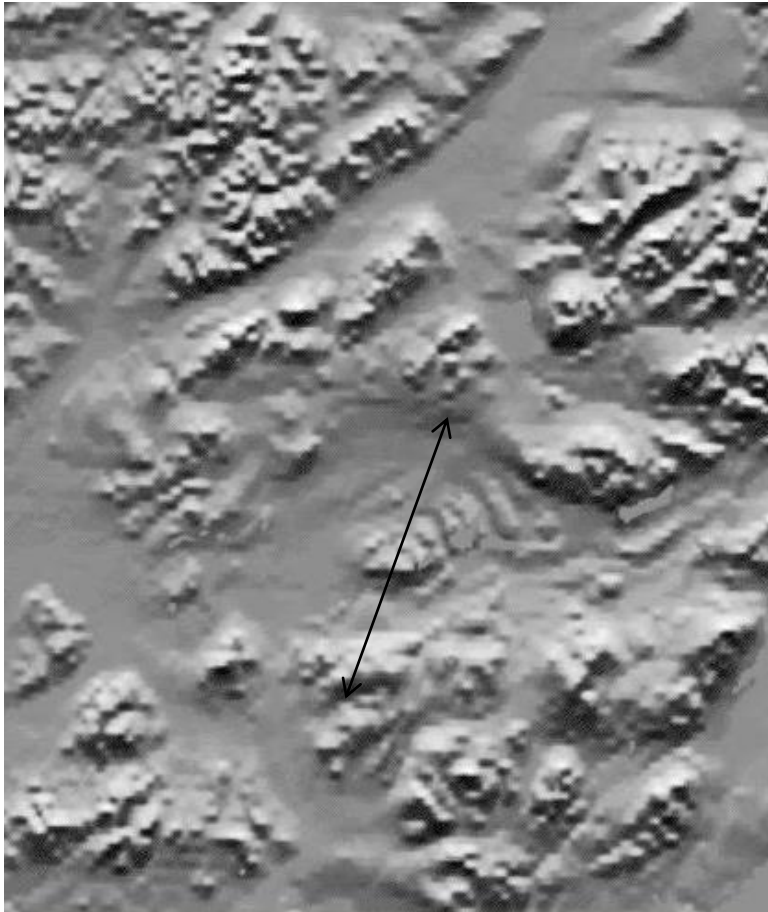
4184m
97 tr/cm 3.0 IPS

HW82-208
SE

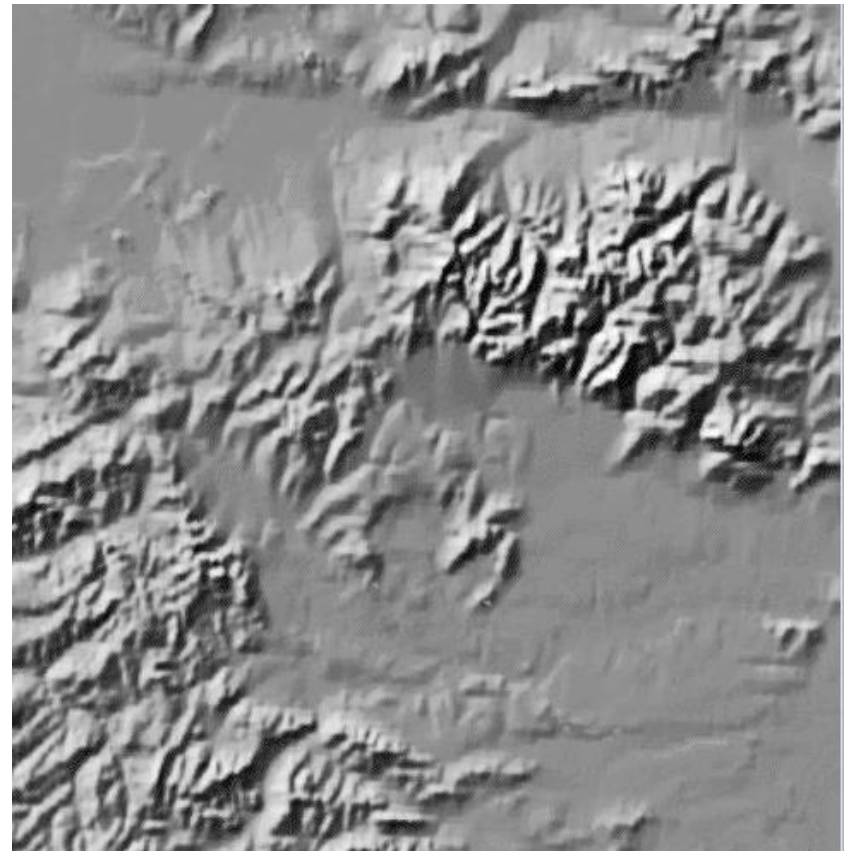
PROBABLE & POSSIBLE - EARTH

- Alaska
- Lower 48
- Southeast Asia
- South America
- World





Arrow is 33.3 km diameter. Slight magnetics central and encircling maxima. Volcanic?

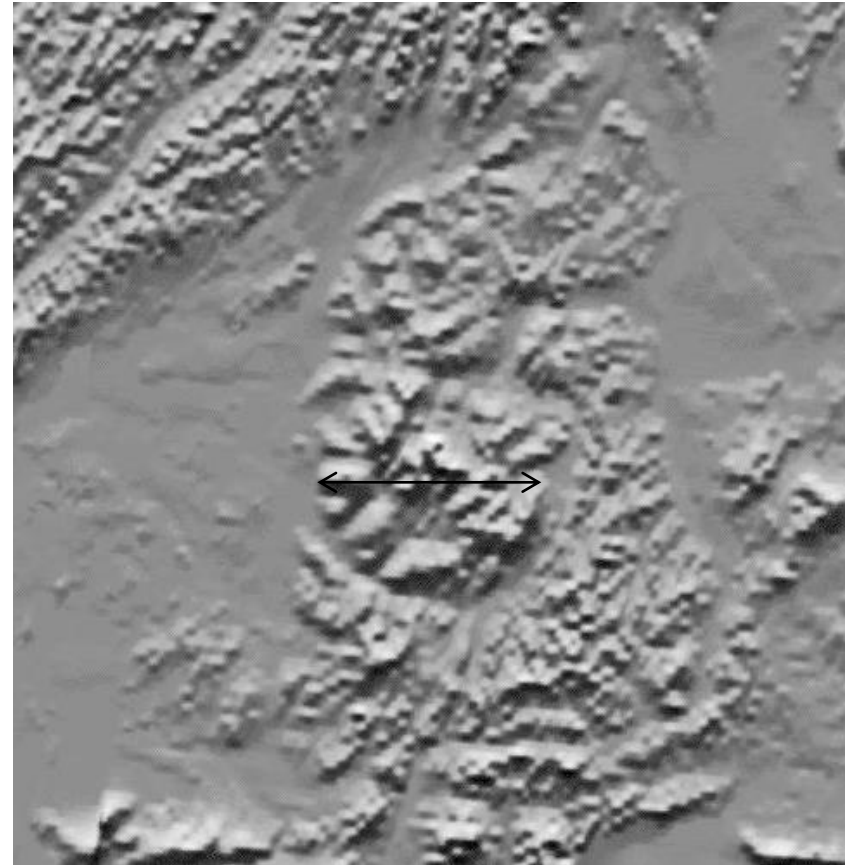


Inner dimple diameter is 11.4 kilometers.
Magnetics minima in center.

Alaska shaded relief DEM. Possible impact craters.

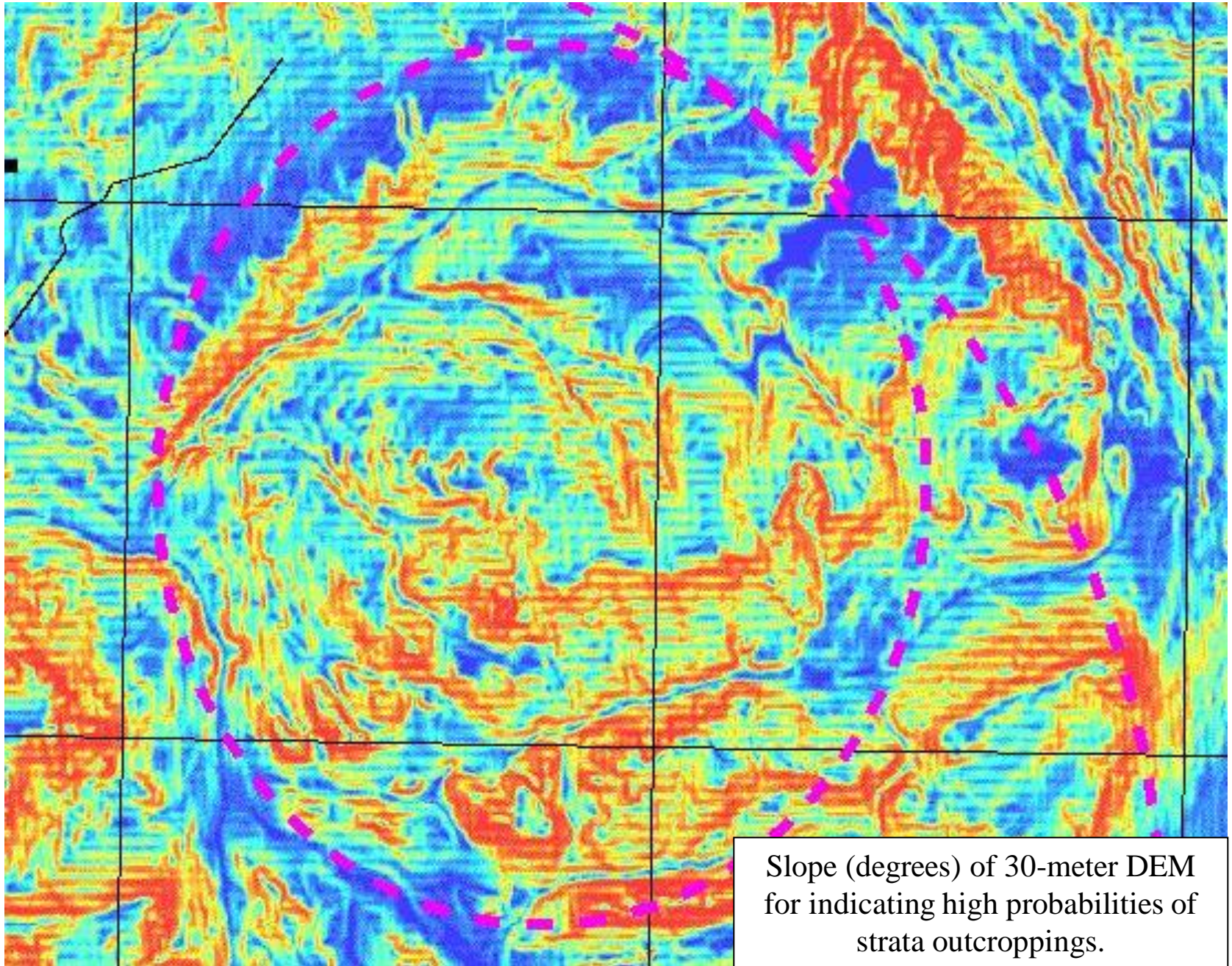


Approximately 70 km diameter from northwest to southeast rims.

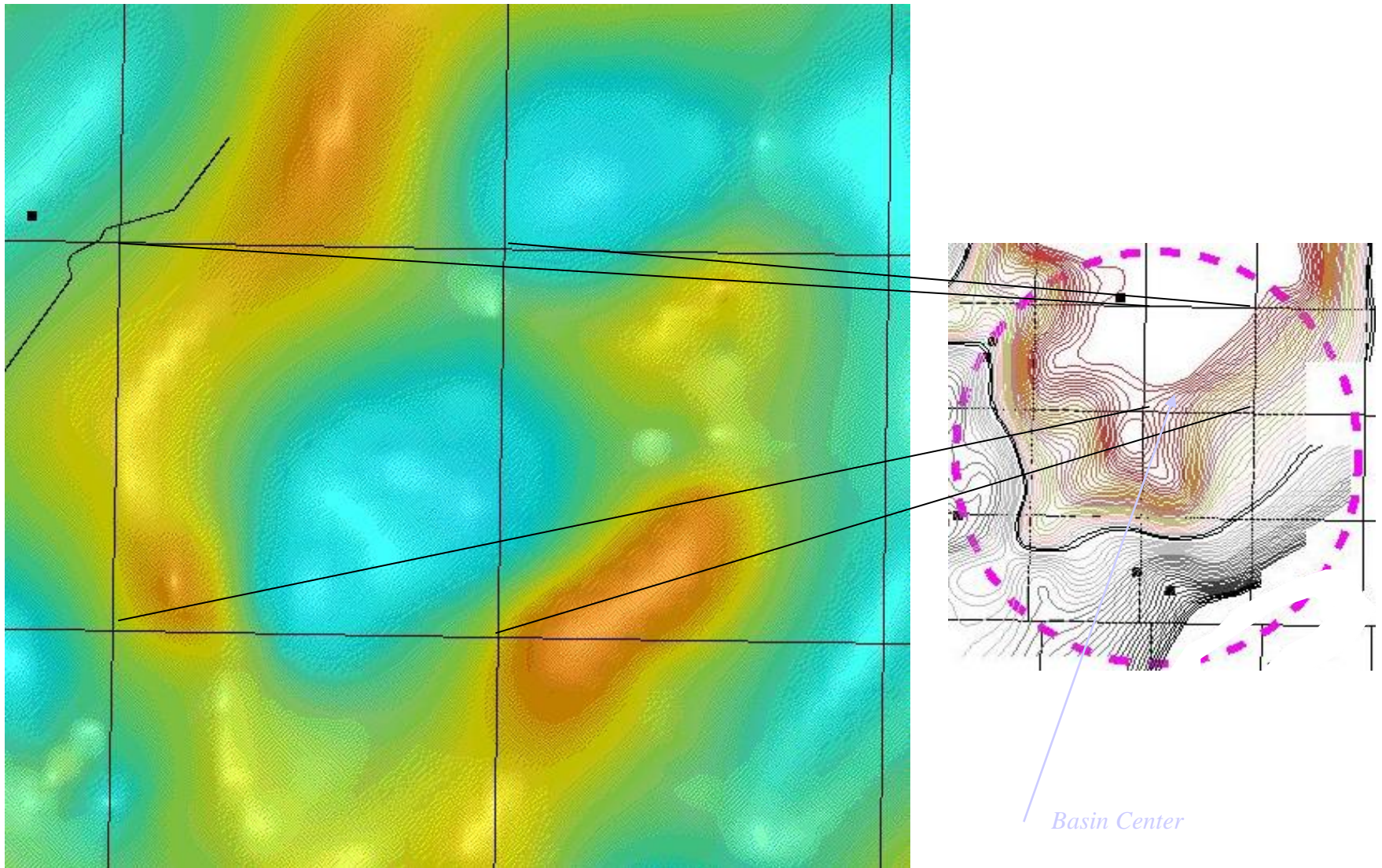


Approximately 29 km diameter west to east diameter (arrow). Magnetics maxima coincident with topographic anomaly. Volcanic?

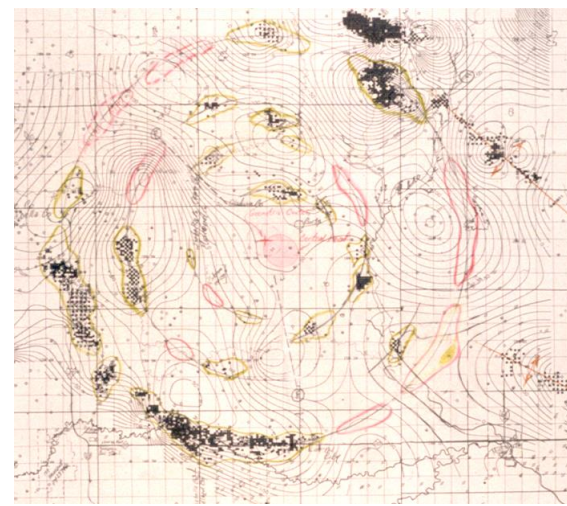
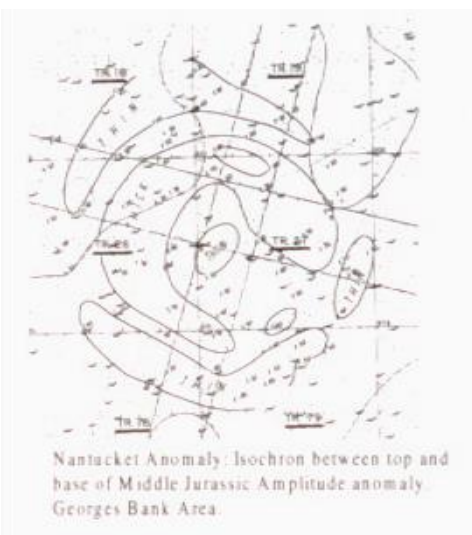
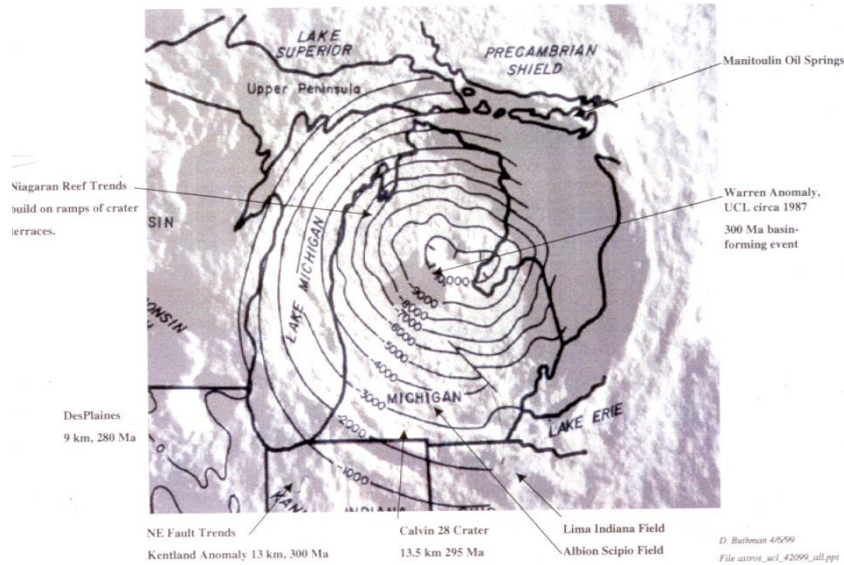
Alaska shaded relief DEM. Possible impact craters.



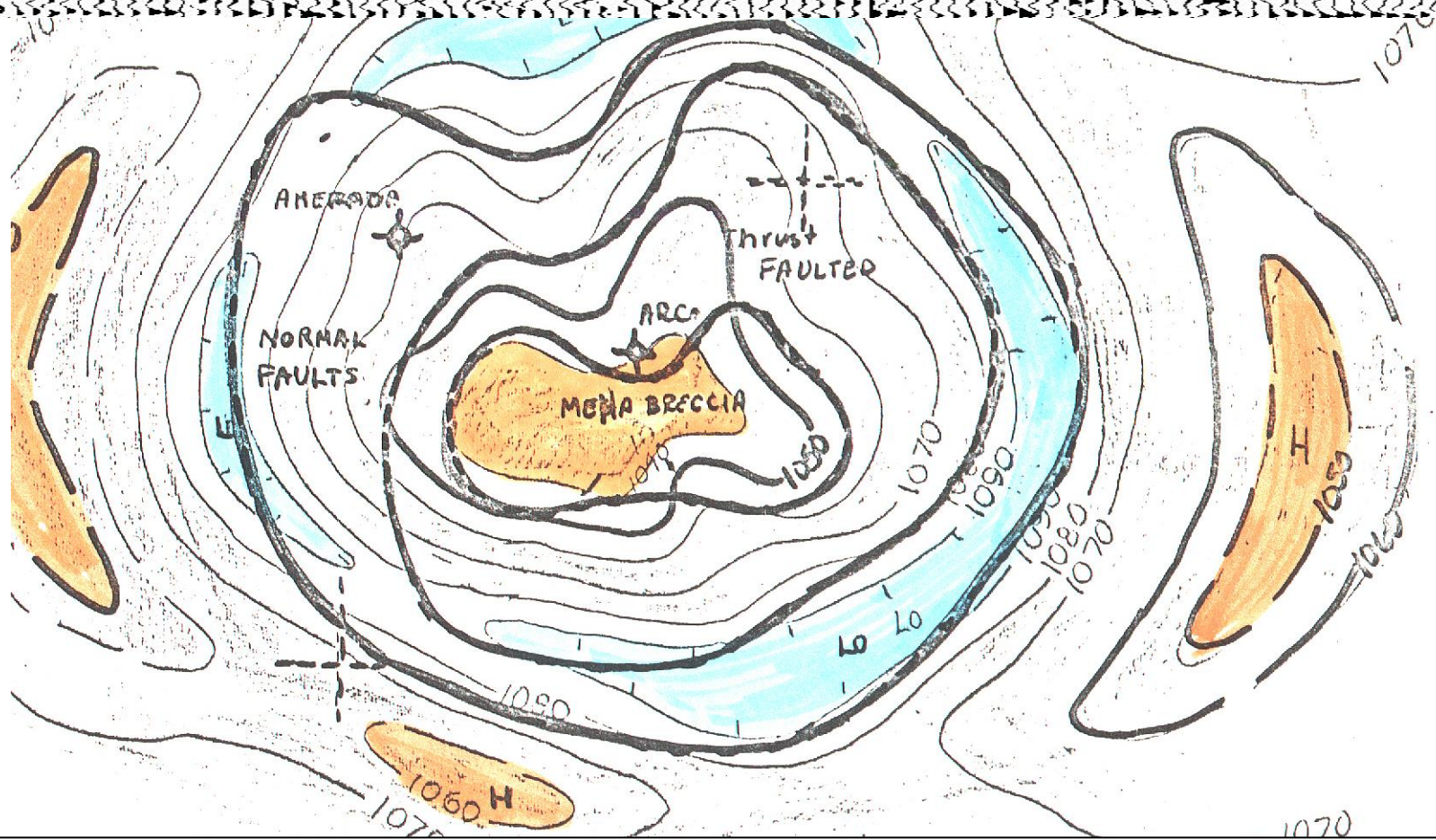
Slope (degrees) of 30-meter DEM
for indicating high probabilities of
strata outcroppings.



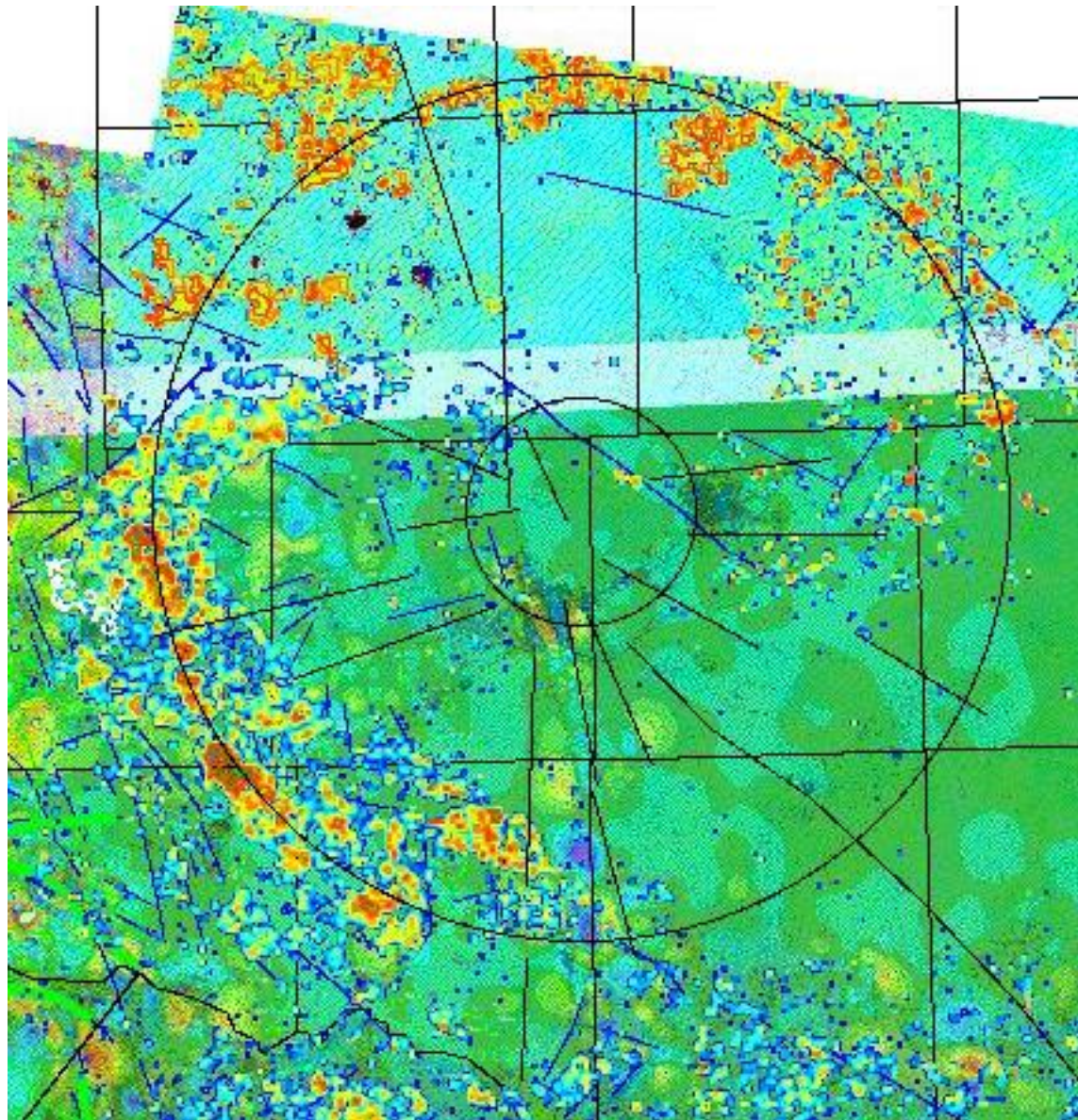
Potential buried impact crater, Alaska. Left: gravity, right: base of crater excavation seismic time horizon.



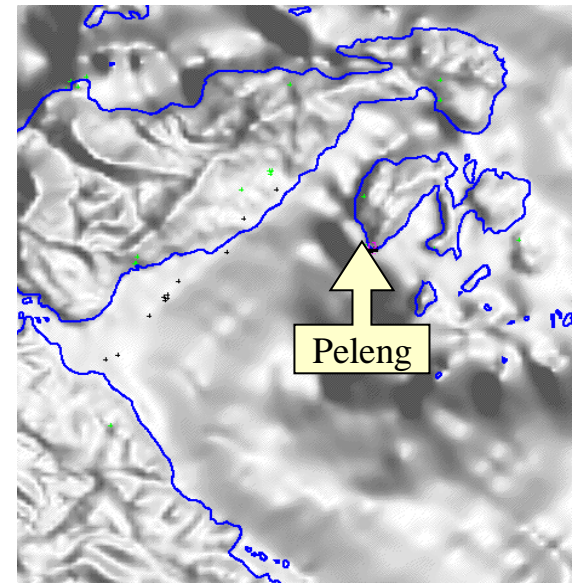
Three possible impact craters based on morphology, seismic horizon mapping, and oil and gas field trend distributions.



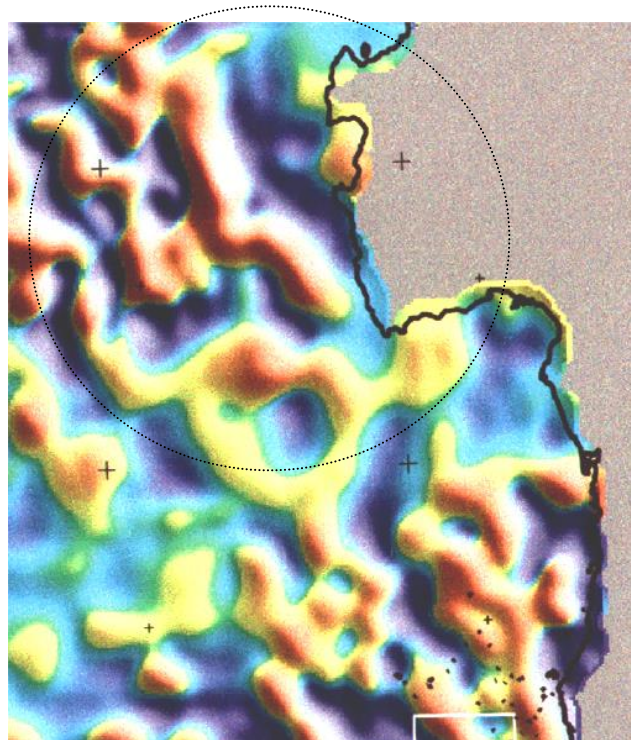
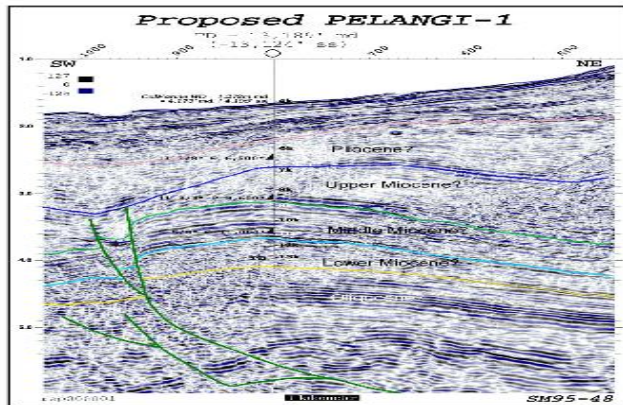
Chimney Prospect, Garfield County, Montana, structure map “drawn from memory” (P. Lindquest). Structure has 250’ of relief on the central peak and is 2 miles in diameter. Arco 1-BNRR encountered oil shows at TD in tight sedimentary rock. Seismic line cutout 24-fold CDP from Plawman & Hager, Arco, in Bally, 1983.



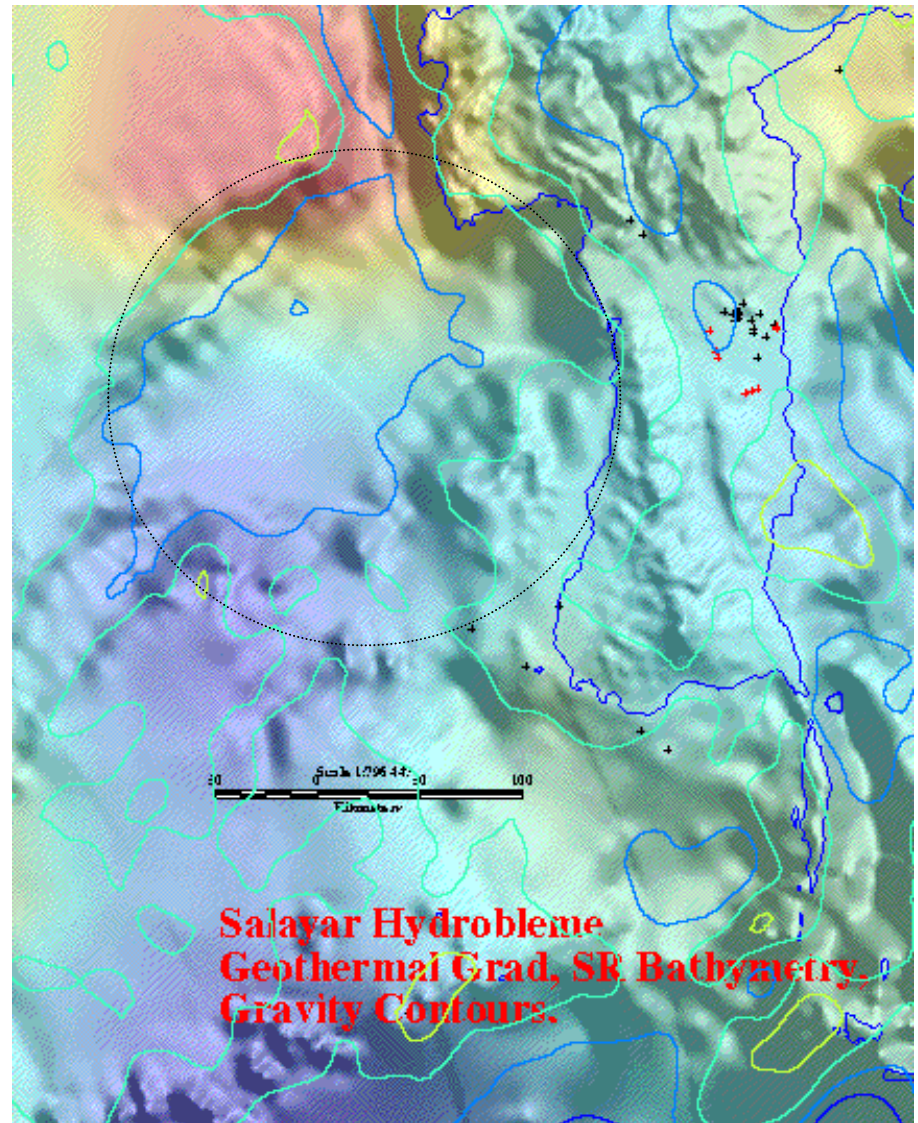
Inner ring diameter of 34 kilometers. Second order derivative on Devonian, TM Thermal Band 6 contours with threshold, faults, and TM PC 1-2-3.



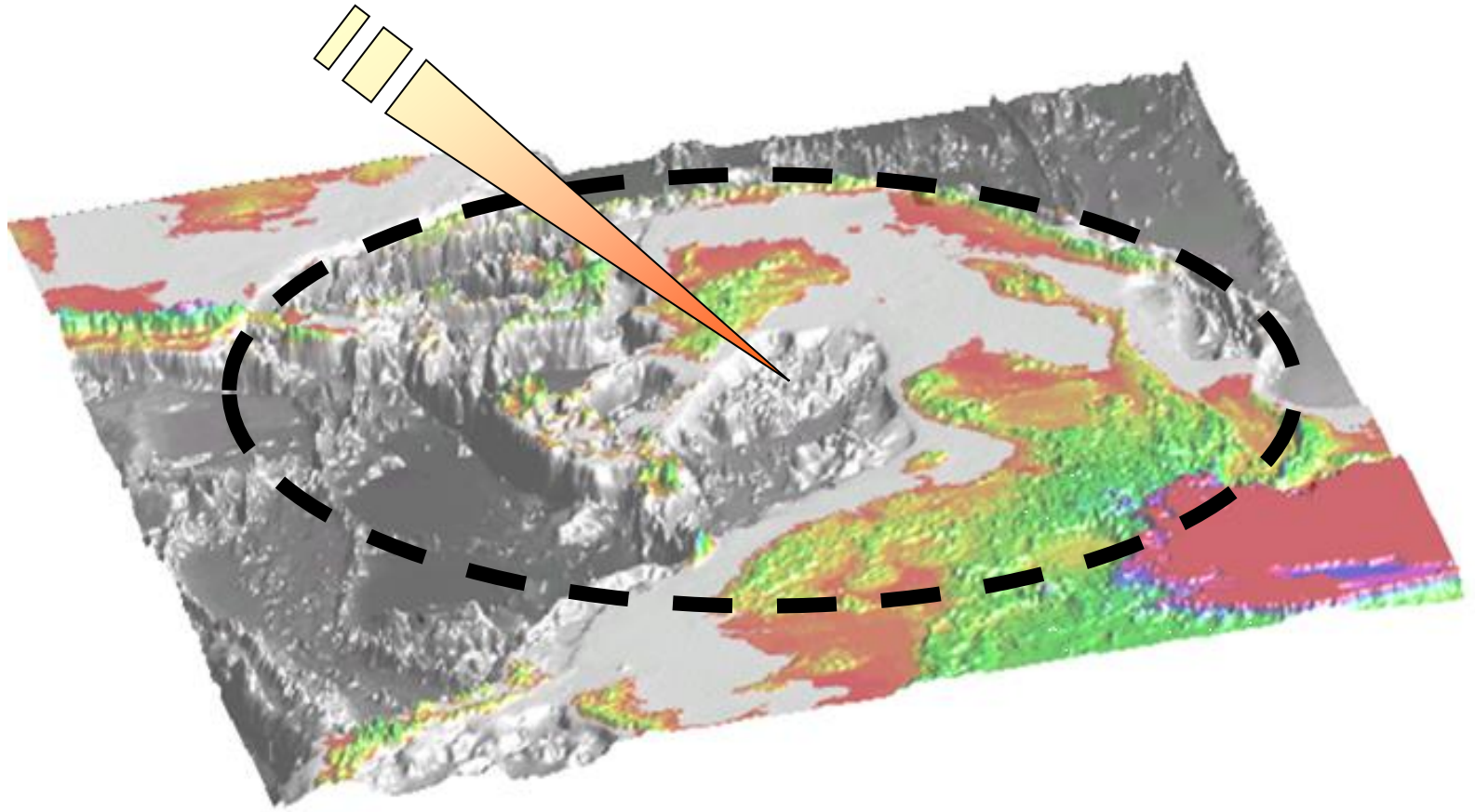
C-Band Radar, Peleng Impact Crater, Indonesia.

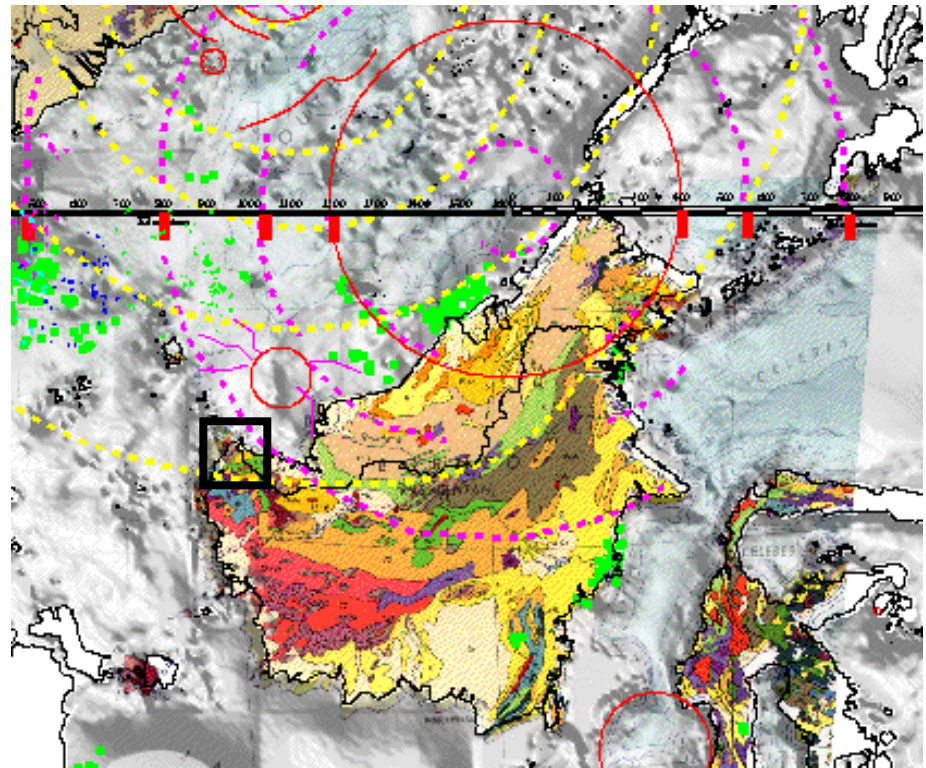
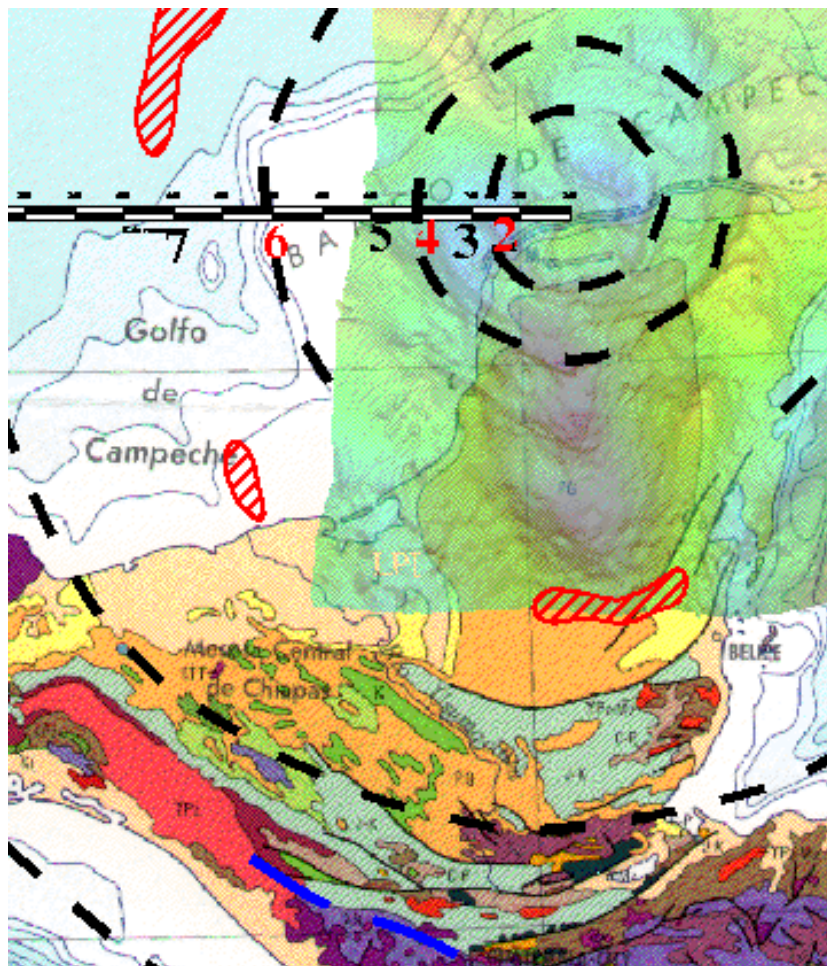


Salayar Hydrobleme, South Makassar Straits, Indonesia. Getec Vertical Derivative RTP Magnetic Intensity.



Salayar Hydrobleme, South Makassar Straits, Indonesia. Shaded relief bathymetry and satellite gravity colorfill.





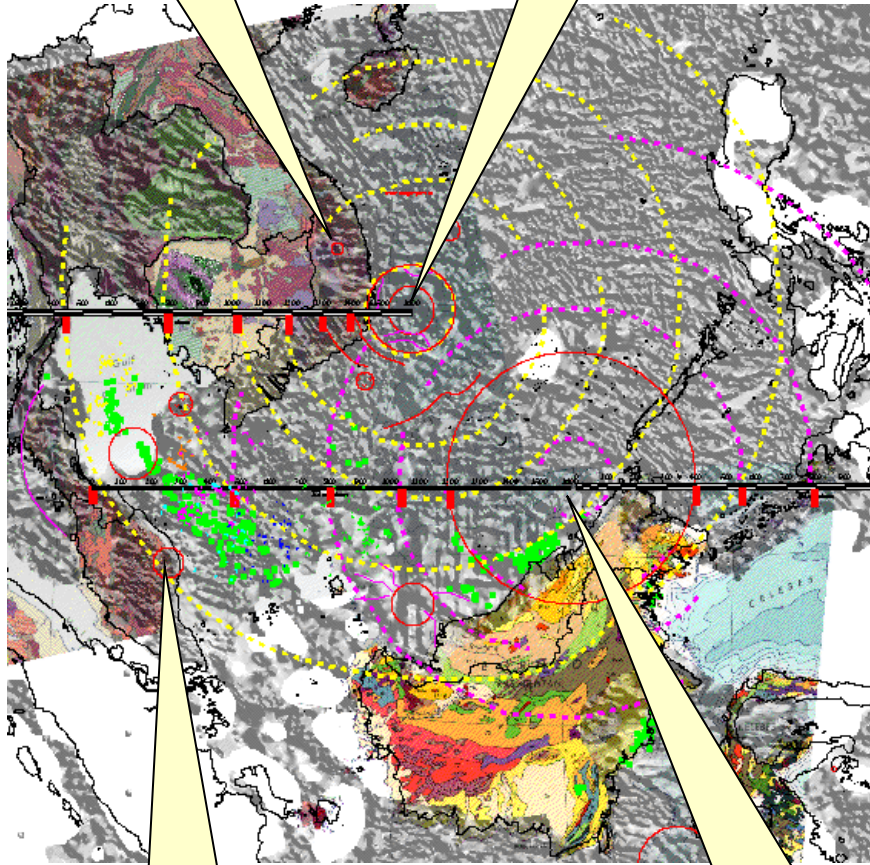
Inset box is Scansar SAR Natuna #8759.

Comparison between onshore geology at Chicxulub multiringed impact basin, Gulf of Mexico, and onshore geology in the South China Sea. Two multiringed Copernican impact basins (hydroblemes) proposed for Ben Goi (Mid-Miocene, Vietnam offshore) and South China Sea (Eocene) exhibit interference patterns which controlled tectonic deformations in the Schwaner Mountains and in the Crocker Belt. These onshore discordant mountain trends have lead to hypothesizing that Borneo has rotated clockwise, and then counterclockwise, since the Eocene. Without evoking the unlikely rotational behavior of Borneo to explain the onshore geology, the superimposition of two large multiringed impact basins more simply explains this phenomenon.

Impact origin of the South China Sea bathymetric depression.
Level: MSc ; Universiti Sains Malaysia
11800 USM, Penang, Malaysia.
Supervisor: Assoc. Prof. Madya Leong Lap Sau
e-mail: lsleong@usm.my

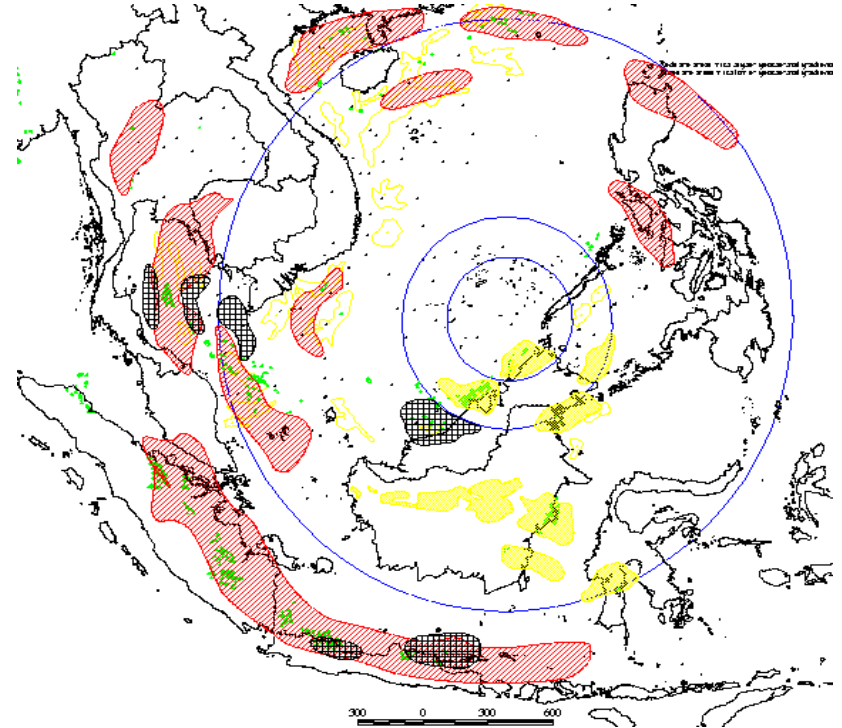
Holocene Event

Ben Goi Event



Bukit Paloh Events

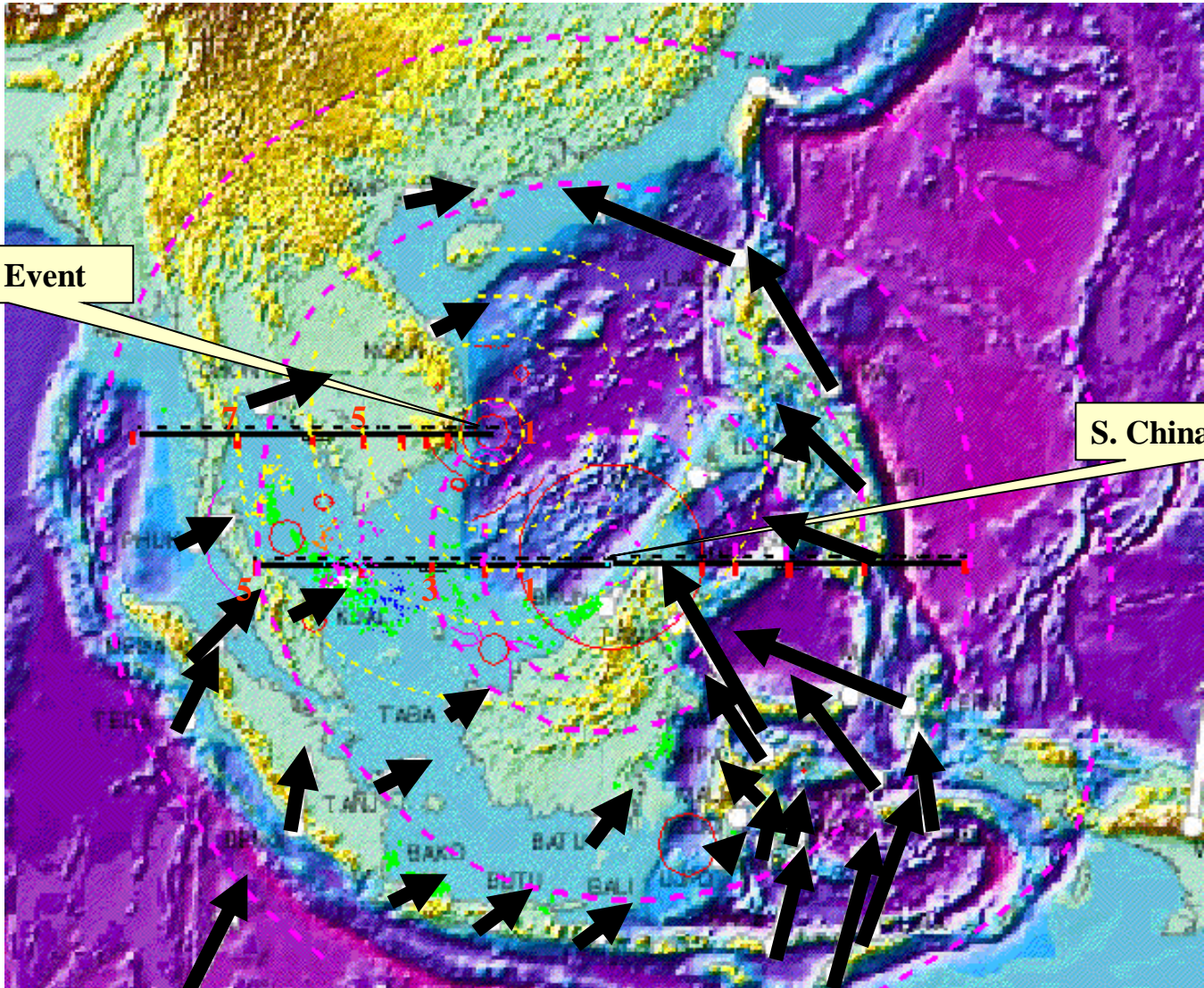
S. China Sea Event



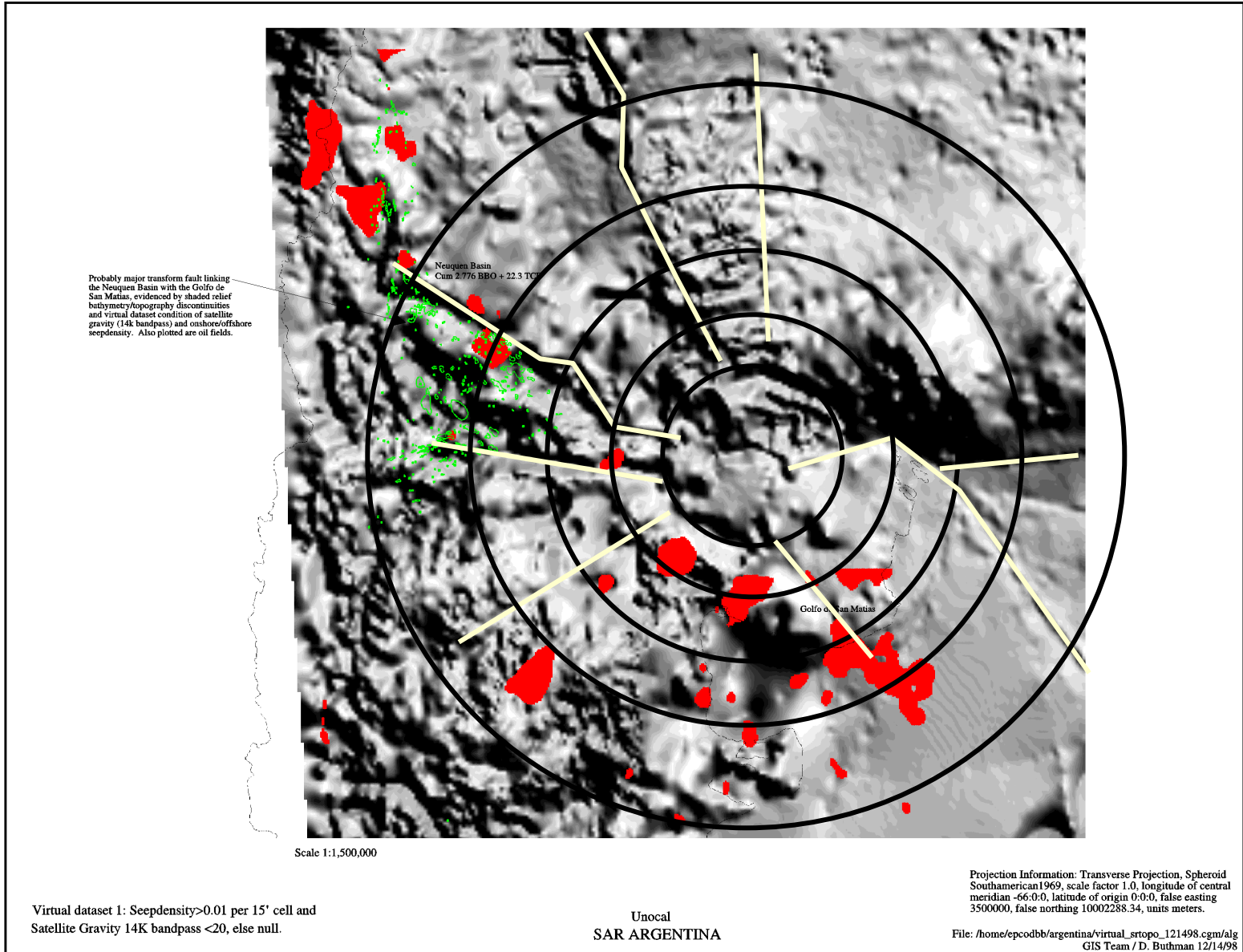
Southeast Asia Crater Tectonics interpretation. Shaded relief CCOP magnetics, Geologic Maps, oil and gas fields (left). Source rock facies distributions: red=lacustrine, yellow=deltaics, black=terrigenous.

Ben Goi Event

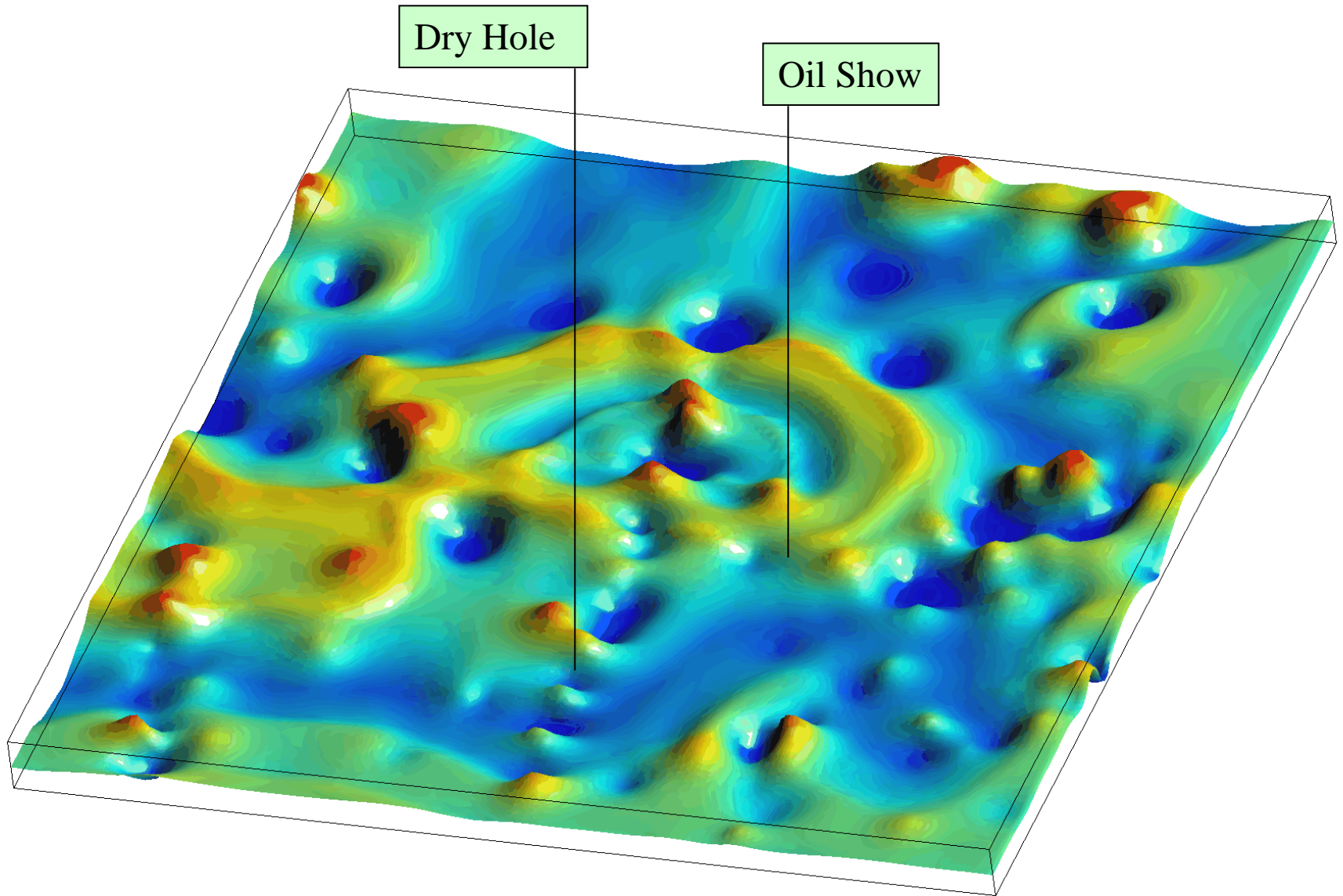
S. China Sea Event



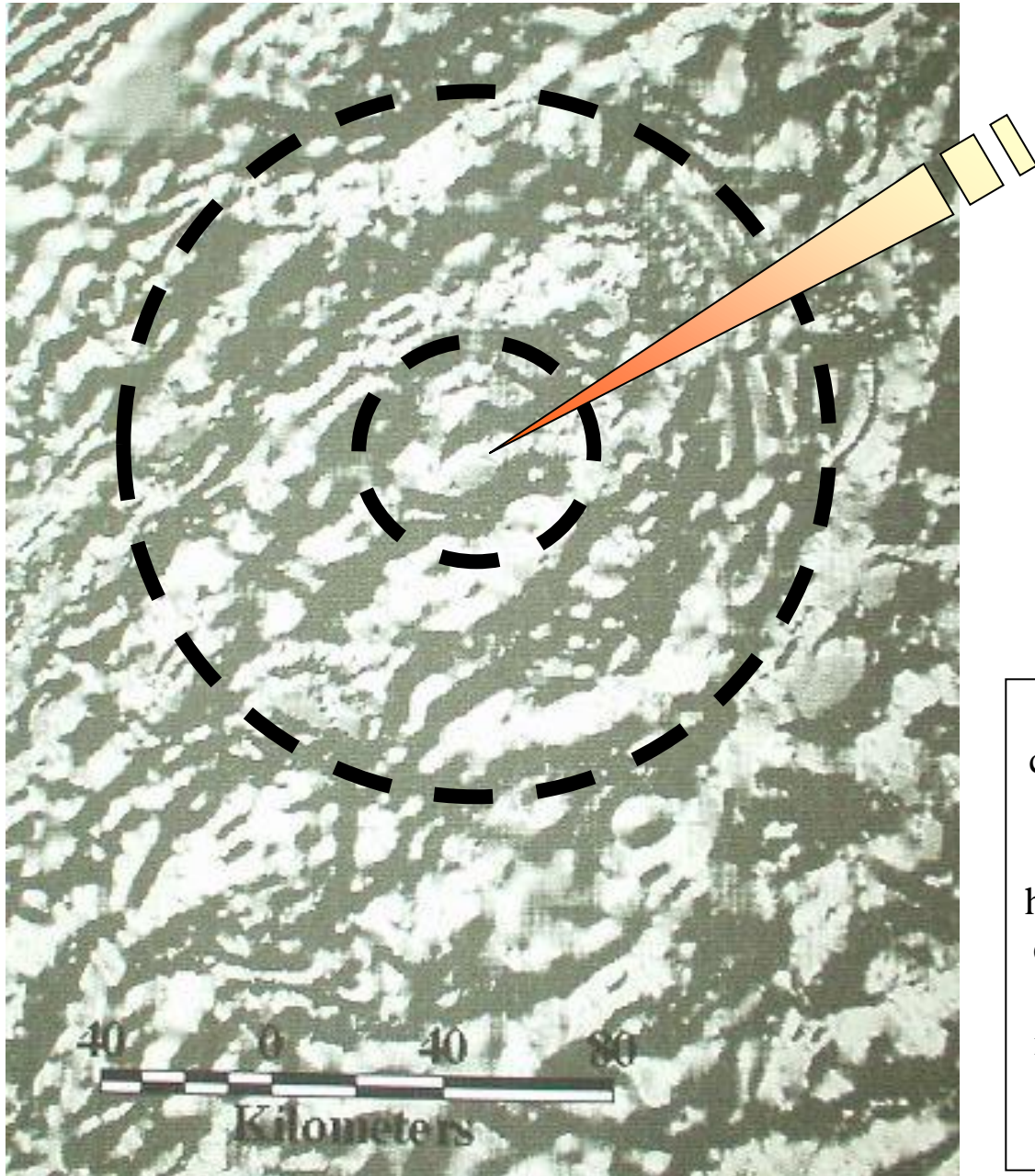
South China Sea Copernican crater tectonics interpretation with DOTSEA's modern geodynamics earth movement measurement vectors (GPS). The earth movements may indicate complex plate interactions, or they may alternately indicate slow supra- and sub-crustal infilling of the multiringed basin depression.



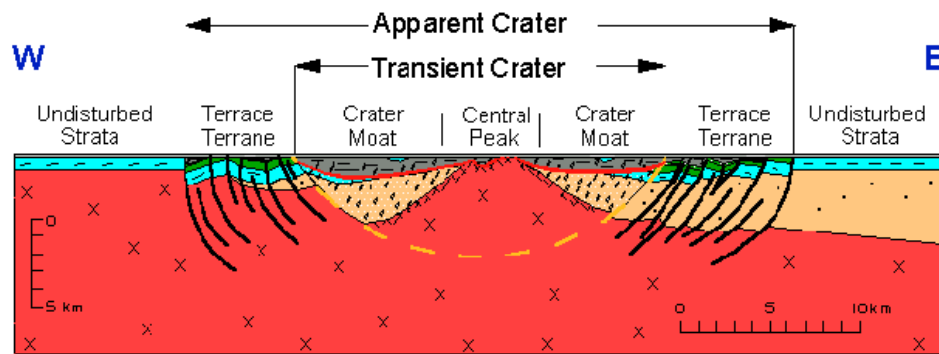
Multibasin crater geometric analysis, Neuquen and San Matias Basins, Argentina, Shaded relief topography and bathymetry with gravity / SPT-SAR seepdensity virtual GIS query.



20K Residual Gravity 3D perspective. Unspecified Location, Alaska Interior.



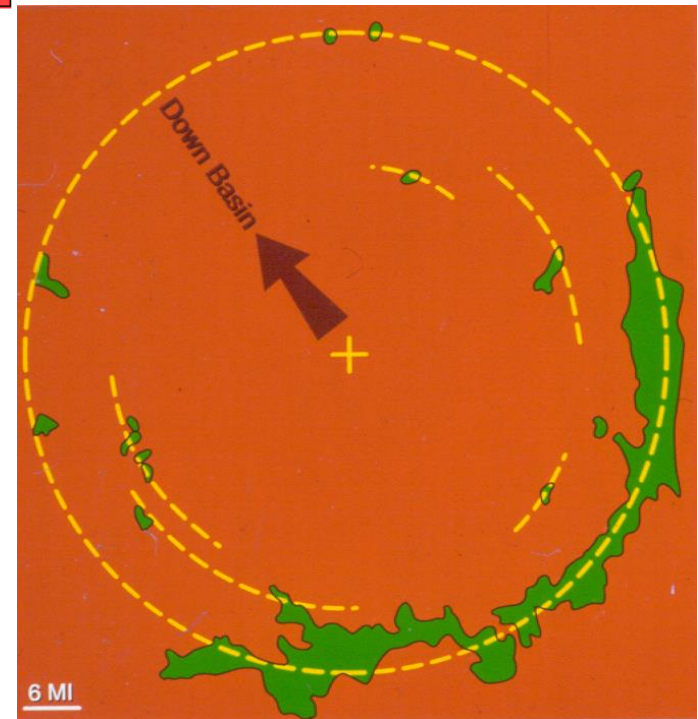
Potential Copernican impact crater with a diameter exceeding 150 kilometers. This basin is one of the most prolific hydrocarbon basins on Earth. So entrenched are plate tectonicists in their paradigms here that the mere speculation of this being a crater has evoked fear, anger, and ridicule.



- | | | | |
|--|---|--|----------------------------------|
| | Glacial Drift | | Cretaceous Rocks |
| | Fall-Back (Suevite) | | Paleozoic Strata |
| | Phanerozoic Clast Breccia (Debris Flow) | | Proterozoic Red Clastic Rocks |
| | Transported, Brecciated Strata | | Proterozoic Crystalline Basement |
| | Brecciated Crystalline Rock | | Transient Crater |

Cross-Section of the Manson Impact Structure

by R.R. Anderson

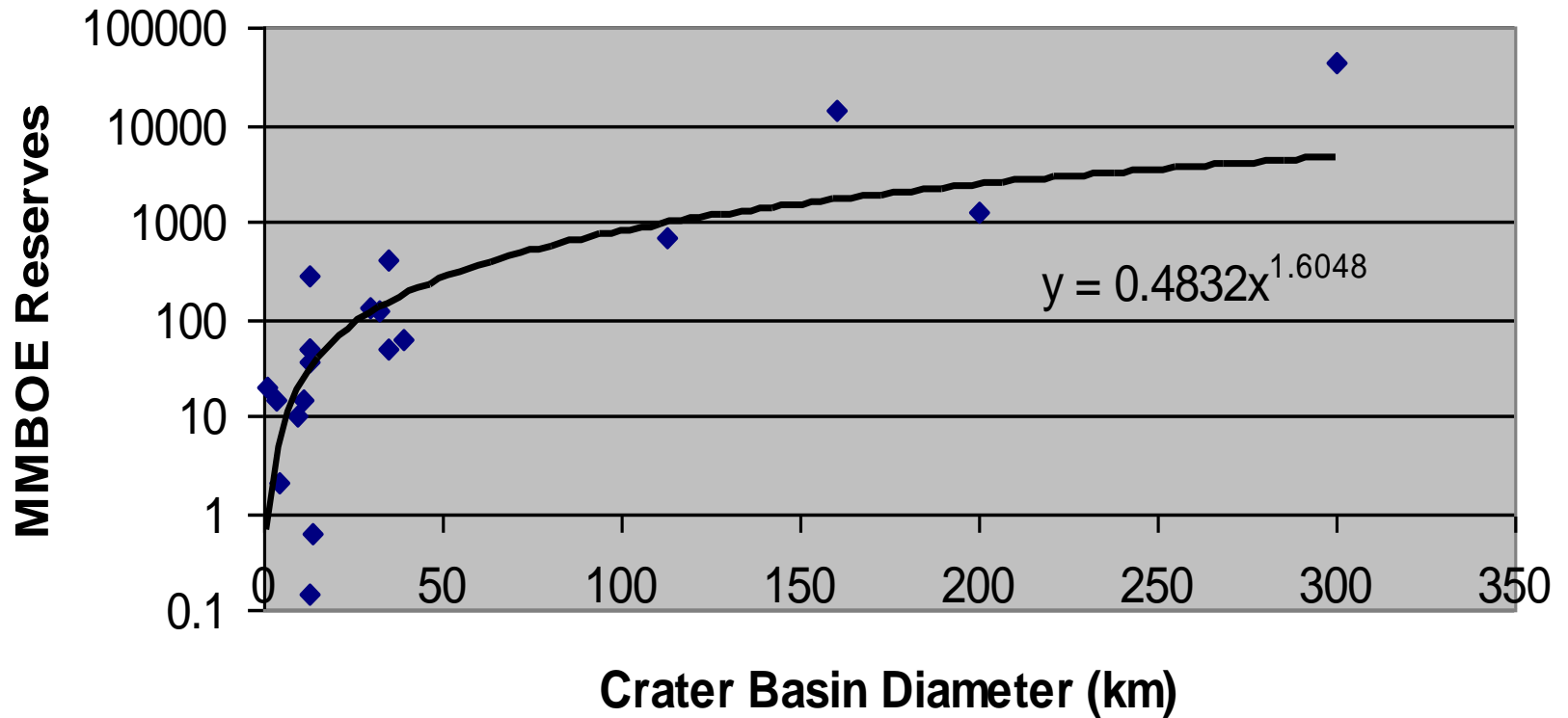


Generalized trapping and reservoir developments at impact craters. Cross section shows structural elements typical of conventional hydrocarbon entrapment, such as within the central peak and along the terraced terrain or encircling ring anticlines. Most oil pools of the 20 reported be productive from impact related features, have undergone basin tilting long after formation of the craterform structure; consequently, hydrocarbon migration within the rings will be preferential toward the out of basin direction.

	Dia (km)	Reserves	Reserves	MMBOE
<i>Viewfield, Saskatchewan</i>	1.24	20	<i>MMBO</i>	20
<i>Newporte, N. Dakota</i>	3.2	15	<i>MMBO</i>	15
<i>Lyles Ranch (Bee Bluff), Texas</i>	4	2	<i>BCFG</i>	2
<i>Red Wing Creek, N. Dakota</i>	9	10	<i>MMBO</i>	10
<i>Hartney, Manitoba</i>	11.2	15	<i>MMBO</i>	15
<i>Marquez, Texas</i>	12.7	0.15	<i>MMBOE</i>	0.15
<i>Ames, Oklahoma</i>	12.8	50	<i>MMBO</i>	50
<i>Avak, Alaska</i>	12.8	37	<i>BCFG</i>	37
<i>Steen Field, Alberta</i>	12.8	50	<i>MMBO</i>	50
<i>Sierra Madera, Texas</i>	13	270	<i>BCFG</i>	270
<i>Cass Co., Michigan</i>	13.6	0.6	<i>MMBO</i>	0.6
<i>Central Oklahoma</i>	30	130	<i>MMBOE</i>	130
<i>Ochiltree, Texas</i>	32	120	<i>BCFG</i>	120
<i>Haswell Hole, Colorado</i>	35	50	<i>MMBO</i>	50
<i>Roxanna-Orlando, Oklahoma</i>	35	400	<i>MMBO</i>	400
<i>Warren, Michigan</i>	39	60	<i>MMBO</i>	60
<i>Lima, Indiana</i>	113	700	<i>MMBO</i>	700
<i>Campos Basin, Brazil</i>	160	13800	<i>MMBOE</i>	13800
<i>Bombay, India</i>	200	1296	<i>MMBOE</i>	1296
<i>Chicxulub, Mexico</i>	300	45000	<i>MMBOE</i>	45000
TOTAL:				62025.75

Estimates of impact structure basement rocks reservoirs in the Lower 48 range from 5 BBO to over 105 BBO, based on extrapolation of crater densities in the Canadian Shield (Donofrio, 1997).

Crater Basin Diameter (km) Versus MMBOE Reserves



UNOCAL 76

Alaska Resources

Acknowledgements:

Unocal

M. Hrachovy

